Polypyrrole-Graphene based Flexible Supercapacitors

by

Priya Bhargava

A thesis

presented to the University of Waterloo

in fulfilment of the

thesis requirement for the degree of

Master of Applied Science

in

Chemical Engineering (Nanotechnology)

Waterloo, Ontario, Canada, 2020

Author's Declaration

I hereby declare that I am the sole author of this thesis. This is a true copy of the thesis including any required final revisions, as accepted by my examiners.

I understand that my thesis may be made electronically available to the public.

Abstract

The high interest in wearable technologies has inspired an increased demand for portable, flexible energy storage devices. Currently, most commercial electrochemical energy storage units, such as supercapacitors, are available only in rigid formats, failing to meet the flexibility standards that allow their integration into wearables such as smart textiles and flexible electronics. To achieve flexible supercapacitors, different flexible substrates have been separately reported by various research studies for electrode preparation by coating them with active materials. However, there is a lack of studies comparing these substrates, using the same active material, to investigate their impact on the electrochemical performance of a supercapacitor cell. This can provide important reference and guidance for the design of flexible supercapacitors.

Polypyrrole is a popularly used conductive polymer for supercapacitor applications due to their high areal/specific capacitance, energy density and low cost, but they suffer from poor cycling stability. Herein, reduced graphene oxide has been combined with polypyrrole to obtain an optimized electrode configuration with good cycling stability and areal capacitance. Using this electrode configuration, the electrochemical performance of flexible supercapacitor electrodes and full cells constructed with three commonly used substrates- commercially obtained conductive polyester fabric (Cu:Ni-PET), carbon cloth and stainless-steel wire mesh (SSWM), are compared. Particularly, the effects of substrate properties such as conductivity, morphology, wettability on the morphology and electrochemical performance of the resulting polypyrrole-graphene-polypyrrole sandwich structure electrode are investigated in-depth. It is found that the best electrochemical performance is obtained for Cu:Ni-PET based electrodes with a high areal capacitance of 1412 mF/cm^2 at the current density of 2 mA/cm^2 and capacitance retention of 96.6%

after 3000 cycles. Whereas, carbon cloth-based electrodes show next best performance with 1227 mF/cm^2, followed by SSWM based electrodes with 1030 mF/cm^2 capacitance. The supercapacitor cells show similar results, where cells prepared using Cu:Ni-PET show larger areal capacitance, good cycling stability, and better capacitance retention after 4000 bending cycles compared to carbon cloth and followed by SSWM. The best electrochemical performance of Cu:Ni-PET based supercapacitors are mainly attributed to its high conductivity, good wettability, and unique surface morphology as well as excellent bendability.

Acknowledgements

I take this opportunity to express my gratitude to my supervisors, Dr. Aiping Yu and Dr. Ting Tsui, for their valuable guidance and support in executing my project.

I would also like to acknowledge and thank the readers of this thesis- Dr. Aiping Yu, Dr. Ting Tsui, Dr. Eric Croiset and Dr. David Simakov.

I am thankful to Dr. Michael Pope for advising me during the initial phase of my project. I also extend my thanks to Dr. Wenwen Liu and Dr. Wenyao Zhang for providing me with technical support and mentorship when needed.

I wish to express my profound gratitude to my friend, Amogh Sohoni, for proofreading my thesis.

Finally, I would like to express my gratitude to my family and friends for their constant encouragement and help throughout my project.

Dedication

Dedicated to my parents and Priyansh.

Table of Contents

Author's Declaration ii

Abstract iii

Acknowledgements v

Dedication vi

List of Figures x

List of Tables xiv

List of Abbreviations xv

1.0 Introduction 1

1.1 Project Motivation 1

1.2 Project Aims and Objectives 4

1.3 Report Structure 6

2.0 Background 8

2.1 Supercapacitor Configuration 8

2.1.1 Electric Double Layer Capacitors (EDLCs) 9

2.1.2 Pseudocapacitors 12

2.2 Electrode Materials 14

2.2.1 Carbon-based materials 14

2.2.2 Metal oxide-based materials 16

2.2.3 Conductive polymer-based materials 17

2.3 Characterization 19
2.3.1 Cyclic Voltammetry 19
2.3.2 Galvanostatic Charging Discharging 20
2.3.3 Electrochemical Impedance Spectroscopy 22
2.3.4 Four-Point Probe Method 22
2.4 Flexible Supercapacitors 24
2.4.1 Types of Substrates 27
2.5 Conductive Polymers 30
2.5.1 Introduction to Polypyrrole 30
2.5.2 Polypyrrole Based Flexible Supercapacitors 34
3.0 Polypyrrole-Graphene-Polypyrrole Sandwich Structure for Supercapacitor Electrode 39
3.1 Introduction 39
3.2 Experimental Methods and Characterization 41
3.2.1 Electrode Preparation 41
3.2.2 Chemical and Structural Characterization 43
3.2.3 Electrochemical Characterization 43
3.3 Results and Discussion 43
4.0 Impact of Substrates on Supercapacitor Performance 56
4.1 Introduction 56
4.2 Experimental Methods and Characterization 60
4.2.1 Electrode Preparation using different Substrates 60
4.2.2 Device Assembly 61

4.2.3 Materials and Electrochemical Characterization 61

4.3 Results and Discussion 62

4.3.1 Three-electrode Tests 62

4.3.2 Two-electrode Tests 73

5.0 Conclusions 85

6.0 Recommendations 89

References 91

List of Figures

Figure 1: Ragone plot comparing power density and energy density of different electrochemical energy storage devices (Reproduced from reference [13]). 2

Figure 2: Schematic diagram showing components of a Symmetric Supercapacitor (Reproduced from reference [27]). 8

Figure 3: EDLC Models- (a) Helmholtz Model, (b) Gouy-Chapman Model, (c) Stern Model (Reproduced from reference [27]). 10

Figure 4: Schematic for Four-Point Probe Method (Reproduced from reference [61]). 23

Figure 5: Number of flexible supercapacitors-based research studies conducted over past 10 years (source Web of Science; search time: 18, Jan. 2020). 25

Figure 6: Oxidation (Doping) and Reduction (Dedoping) of Polypyrrole (Reproduced from reference [85]). 31

Figure 7: Number of publications on conductive polymer based flexible supercapacitors over past 10 years (source Web of Science; search time: 18, Jan, 2020). 31

Figure 8: Schematic Illustration for synthesis of PPy-rGO-PPy sandwich structure electrodes. 44

Figure 9: XRD Patterns (a) GO and rGO powder. (b) Blank Cu:Ni-PET substrate, Polypyrrole coated Cu:Ni-PET (PPy-Cu:Ni-PET) and Graphene coated on PPy-Cu:Ni-PET (PPy-rGO-Cu:Ni-PET). 45

Figure 10: SEM Images of (a) blank Cu:Ni-PET fabric (b) PPy- Cu:Ni-PET (c) rGO-PPy- Cu:Ni-PET at 2000X magnification. (d) SEM image at edge of rGO-PPy- Cu:Ni-PET showing rGO coating on PPy particles at 5000X magnification. (e) SEM image of PPy-rGO-PPy- Cu:Ni-PET. 46

Figure 11: Deposition time for electrochemical polymerization of each layer of PPy in electrode with sandwich configuration (PPy-rGO-PPy) and control samples without rGO layer (PPy-PPy). 48

Figure 12: Drying method determination by comparing areal capacitance (mF/cm^2) and capacity retention (%) data. 49

Figure 13: (a) CV curves for electrode with sandwich configuration (PPy-rGO-PPy) at different scan rates. (b) Areal capacitance at different scan rates for electrode with sandwich configuration (PPy-rGO-PPy) and control samples without rGO layer (PPy-PPy). 50

Figure 14: Nyquist plot for PPy-rGO-PPy and PPy-PPy coated on Cu:Ni-PET fabric. 52

Figure 15: Cycling stability comparison between electrode with sandwich configuration (PPy-rGO-PPy), control samples without rGO layer (PPy-PPy) and single layer of PPy deposited on Cu:Ni-PET fabric for 1000 cycles. 52

Figure 16: (a) Cycling stability of electrode with sandwich configuration (PPy-rGO-PPy) for 3000 cycles. (b) CV scans at 50 mV/s for first and 3000th cycle for PPy-rGO-PPy electrodes. 54

Figure 17: (a) Images of blank (top) and PPy-rGO-PPy coated (bottom) Cu:Ni-PET (left), Carbon cloth (centre), SSWM (right) substrates. (b) Qualitative analysis of contact angle using images of water droplet on blank substrates. (c) In-plane electrical conductivity of blank substrates. 63

Figure 18: SEM images at 100X magnification of blank substrates- (a) Cu:Ni-PET fabric, (b) Carbon cloth, (c) SSWM and substrates coated with PPy-rGO-PPy electrode material- (d) Cu:Ni-PET fabric, (e) Carbon cloth, (f) SSWM. 64

Figure 19: CV data of PPy-rGO-PPy on different substrates. CV curves at different scan rates for (a) Cu:Ni-PET (b) Carbon cloth (c) SSWM. (d) Areal capacitance values at different scan rates comparing the three substrates. 66

Figure 20: GCD data of PPy-rGO-PPy on different substrates. GCD curves at different current densities for (a) Cu:Ni-PET (b) Carbon cloth (c) SSWM. (d) Areal capacitance values at different current densities comparing the three substrates. 67

Figure 21: Stability test of PPy-rGO-PPy on different substrates at scan rate of 50 mV/s. 68

Figure 22: Nyquist curves of PPy-rGO-PPy on different substrates- (a) Cu:Ni-PET (b) Carbon cloth (c) SSWM. 69

Figure 23: Bending test of PPy-rGO-PPy on different substrates (a) Cu:Ni-PET (b) Carbon cloth (c) SSWM. (d) Areal capacitance as a function of number of bending cycles for three different substrates. 71

Figure 24: Schematic illustration for assembling full cell using PVA/Na_2SO_4 gel electrolyte. ... 73

Figure 25: Carbon cloth coated with PPy-rGO-PPy in PVA/KOH electrolyte. 74

Figure 26: Voltage window determination using SC full cells prepared with Cu:Ni-PET fabric coated with PPy-rGO-PPy as electrodes. 75

Figure 27: CV data of PPy-rGO-PPy based full cells with different substrates. CV curves at different scan rates for (a) Cu:Ni-PET (b) Carbon cloth (c) SSWM. (d) Areal capacitance values at different scan rates comparing the three substrates. 76

Figure 28: GCD data of PPy-rGO-PPy based full cells with different substrates. CV curves at different scan rates for (a) Cu:Ni-PET (b) Carbon cloth (c) SSWM. (d) Areal capacitance values at different scan rates comparing the three substrates. 77

Figure 29: Ragone plot comparing PPy-rGO-PPy based full cells with different substrates. 78

Figure 30: Stability test of PPy-rGO-PPy based full cells with different substrates at scan rate of 80 mV/s. 79

Figure 31: Nyquist curves of PPy-rGO-PPy based full cells with different substrates. 80

Figure 32: Bending test: CV scans of PPy-rGO-PPy based full cells with different substrates after different number of bending cycles at 10 mV/s (a) Cu:Ni-PET (b) Carbon cloth (c) SSWM. 81
Figure 33: Bending test: CV scans of PPy-rGO-PPy based full cells with different substrates under flat and bent conditions at 10 mV/s (a) Cu:Ni-PET (b) Carbon cloth (c) SSWM. 82

List of Tables

Table 1: Comparison of electrochemical performance of PPy composite based flexible symmetric supercapacitors..... 84

List of Abbreviations

CNTs	-	Carbon Nanotubes
Co_3O_4	-	Cobalt oxide
CQDs	-	Carbon quantum dots
Cu:Ni-PET	-	Commercial conductive polyester fabric coated with copper and nickel obtained from Adafruit Industries
CV	-	Cyclic voltammetry
EDLCs	-	Electrochemical Double Layer Capacitors
EIS	-	Electrochemical impedance spectroscopy
GC	-	Gouy Chapman
GCD	-	Galvanostatic charge-discharge
GO	-	Graphene oxide
HCl	-	Hydrochloric acid
H_2O_2	-	Hydrogen peroxide
H_2SO_4	-	Sulphuric acid
H_3PO_4	-	Phosphoric acid
$KMnO_4$	-	Potassium permanganate
KOH	-	Potassium hydroxide
MnO_2	-	Manganese dioxide
Na_2SO_4	-	Sodium sulfate
NiO	-	Nickel oxide
PANI	-	Polyaniline
PPy	-	Polypyrrole

PPy-PPy	-	Control samples consisting of two layers of polypyrrole deposited on a substrate
PPy-rGO	-	An rGO layer deposited on polypyrrole coated substrate
PPy-rGO-PPy	-	Sandwich configuration where rGO layer is deposited between two layers of polypyrrole on a substrate
PVA	-	Polyvinyl alcohol
rGO	-	Reduced graphene oxide
RuO_2	-	Ruthenium (IV) oxide
SEM	-	Scanning Electron Microscopy
SSWM	-	Stainless steel wire-mesh obtained from Alfa Aesar
TsOH	-	p-Toluenesulfonic acid
XRD	-	X-ray Diffraction

1.0 Introduction

1.1 Project Motivation

With the fast depletion of non-renewable resources such as fossil-fuels and the alarming impact of greenhouse-gas emissions and environmental pollution, it has become extremely important to develop highly efficient energy generation and storage devices. Over the past few decades, many renewable energy sources have been exploited to meet the sustainable development requirement. However, due to the unstable and intermittent nature of these renewable energy sources, the development of a stable and efficient energy storage technology is significant [1]–[3]. These energy storage technologies include batteries and supercapacitors, which have been extensively investigated over the recent years in both academia and industry [3], [4]. Out of these two popular energy storage devices, even though batteries can provide higher energy density, they suffer from lower power density compared to supercapacitors as shown in the Ragone plot (Figure 1). Supercapacitors hold advantages such as fast charge/discharge capacity, high reliability, long cycle life, wide operating temperature range, and low environmental impact, making them promising energy storage devices [5]–[8]. Their high-power density is useful for applications ranging from wearable electronics to medical devices and to hybrid electric vehicles.

Wearable electronics have gained a lot of traction in recent years and the market size has increased rapidly. Supercapacitors can be used as energy storage devices for almost every wearable electronics technology. Wearable technologies include but are not limited to implantable medical equipment, smart health monitoring devices, smart watches, flexible sensors, military electronics [9], [10]. With its ever-growing market size and the demand for wearable devices with a small

form-factor, there is an increased need for miniaturization of energy storage devices such as supercapacitors while maintaining their flexibility, lightweight, safety, and efficiency for easy incorporation into a wearable device with small form factor [11]. Traditional devices such as button supercapacitors are difficult to integrate into wearable electronics due to their bulkiness and rigidity. Therefore, there has been an increased focus on developing flexible, stretchable and lightweight supercapacitor devices that can maintain their performance even under bending conditions [4], [8], [12].

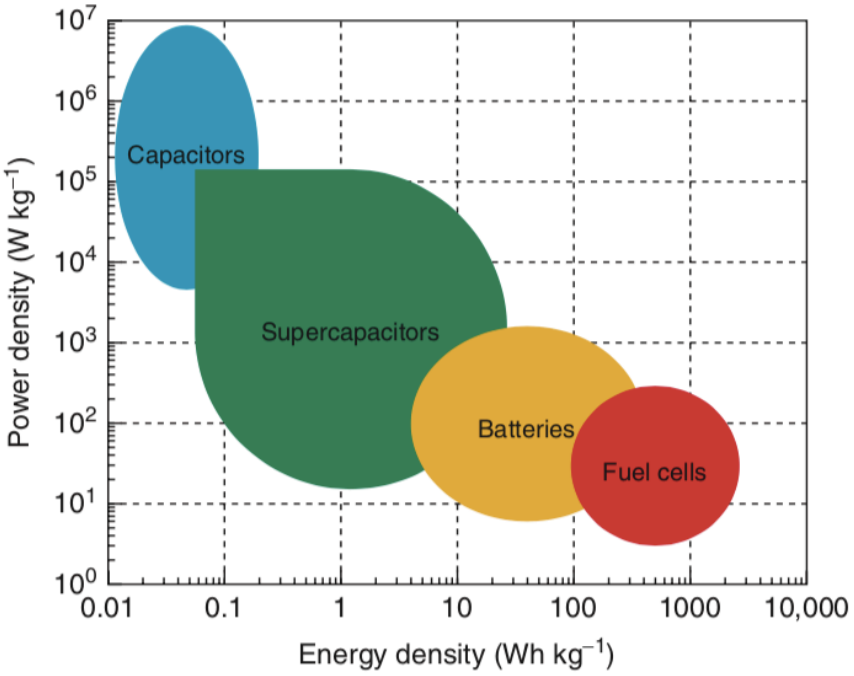

Figure 1: Ragone plot comparing power density and energy density of different electrochemical energy storage devices (Reproduced from reference [13]).

Supercapacitors store energy via two different charge storage mechanisms- electric double layer capacitors (EDLCs) and pseudocapacitors [1], [13]. EDLCs store energy via physical adsorption of ions from the electrolyte on the surface of the electrode material and does not involve faradic redox reactions. This mechanism is exhibited by carbon-based materials, that have high electrical

conductivity and specific surface areas, such as graphene, activated carbon, and carbon nanotubes (CNTs) and their derivatives [1], [14]. The charge storage capability of EDLCs depends on the active surface and presence of reaction sites. Thus, they have a lower energy density. Compared to EDLCs, pseudocapacitors involve fast, reversible faradaic redox reactions at the surface of active material. Popularly used pseudocapacitor materials include metal oxides such as RuO_2, MnO_2, and conductive polymers such as polypyrrole (PPy), polyaniline (PANI). These pseudocapacitors show 10-100 times greater specific capacitance than the materials exhibiting EDLCs [15]. They have higher energy storage capabilities due to the nature of their charge storage mechanism, where faradaic redox reactions occur at the surface as well as in the bulk near the surface of the active material [16]. Within pseudocapacitors, conductive polymers have several advantages over metal oxides and make a better choice for supercapacitor electrode material. These advantages include excellent electrical conductivity, large theoretical specific capacitance, low cost, mechanical flexibility, ease of fabrication and ease of deposition on a substrate [1], [15].

Polypyrrole (PPy) is one of the popular conductive polymers used in the supercapacitor devices due to its high conductivity (0.3- 500 S/cm), good redox properties, environmental stability, and simple synthetic procedures [1], [17]–[19]. PPy based supercapacitor device can deliver a large areal capacity of 505 mF/cm^2 at a current density of 2.0 mA/cm^2 [20]. However, PPy has its limitations for application in high-performance supercapacitors, just like other conductive polymers. It suffers from poor cycling stability due to repeated swelling and shrinking of polymer chains during the long-term charging-discharging processes. To overcome this limitation, PPy can be combined with a high surface area carbon-based material such as graphene to improve its chemical and structural stability. Also, by avoiding the bulk film of PPy in the electrode structure,

the penetration of electrolyte ions can be allowed to maximize the utilization of active material [21]. By designing a configuration for electrode structure, where graphene is incorporated into the PPy films, a supercapacitor device with good cycling stability can be fabricated [18].

Over recent years, a lot of studies on PPy based flexible supercapacitors have been conducted due to ease of deposition of PPy on a conductive substrate. Studies on PPy-based flexible supercapacitors have separately reported applications of flexible substrates such as carbon cloth [22], metallic foils or wire meshes [23], and carbonized or metal-coated/blended fabrics [9], [24]. There is a lack of studies comparing these substrates using same active materials. The role of substrate in the overall electrochemical performance of the supercapacitor is often under-looked. Therefore, it is important to conduct a comparison study using different substrate materials to investigate and understand its role in flexible supercapacitor devices. The work presented here designs an optimized electrode configuration and uses it for comparing three different conductive and flexible substrates to investigate impact of properties of the substrate on electrochemical performance of their respective flexible supercapacitor electrodes and devices.

1.2 Project Aims and Objectives

Fabrication of a flexible supercapacitor device requires a flexible substrate coated with a designed electrode configuration. In this work, PPy and graphene are used as the active material to design electrodes for the supercapacitor device. The designed electrode configuration is used to compare three different substrates- a commercially obtained copper-nickel coated conductive polyester fabric (Cu:Ni-PET), carbon cloth and stainless steel wire mesh (SSWM), to investigate the role of a substrate on the electrochemical performance of the supercapacitor. These conductive substrates

provide flexibility and act as a current collector in the supercapacitor device. Following are the objectives, that need to be met to fabricate a flexible supercapacitor device with superior performance and to evaluate the impact of substrate properties on the electrochemical performance of the device:

Objective #1: Design the electrode configuration by depositing PPy on a flexible substrate and incorporating graphene sheets into the electrode structure to enhance the cycling stability of the PPy chains. This includes the optimization of synthesis procedures for obtaining the designed electrode configuration.

Objective #2: Compare three different substrates for their role in influencing the electrochemical performance of the supercapacitor device. The three flexible substrates chosen are- carbon cloth, SSWM, and Cu:Ni-PET. They are deposited with the same electrode configuration, determined from objective 1, and are analyzed using three-electrode tests. The performance of electrodes is assessed based on areal capacitance, cycling stability and the effect of mechanical bending on the capacitance.

Objective #3: Fabricate flexible quasi-solid-state supercapacitor device by preparing polyvinyl alcohol (PVA) based aqueous gel-electrolyte. The aqueous gel electrolyte needs to be compatible with all three substrates. The electrochemical performance of the supercapacitor device (two-electrolyte test), fabricated using each substrate, is analyzed under bending conditions to satisfy flexibility criteria for the device.

1.3 Report Structure

This research project focuses on developing PPy and graphene-based flexible quasi-solid-state supercapacitor device using a gel electrolyte that can exhibit good cycling performance while maintaining its flexibility for potential integration in a wearable device. Three different flexible substrates are compared for obtaining a high electrochemical performance even under bending conditions. Section 2 provides a brief background on supercapacitors, their energy storage mechanisms, and commonly used electrochemical characterization techniques. This section also discusses the demand and challenges associated with flexible supercapacitors and the role of substrate materials in the overall performance of a flexible device. It introduces the conductive polymer-PPy and provides a literature review on PPy application and limitations as a supercapacitor electrode. This section also includes mitigation strategies to overcome limitations of PPy as an active material for supercapacitors.

Section 3 introduces the proposed PPy and graphene-based sandwich structure of electrodes for the supercapacitor device, satisfying objective 1 from Section 1.2. It discusses their synthesis methods and evaluates the electrochemical performance of the sandwich structure against the control samples. It also discusses results from physical characterization to understand the enhancement in the performance of electrode material. All the results related to electrochemical performance are obtained using three-electrode tests.

Section 4 compares three different substrates using the electrode configuration determined in Section 3. It also presents the fabrication procedure of the supercapacitor device. Thus, this section satisfies objectives 2 and 3 from Section 1.2. The blank substrates are compared in terms of their

in-plane electrical conductivity, wettability, surface morphology, structure and cost. The electrochemical performances are analyzed using three-electrode and two-electrode tests. Two-electrode tests involve use of a PVA-based aqueous gel electrolyte to assemble the supercapacitor device. The electrochemical performance of electrodes and full cells prepared based on different substrates are compared. The flexibility criteria are satisfied by analyzing the electrochemical performance of the device under bending conditions. Finally, section 5 concludes the work described in this thesis, and section 6 provides recommendations related to future work that can aid in further improving the performance of the supercapacitor device.

2.0 Background

2.1 Supercapacitor Configuration

Supercapacitors' ability to store and deliver energy was demonstrated and patented for the first time by Becker in 1957 (US Patent 2 800 616) [25] and ever since has attracted attention in both industry and academic field. A supercapacitor typically consists of two electrodes placed in a sandwich structure with a separator film between them as shown in Figure 2. The electrodes are adhered to current collectors that transport electrons to external load. The key advantage of supercapacitors is that they overcome performance issues such as poor energy storage capabilities and lower power output of traditional electrolytic capacitors and batteries, respectively [26], [27]. Therefore, supercapacitors have a wide variety of applications involving dynamic operations from wearable electronics to medical devices, and hybrid electric vehicles [28].

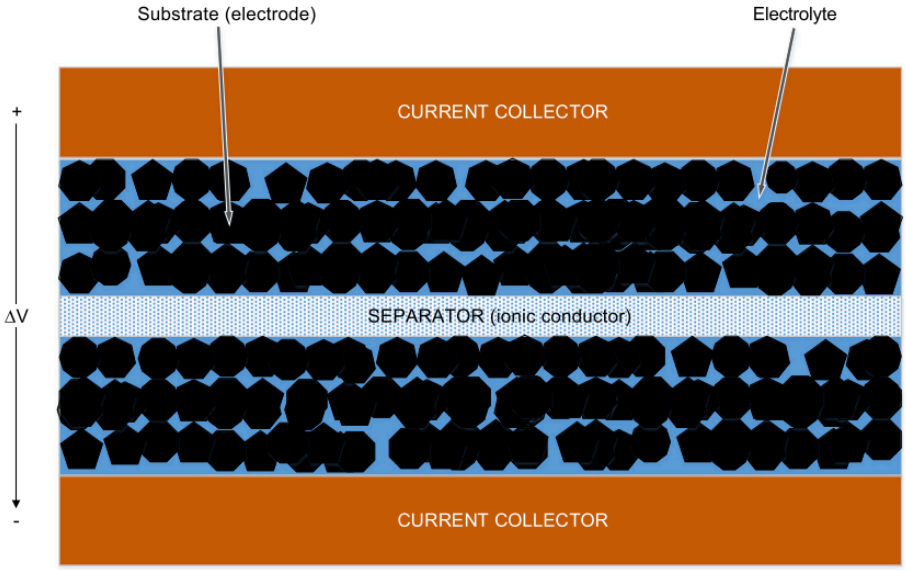

Figure 2: Schematic diagram showing components of a Symmetric Supercapacitor (Reproduced from reference [29]).

Supercapacitors are distinguishable as EDLCs or pseudocapacitors based on their charge storage mechanisms. In EDLCs, physical charge accumulation occurs at the interface between electrode

and electrolyte materials. Whereas, in the pseudocapacitors, the electrode material undergoes electrochemical reaction to store charges during the charging-discharging process.

2.1.1 Electric Double Layer Capacitors (EDLCs)

EDLCs are obtained from high surface area carbon-based materials as electrodes. These materials form two charged layers at the electrode/electrolyte interface when placed into a liquid, as shown in Figure 3. The first charged layer creates a standing electric field that attracts counter ions of the electrolyte to form the second charged layer. These charged surfaces provide supercapacitors the ability to store potential-dependent charges [30]. The electric double layer formation can be explained using several models and theories.

The Helmholtz double layer theory is the earliest model that defined the electric double layer formation. According to this model, when an electrode of surface area A is polarized, a condensed layer is formed in a plane parallel to the electrode surface by oppositely charged ions from the electrolyte to achieve charge neutrality at a distance d from the electrode surface as shown in Figure 3 (a) [31]. This condensed layer and charged surface of the electrode together are known as the electrical double layer. The Helmholtz double layer can be treated as an electrical capacitor of capacitance C_H defined by Equation 1

$$C_H = \varepsilon_0 \cdot \varepsilon_r \cdot \frac{SA}{d} \quad (1)$$

Where,

ε_0 is vacuum permittivity (8.854 x 10^{-12} F/m)

ε_r is relative permittivity of the electrolyte

SA is the surface area of the electrode

d is the effective thickness of the double layer

d can be approximated as the Debye length. However, this theory is very simple and does not adequately describe what happens in nature [29].

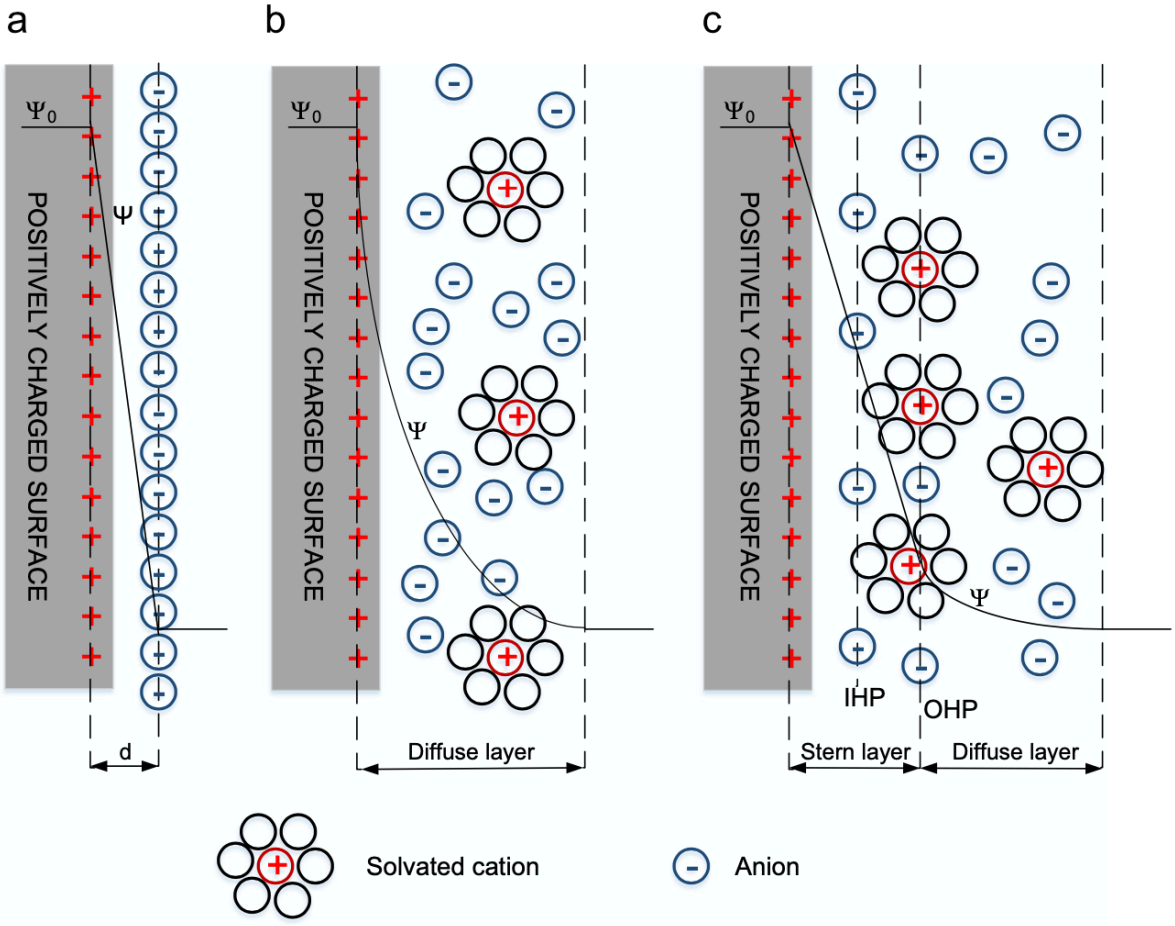

Figure 3: EDLC Models- (a) Helmholtz Model, (b) Gouy-Chapman Model, (c) Stern Model (Reproduced from reference [29]).

Later, Gouy-Chapman (GC) model made a more accurate description of the double layer mechanism, where a charged surface of the electrode is surrounded by an equal amount of oppositely charged ions from the given electrolyte. But these ions are not rigidly held to the electrode surface as shown in Figure 3 (b) [32]. Since ions diffuse into the liquid phase until a

counter potential generated by their departure restricts them, this model is also called the diffuse model. The concentration of the counter ions follows Boltzmann distribution, and therefore, ion concentration decreases exponentially with distance from the electrode surface to the electrolyte bulk. However, ions are assumed to be point charges in this model, and therefore, they are allowed to approach the charged surface without any limit. This model also fails for highly charged double layers [31], [33]. These drawbacks of GC theory were overcome by Stern model that combines both the Helmholtz and GC models.

Stern model assumes that ions of the electrolyte have a finite size, and therefore, have a limiting approach to the electrode surface. It also considers ion accumulation closer to the charged surface and hydrodynamic motions of ions in the diffuse layer. In this model, ions are distributed across two regions- an inner region called the Stern layer or compact layer, and outer diffuse layer, as shown in Figure 3 (c). Within the Stern layer, ions are strongly adsorbed on the electrode surface. The Stern layer itself consists of adsorbed ions that form an inner-Helmholtz plane, and non-adsorbed ions that form the outer Helmholtz plane. The diffuse layer is explained using the GC model and formed as a result of the kinetic energy of counterions. These two layers are equivalent to two capacitors in series, and thus, the total capacitance of the electrode material (C_{DL}) is given by using Equation 2

$$\frac{1}{C_{DL}} = \frac{1}{C_S} + \frac{1}{C_D} \tag{2}$$

Where,

C_S is the capacitance in the Stern layer

C_D is the capacitance in the diffusive layer

C_{DL} is the total capacitance of electrode material

The theoretical value of capacitance for EDLCs can be derived using the thickness of the double layer which is also known as Debye length. The total capacitance C_{DL} at electrode/electrolyte interface using Debye length, Stern layer thickness and Equation 1, is given by Equation 3

$$\frac{1}{C_{DL}} = \frac{1}{C_S} + \frac{1}{C_D} = \frac{\lambda_D}{\varepsilon_0 \varepsilon SA} + \frac{\delta}{\varepsilon_0 \varepsilon SA} \quad (3)$$

Where,

C_{DL} is total capacitance at electrode/electrolyte interface

ε_0 is vacuum permittivity (8.854 x 10^{-12} F/m)

ε is relative permittivity of the electrolyte

SA is the surface area of the electrode

λ_D is the thickness of the double layer (Debye length) in the diffuse layer

δ is the thickness of the Stern layer

In summary, EDLCs involve electrode materials that form an electric double layer upon contact with an electrolyte. Various models can be used to explain the electrical double layer formation, out of which, Stern model is popularly used to understand the mechanisms involved in the double layer formation.

2.1.2 Pseudocapacitors

Pseudocapacitors involve a faradaic charge storage mechanism, where fast and reversible redox reactions occur on the electrode surface, and the passage of charge across the double layer

generates a faradaic current [27]. The faradaic charge transfer mechanism depends on voltage. So, the pseudocapacitance is, in turn, dependent on voltage. The materials exhibiting pseudocapacitance have an electrical response similar to double-layer capacitors since the state of charge is proportional to the potential with capacitance as proportionality constant. Many different electrolytic processes such as electrosorption, redox reactions and intercalation systems give rise to pseudocapacitance [34]. These materials are different from battery-type materials since their kinetics is limited by surface-based processes compared to diffusion-related reactions that occur in the battery electrodes [29]. Unlike batteries, making/breaking of bonds or phase changes do not occur in pseudocapacitors. These materials are distinguishable by reversible doping/de-doping of conductive polymers such as PPy, PANI, redox reactions of transition metal oxides such as RuO_2, MnO_2, and Co_3O_4 and other materials with redox states [13], [27], [35].

There are three different electrochemical processes associated with pseudocapacitors- (1) surface adsorption of electrolyte ions, (2) redox reactions involving the electrolyte ions and (3) doping/de-doping of conductive polymer. The first two processes are surface-based mechanisms, so the specific surface area of electrode material plays a crucial role in impacting overall supercapacitor performance. In the case of doping/de-doping process occurring in conductive polymers, the surface area does not influence capacitance as it relies on the bulk of the material [35]. The electrical conductivity of the conductive polymers is an important factor in influencing the performance of supercapacitors since this ensures proper distribution and collection of the electric current.

In pseudocapacitors, electrochemical processes occur at the electrode surface as well as in bulk near the surface. Therefore, they exhibit higher specific capacitance and energy density than EDLCs. It has been reported that the electrostatic capacitance of a pseudocapacitor can be 10-100 times higher than that of an EDLC, making them desirable for application in next-generation electrochemical supercapacitors [34]. However, they have lower power density than EDLC since faradaic reactions are slower than non-faradaic reactions. Furthermore, pseudocapacitors suffer from lower cycling stability due to redox reactions occurring at the electrode surface [29]. For example, conductive polymers undergo swelling and shrinking during charging-discharging cycles, leading to poor mechanical and cycling stability [29], [35], [36].

2.2 Electrode Materials

A supercapacitor typically consists of three components- 1) electrode, 2) current collector, and 3) electrolyte. Out of these components, the electrode material plays a crucial role since it determines the capacitance and charge storage mechanism in the device. Therefore, current research studies focus on developing new electrode materials or combining different electrode materials to form novel composites or electrode configurations [27]. The electrode materials for supercapacitors are commonly classified into three categories: 1) carbon-based materials, 2) metal-oxide based materials, and 3) conductive polymers.

2.2.1 Carbon-based materials

Carbon-based materials are desirable electrode materials for supercapacitors due to their abundance, low cost, ease of processing, excellent conductivity, high specific surface area, high chemical/thermal stability and non-toxicity [37]–[39]. They store charges via electrochemical

double layer mechanism at the electrode/electrolyte interface and do not involve the bulk of the material as discussed in Section 2.1.1. The capacitance of these materials predominantly depends on the electrochemically accessible surface area. Various factors, such as specific surface area, electrical conductivity, surface functionality, and pore size, volume, and distribution, can significantly influence the electrochemical performance of these materials [40]–[42]. Initial research focused on increasing the pore volume of carbon materials for developing high surface area materials. However, the capacitance of these materials increased to a limited extent because not all micropores are electrochemically accessible to form a double layer. Thus, apart from the surface area, pore size and distribution should also be optimized to achieve high performance for carbon materials.

Widely studied carbon-based materials are activated carbon, CNTs, and graphene. Activated carbon is the most commonly used carbon material for supercapacitor applications due to its large surface area, low cost, and good electrical conductivity. They are derived via physical or chemical activation of carbonaceous materials such as coal, wood, coconut shells, nutshells, polymers. Physical activation involves thermal treatment at high temperatures using oxidizing/reducing agents, and chemical treatment involves chemical agents such as potash or metal chlorides [35]. Various studies have come up with different activation procedures to increase the surface area and pore volume of the activated carbon. However, excessive activation can lead to a very high pore volume, which reduces material density and conductivity, and therefore, lowers their power density. Currently, studies related to these materials focus on controlling their pore size distribution and pore structure [43].

CNTs are another important electrode material for EDLCs because of their intrinsic flexibility, light-weight, electrical conductivity, and high surface area [44]. However, factors such as micropores, purity of the material, and internal resistance limit their electrochemical performance [27], [29]. Graphene sheets are prominent electrode material due to their high cyclic life, excellent physiochemical properties, and improved capacity [45]. Graphene exhibits various advantages such as good flexibility, high specific surface area (2630 m^2/g), good electrical conductivity, and processability [46]–[48]. They have a surface area similar to that of activated carbon (up to 3000 m^2/g) [49], and higher than CNTs (1600 m^2/g) [44]. However, van der Waals forces between adjacent sheets cause them to restack, lowering their surface area and hence, their energy density.

2.2.2 Metal oxide-based materials

Metal oxide-based supercapacitor electrode materials exhibit high specific capacitance, and hence, can provide higher energy density than carbon-based materials. These materials not only store energy via electrochemical double layer formation but also exhibit pseudocapacitive behavior, where reversible faradaic reactions occur within an appropriate potential window, as explained in Section 2.1.2. For a metal oxide to be applicable for supercapacitor application, it must be electronically conductive, must have multiple oxidation states that can coexist without causing irreversible phase changes, and its oxide lattice should allow intercalation of protons in and out during reduction and oxidation, respectively [27]. Some of the metal oxides used for supercapacitor electrode fabrication are ruthenium oxide (RuO_2) [50], manganese oxide (MnO_2) [51], cobalt oxide (Co_3O_4) [52], nickel oxide (NiO) [53]–[55]. Ruthenium and manganese oxides are the most popular pseudocapacitive materials [29].

RuO_2 is the most extensively studied pseudocapacitive material due to its highly reversible redox reactions, wide potential range, three oxidation states accessible within a voltage window of 1.2 V, high specific capacitance, and long cycle life [27], [56]. In RuO_2 electrodes, the majority charge storage occurs through the pseudocapacitance mechanism, with only 10% of charge accumulated via double layer formation [29]. Supercapacitors using amorphous and hydrous RuO_2 as an active material exhibit high specific capacitance. However, this metal oxide has a very high cost and is toxic to the environment. Hence, researchers have investigated many alternative metal oxides. One such oxide is MnO_2 that presents advantages such as low cost, low toxicity, and high theoretical capacitance. However, low surface area, dissolution problem, and low conductivity limit the performance of the material [27].

Metal oxides generally have lower conductivity, which in turn lowers the specific capacitance of the material. Even though they have better electrochemical stability than conductive polymers, they suffer from issues such as limited surface area, high cost and low conductivity [15].

2.2.3 Conductive polymer-based materials

Conductive polymers consisting of conjugated double bonds, are semiconducting in the neutral state but become conductive upon doping of these polymer networks. They store charges via the pseudocapacitance mechanism when used as a supercapacitor electrode. When oxidation occurs, ions from electrolyte transfer to the polymer backbone. When reduction takes place, the ions are released back into the electrolyte. Since the redox reactions are not limited to the surface but also involve the entire polymer network, therefore, these materials grant higher capacitance than metal oxides. Thus, conductive polymers have high conductivity, flexibility, specific capacitance, and

energy density, and low cost compared to metal oxides [43]. Therefore, they are extensively being studied for supercapacitor applications.

The most popularly investigated conductive polymers for application in supercapacitor electrodes are PANI, PPy, and their derivatives. These conductive polymers can be synthesized via chemical or electrochemical polymerization of the relevant monomer, where each method has its advantages and disadvantages. Their conductivity can be tuned up to 10^4 S/cm using different doping agents and doping levels [57], [58]. Their electrochemical properties depend on the synthesis conditions such as temperature, doping level, solvent, current density, reaction duration, pH of the electrolyte during the polymerization process [19], [59]. The synthesis conditions can affect the effective surface area of polymer films, which in turn can lower the performance of the conductive polymer-based supercapacitors.

Although conductive polymers can provide supercapacitors with good energy density, they suffer from poor cycling stability due to swelling and shrinking of polymer chains during charging-discharging cycles. The structural degradation of conductive polymers during fast charging-discharging cycles, in turn, lowers their electrochemical performance significantly. Therefore, researchers are focusing on modifying the structure design of the electrode to increase the stability of these polymers [43]. Conductive polymers are often combined with carbon-based materials, using different electrode configurations, to increase their stability and hence, improve their life cycle [13].

2.3 Characterization

2.3.1 Cyclic Voltammetry

Cyclic Voltammetry (CV) is a widely used method to measure the electrochemical performance of energy storage devices. A potentiostat or a battery tester can generate CV scans. In this method, cyclic voltammograms obtained are used to calculate the specific/areal capacitance of material in a three-electrode setup, and specific/areal capacitance of a supercapacitor in a two-electrode setup. It can also be used to determine cycling stability. During a CV scan, a linearly changing potential is applied across two electrodes to record instantaneous current passing between the working electrode and the counter electrode. The potential range used for CV is called a potential window and the rate of change in potential with respect to time is called scan rate. The CV is an important technique used in electrochemistry since it can probe a species to undergo forward as well as reverse scan within a few seconds.

The specific and areal capacitance of a supercapacitor electrode material can be evaluated from CV data, at a given scan rate, using Equation 4 and 5 respectively.

$$C_s = \frac{1}{mv\Delta V}\int_{V_1}^{V_2} idV \tag{4}$$

$$C_A = \frac{1}{Av\Delta V}\int_{V_1}^{V_2} idV \tag{5}$$

Where,

C_S is specific capacitance in F/g

m is mass loading of the active material in the electrode in g

v is the scan rate of CV in V/s

ΔV is the potential window of CV curve in V (V_2-V_1)

i is the current density in mA/g or mA/cm^2

C_A is areal capacitance in F/cm^2

A is the area of electrode material in cm^2

The potential scan rate can be used to analyze electrode kinetics in a supercapacitor. The increase in scan rate of CV scan results in a decrease in the calculated areal capacitance due to the reduction in efficiency of ion diffusion at high scan rates. At lower scan rates, ions in electrolyte have enough time to penetrate the pores of the electrode material, resulting in high capacitance value. The information provided by CV curves, such as the shape of CV or relationship between scan rates and their corresponding capacitances, makes it possible to detect whether the material exhibits EDLC or pseudocapacitive behavior during the charging-discharging process [35].

2.3.2 Galvanostatic Charging Discharging

Galvanostatic Charging/ Discharging (GCD) is another commonly used technique for characterizing electrochemical capacitors to evaluate performance parameters such as capacitance, ESR, cycle stability, energy density, and power density. It can be used in three-electrode or two-electrode systems. It involves repetitive cycles of charging and discharging of the device where charging occurs at a constant current and discharging takes place in a specific time or voltage range. Cell voltage is recorded with respect to time during charging-discharging cycles. Equation 6 and 7 can be used to calculate the specific and areal capacitance from the GCD cycle, respectively.

$$C_s = \frac{i_{d,S}\Delta t}{mV} \quad (6)$$

$$C_A = \frac{i_{d,A}\Delta t}{AV} \quad (7)$$

Where,

C_s is the specific capacitance in F/g

$i_{d,S}$ is the current density during charging-discharging cycles in A/g

Δt is the time required for cell to completely discharge in s

m is mass loading of active material in g

V is the maximum voltage of the potential window in V

C_A is the areal capacitance in F/cm^2

$i_{d,A}$ is the current density during charging-discharging cycles in A/cm^2

A is the area of the electrode

The energy and power densities of a supercapacitor device can be calculated from GCD data using Equation 8 and 9.

$$E = \frac{CV^2}{(2 \cdot 3600)} \quad (8)$$

$$P = \frac{E \times 3600}{\Delta t} \quad (9)$$

Where,

E is volumetric energy density in Wh/cm^2

C is the volumetric capacitance of supercapacitor device in F/cm^2

V is the voltage window in GCD

P is volumetric power density in W/cm^2

Δt is the discharge time in s

2.3.3 Electrochemical Impedance Spectroscopy

Electrochemical Impedance Spectroscopy technique assesses the capacitive performance of an electrode material for an energy storage device, and to determine the contribution of the electrodes and electrolytic processes in the electrical performance of the material. EIS data is collected at the open-circuit potential by applying a small voltage amplitude of 5 to 10 mV over a wide frequency range of 30 mHz to 200 kHz. Using the EIS data Nyquist plot can be obtained, which graphically represents the imaginary part of impedance, Z", vs real part of impedance, Z'. This plot consists of three regions: (1) a semicircle at high frequency ($>10^4$Hz) that presents the interface resistance (2) a high to medium frequency range (10^4 to 1 Hz) showing pseudo-charge or charge transfer resistance (3) a vertical line along the imaginary axis at low frequency indicating capacitive behavior [60]. The charge transfer resistance can be determined by calculating the semicircle diameter in the plot. Thus, EIS is an important tool in assessing the electrical performance of an energy storage device.

2.3.4 Four-Point Probe Method

The four-point probe is a commonly used method for the measurement of thin film conductivity using superficial contacts. This method involves placing four-point probes collinearly and with equal spacing between them on the surface of a sample. Figure 4 shows the four-point probe setup where the current passes through outer probes 1 and 4, and the potential measured between probes

2 and 3. In this method, the error contribution from electrical contacts is absent since the current and voltage leads are separated [61]. The conductivity of a film can be measured using equation 10.

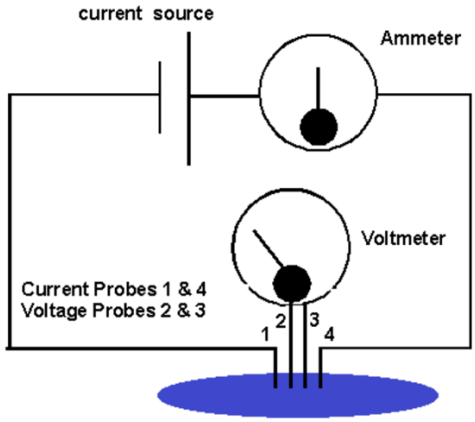

Figure 4: Schematic for Four-Point Probe Method (Reproduced from reference [62]).

$$\sigma = \left(\frac{1}{1000\ 2\pi d}\right)\left(\frac{I}{V}\right) \tag{10}$$

Where,

σ is the electrical conductivity in S/cm

V is the potential drop in mV

I is current in μA

d is the spacing between two probes in cm

In the case of thin metallic films, the length of the film is much longer than its thickness. The electrical conductivity of such thin films is determined using equation 11.

$$\sigma_t = \frac{ln2}{1000\ \pi t}\left(\frac{I}{V}\right) \tag{11}$$

Where,

σ_t is the electrical conductivity of thin films in S/cm

V is the potential drop in mV

I is the current in μA

t is the thickness of the thin film in cm

2.4 Flexible Supercapacitors

With increased market adoption, flexible electronic devices are becoming an essential component in day-to-day activity. Portable and wearable electronic devices are being rapidly developed in various fields such as foldable electronic display, high-performance sportswear, new classes of potable power, military and implantable medical equipment, smartphones. This has led to an increase in the demand for cheap, flexible and lightweight energy storage devices with high energy density [9], [63], [64]. Traditional energy storage devices, such as batteries and button supercapacitors, cannot provide high power needed without becoming too heavy, bulky, or rigid [12]. Their rigid structure inhibits their performance under bending conditions, preventing them from being incorporated in the flexible electronic devices. The traditional electrode fabrication processes involve use of main active material, insulative binders and conductive additives to prepare a slurry. These binders and additives inhibit the electrochemical performance of supercapacitors and batteries as they constitute 20-30% of the slurry, creating dead volume in the electrode since they make a negligible contribution to the overall electrochemical performance [65]. The commercial supercapacitors use activated carbon as the active material that has a rigid microstructure, making the electrode material inflexible. Upon bending such electrodes, the active material can crack or peel off from the current collector irreversibly [66]. Also, the use of liquid electrolyte in conventional supercapacitors pose a safety concern as the electrolyte can leak when

the energy storage device is deformed. Thus, conventional supercapacitors cannot be well integrated into flexible portable and wearable electronic devices due to their inflexibility, bulkiness, and safety concerns related to leakage of liquid electrolyte [67].

To overcome these challenges faced by traditional energy storage devices, researchers have been focusing on research and development of flexible and safe energy storage devices such as flexible supercapacitors to meet requirements of modern wearable electronics and environmental concerns [63]. Flexible quasi-solid-state supercapacitors have attracted a lot of attention for use in flexible electronics due to their rapid charge/discharge processes, long cycle life, high power density, and flexibility [23]. In fact, in the past ten years (2009-2019), there has been an increasing number of research studies conducted on flexible supercapacitors in the electrochemical field, as shown in Figure 5 (source Web of Science; search time: 18, Jan, 2020), indicating a growing demand for developing such devices.

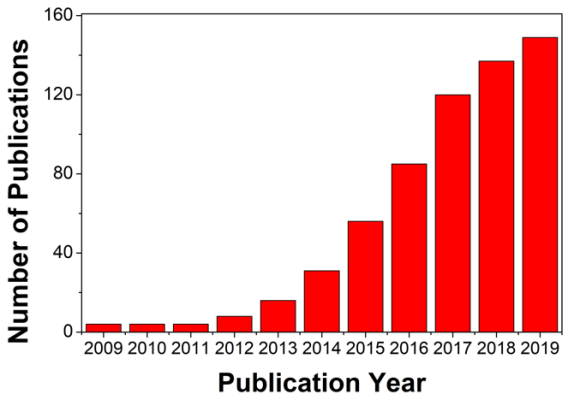

Figure 5: Number of flexible supercapacitors-based research studies conducted over past 10 years (source Web of Science; search time: 18, Jan. 2020).

The main challenge for flexible supercapacitors is to maintain its electrochemical performance under continuous mechanical deformation such as bending, even for long-time cycles. They also require electrodes designed without the use of binding agents or conductive additives while

exhibiting high electrochemical performance. To deal with the safety concern related to leakage of liquid electrolytes, gel electrolytes are a suitable alternative for obtaining a supercapacitor device in a quasi-solid state. The gel electrolyte consists of a liquid electrolyte dissolved in a polymer matrix such as polyvinyl alcohol (PVA). Thus, to obtain a flexible quasi-solid-state supercapacitor device, electrode material must be designed and fabricated such that it exhibits high mechanical flexibility, energy density, power density as well as cycling stability, and it must be used with a compatible gel electrolyte and a separator.

The electrode material is a key component in a flexible supercapacitor design that can provide the device with lightweight, high conductivity, flexibility, and high-power density. An electrode material is composed of active material that participates is supercapacitor mechanisms to store charges and flexible substrate material generally serves as a current collector in the supercapacitor design. Many different kinds of flexible materials such as metallic yarns or wire meshes or foils ([23], [68]), papers ([69], [70]), fibers/yarns ([71], [72]), polymeric films ([73], [74]) and fabrics ([12], [75]) have been used to serve as substrate in the electrode materials for flexible supercapacitors. Each type of substrate has its advantages and disadvantages. Substrates that are electrically insulating in nature need to be made conductive by either depositing metal coatings onto them or, by carbonizing in cases of carbon-based fabrics/fibers such as cotton. However, the carbonized cotton fabric has been reported to possess low specific capacitance, and the carbonization process might reduce the mechanical strength of the cotton fabric, decreasing its flexibility [9].

2.4.1 Types of Substrates

Although freestanding active material films can also be used as the electrode material for a flexible supercapacitor, they tend to be fragile and can flake off during prolonged bending conditions [4]. To deliver mechanical flexibility to the active material, for flexible supercapacitors, different types of substrates can be used as a support. The mechanical properties of these substrate materials have a crucial role in the electrode fabrication of a flexible supercapacitor device. Additionally, the substrate material can serve as a current collector if it is either inherently conductive or made conductive by processing. Some of the commonly used substrates are flexible metal substrates stainless-steel wire meshes/foils (SSWM/foils), carbon-based and/or porous electrodes (carbonized textile fabric, carbon cloth), and metal-coated textile fabrics.

Many metal substrates such as copper foil [76], nickel foam [77], aluminum foil [68], SSWM or foils [23], [78], have been used as supercapacitor substrate. These metallic substrates have high conductivity and mechanical strength, making them an interesting choice for flexible supercapacitors. In the case of stainless-steel based substrates, a study has shown that the stainless-steel foil has several disadvantages over SSWM for depositing active material such as conductive polymers. Thick films of polymer tend to form on these foils due to which polymer chains undergo huge volume change as a result of their swelling/shrinking under repetitive charging-discharging cycles [79]. The conductive polymers also have poor adhesion to stainless steel foil compared to SSWM. Many studies have used SSWM as a substrate material for flexible supercapacitors. In one study, PPy was electrochemically polymerized onto SSWM using sodium toluenesulfate and p-toluenesulfonic acid as doping agents. The specific capacitance of supercapacitor fabricated using this electrode material could effectively be enhanced from 170 F/g to 214 F/g at a specific current

of 0.5 A/g by applying a 20% strain [78]. Another study involved electrochemical co-deposition of carbon quantum dots and PPy onto the SSWM substrate. The all-solid-state supercapacitor, fabricated using these electrodes with PVA/LiCl gel electrolyte, exhibited areal capacitance of 315 mF/cm^2 at a current density of 0.2 mA/cm^2 and capacitance retention of 85.7% after 2000 cycles [23].

Textile materials have gained a great interest of researchers for application in supercapacitor substrate. Carbon cloth is the most popularly used substrate for flexible supercapacitor applications. It is an inexpensive, conducting textile with high surface area, made from woven bundles of carbon fibers [80]. It is highly flexible with excellent strength [81]. A study reported a one-step spray technique for fabricating flexible electrodes using poly(3,4-ethylene dioxythiophene) polystyrene sulfonate (PEDOT:PSS), reduced graphene oxide (rGO), and carbon cloth [82]. Treatment of carbon cloth/PEDOT:PSS/rGO electrodes with H_3PO_4 resulted in a specific capacitance of 170 F/g at 10 mV/s, and an excellent cyclic and bending stability. After 2000 cycles, 100% capacitance retention was obtained, and 95% capacitance was retained under bending condition. Another study prepared nitrogen-doped graphene-enhanced polyacrylic acid/polyaniline composites deposited on carbon cloth [81]. A symmetric supercapacitor fabricated with 20 wt% PANI carbon cloth electrodes has a high specific capacitance of 68F/g at 1 A/g and retains full capacitance under large bending angles. They also exhibit good cycling stability, with 83.2% capacitance retention, after 2000 cycles. One study sequentially electrodeposited MnO_2 and PPy on carbon cloth to obtain flexible electrodes that possessed high specific capacitance of 325 F/g at a current density of 0.2 A/g and 70% capacitance retention at a high current density of 5 A/g after 1000 cycles [22]. Carbonized fabrics are another carbon-based

textile material used as supercapacitor electrodes. One study utilized such carbonized cotton fabric coated with electrochemically polymerized PPy to develop supercapacitor electrodes with high areal capacitance of 3596 mF/cm^2 at a current density of 2 mA/cm^2 and high stability with capacitance retention of 96.5% after 4000 cycles. However, it retained only 75.6 % capacitance after 200 bending cycles [9].

Metal coated textile fabrics have also gained attention in recent years [83]. The metal coating provides the fabric with an electrical conductivity that allows it to act as a current collector in the supercapacitor assembly. The metal coating can also provide them with higher tensile strength [83]. Metals like nickel, copper, and silver are commonly coated on textile fabrics to make them conductive. A study reported the use of nickel-coated cotton fabric deposited with alternative layers of rGO and MWCNT [43]. All-solid-state supercapacitor device fabricated using these electrodes displayed EDLC behavior and was able to reach a high performance of 2.7 mF/cm^2 at 20 mA/cm^2 and 0 capacitive decay after 10000 bending tests. Another study used nickel coated polyester fabric deposited with Ni-metal organic framework (MOF) and rGO that reached areal capacitance of 260 mF/cm^2 at a current density of 2 mA/cm^2 [84]. Thus, metal-coated textile fabrics are a good choice as a substrate for the supercapacitor electrode.

It is important to compare these substrate materials using the same active materials, with so many choices available for substrates of flexible supercapacitor devices. It is also important to compare various properties of flexible substrates such as conductivity, wettability, structure, and surface morphology that can affect the morphology and electrochemical properties of the resulting electrodes. Conductivity is an important property since high conductivity ensures that the material

acts as a good current collector by efficiently transporting electrons to external load. In the deposition methods involving electrochemical techniques, good conductivity can influence the growth rate of polymerization. A higher conductivity increases the efficiency of electrochemical polymerization [85]. The good wettability of material towards water can aid in the deposition of active material where aqueous solvents are involved. The structure and surface morphology of the substrate is another important factor since they can, in turn, affect the surface morphology of the active material deposited on them. Comparing these properties of substrates as well as electrochemical properties of the respective electrodes or full cells will allow a better understanding of the role of substrate material in the overall electrochemical performance of a supercapacitor.

2.5 Conductive Polymers

2.5.1 Introduction to Polypyrrole

Owing to the poor cycle life and high cost of transition metal oxides electrode, and lower capacitance of carbon-based nanomaterials electrode, conductive polymers have gained a lot of attention for supercapacitor application [23]. Conductive polymers, such as PANI, PPy, and polythiophene, are semiconducting polymers with double bond conjugation, that exhibit electronic properties upon doping, in their oxidized or reduced forms (Figure 6). These polymers are conductive due to the presence of double bond conjugation that allows electrons to freely move within the physical limit of the polymer chain. Conductive polymers exhibit pseudocapacitive behavior and hold advantages such as inherent flexible polymeric nature, lower cost, and higher conductivity than metal oxides. Due to such advantages, there has been an increasing number of

publications on conductive polymer-based flexible supercapacitors over the past ten years, as shown in Figure 7.

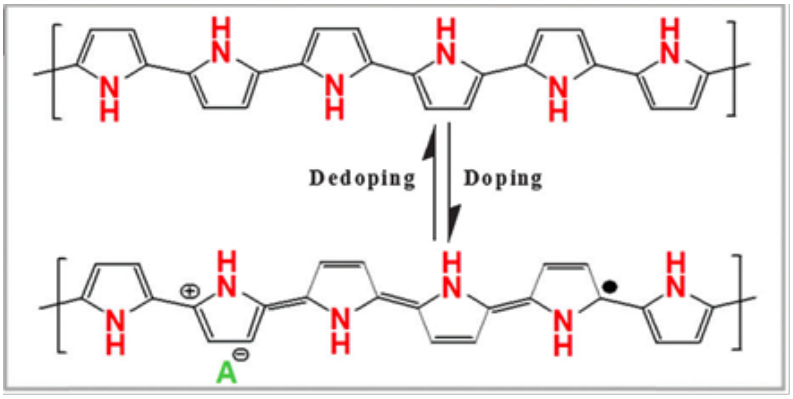

Figure 6: Oxidation (Doping) and Reduction (Dedoping) of Polypyrrole (Reproduced from reference [86]).

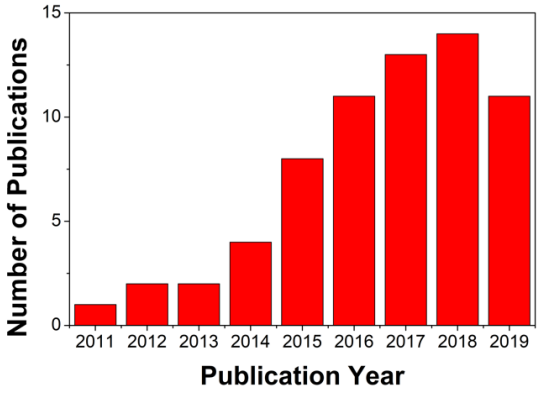

Figure 7: Number of publications on conductive polymer based flexible supercapacitors over past 10 years (source Web of Science; search time: 18, Jan, 2020).

Many conductive polymers have been used for supercapacitor electrodes, out of which PPy has been most extensively studied polymer due to its high conductivity ranging from 0.3 to 500 S/cm [19], [86] and superior flexibility compared to polyaniline and polythiophene [15], [86]. They also have good redox properties, low cost, good thermal and chemical stability, and simple synthesis methods [1], [87]. Its properties depend on synthesis conditions such as type of dopant, deposition time in case of electrochemical polymerization or reaction time in case of chemical oxidation, the

ratio between dopant and monomer, and type of electrolyte used. It can be easily synthesized via electrochemical or chemical oxidation methods due to its commercially available, water-soluble, and easily oxidizable monomer. Each synthesis method has its own advantages and disadvantages.

The chemical oxidation procedure involves the addition of pyrrole monomer in a solvent containing oxidant and doping agents under the desired temperature. PPy can be obtained in the powder form using the filtration method. The reaction duration and temperature can be tuned depending on the desired end property. Different oxidizing agents such as $FeCl_3$, ammonium persulfate, and doping agents such as phytic acid, p-toluenesulfonic acid, 1,5-naphthalene disulfonic acid can be used [1], [19]. Water has been reported to be the best solvent for polymerization to achieve the desired conductivity [19]. During chemical polymerization, when the polymer matrix acquires a positive charge, to maintain the electroneutrality, counterions are incorporated into the matrix from the reaction solution. These counterions are usually the anions of chemically oxidized or reduced products of the oxidant.

This polymerization method is useful for synthesizing dispersed PPy particles of varying size, ranging from several nanometers to several micrometers, in an aqueous solvent, as well as conductive composites. Chemical polymerization has the advantage of being fast and simple. It allows the production of bulk quantities in aqueous or non-aqueous solution and does not require any special equipment [88]. However, this method provides a limited range of conducting segments in the polymer due to the limitation in the number of counterions that can be incorporated. Also, PPy synthesized by conventional polymerization methods is insoluble in common solvents due to strong inter-chain interactions. Therefore, the chemical polymerization

method is not suitable for flexible supercapacitor applications where uniform and strong deposition of a polymer film on a substrate is desirable.

The disadvantages of the chemical polymerization process can be overcome by using the electrochemical polymerization method. This method involves oxidation of monomer directly at the surface of an electrode by application of an anodic potential. This method directly synthesizes the polymer in a doped state. The monomer is first dissolved in the desired solvent using a particular doping agent. Subsequently, two electrodes are immersed in this solution, and potential is applied to cause oxidation of monomer. The cationic radicals generated form a dimer using the C-C coupling mechanism [86]. The electropolymerization process can be performed using cyclic voltammetry, galvanostatic (constant current) or potentiostatic (constant potential) methods. In case of potentiostatic method, oligomeric products are obtained with subsequent reactions since the oxidation potential of dimers is 0.2 V (vs Ag/AgCl), much lower than 0.8 V (vs Ag/AgCl) for the monomers [19], [89], [90]. Thus, formation and oxidation of polymer occur simultaneously in this method, and counterions are incorporated in the polymer matrix [91]. As the molecular weight of oligomers increases, they become increasingly insoluble in the solvent and hence, deposit on the electrically conductive anode material [91].

The properties of electrochemically polymerized PPy films can alter with the variation of substrate material, solvent, doping agent type and concentration, and electrode potential/current density. The main advantage of this process is that the thin PPy films can be deposited directly on to the material, and the film thickness can be controlled using the deposition time [19]. The film quality depends on factors such as the concentration of monomer and electrolyte, solvent, applied

potential, temperature, pH, and properties of substrate material. For example, the polymerization rate was found to decrease with an increase in pH of the medium. The polymerization rate lowered because, in alkaline and neutral solutions, the cation radicals degenerated by PPy oxidation get deprotonated to form neutral radicals [92]. Absence of water in the solvent can also result in poorly adhering, non-uniform films and increasing the amount can improve adherence [93]. Properties of a substrate can impact the morphology of the polymer film. A substrate with high electrical conductivity experience high rate of electrochemical polymerization. This leads to formation of large number of nucleation sites that grow into clusters as a result of a high growth rate. Thus, use of highly conductive substrates increases the efficiency of electrochemical polymerization and result in polymer films with granular and porous morphology [85].

The major drawback of electrochemical polymerization process is that it is difficult to optimize all the parameters affecting film properties in a single experiment [19]. Also, this polymerization process is difficult to scale up for mass production.

Overall, the films obtained though electrochemical polymerization provides good conductivity and adherence to the electrode surface. In the case of flexible supercapacitors, such strongly adhering films are desirable to maintain their electrochemical performance under bending conditions. However, only limited techniques are available to characterize these PPy films.

2.5.2 Polypyrrole Based Flexible Supercapacitors

PPy polymer is the most extensively studied material for its application in the electrodes for batteries and supercapacitors. Depending on the synthesis process, PPy based electrodes have been

reported to exhibit high specific capacitance in the range of 500 to 3400 F/g. Their specific capacitance is comparable to that of the pseudocapacitive metal oxides and significantly larger than that of carbon-based electrodes [94]. PPy has gained popularity as a highly researched conductive polymer for applications in high-performance flexible supercapacitors due to their electrochemical reversibility, electrical conductivity, a fast charge-discharge mechanism, and the wide potential window [18].

Yuan et al. used a simple soak and polymerization process to fabricate PPy coated paper as a flexible electrode that exhibited constant conductivity after 100 bending cycles [95]. However, this material has not been reported to have achieved high electrochemical performance yet. Another study reported the synthesis of PPy coated nylon fabric for supercapacitor applications [17]. This conductive textile endured 1000 stretching cycles under 100% strain while retaining its electrical conductivity and electrochemical properties, providing a highly stretchable supercapacitor electrode for use in wearable electronics. However, the cycling stability achieved was lower in terms of practical application.

Like most of the conductive polymers, PPy suffers from poor cycling stability performance due to swelling and shrinking as well as counterion drain effect, during the charging/discharging process [94], [96]. When PPy undergoes oxidation (Figure 6), positively charged nitrogen groups are generated on the polymer chains that are neutralized by diffusion of counterions from the electrolyte into the polymer backbone, making PPy swell. Whereas, upon reduction, injected electrons neutralize the polarons, and counterions diffuse back into the electrolyte, causing PPy chains to shrink. With repeated cycles of oxidation-reduction, PPy experiences structural

pulverization that ultimately deteriorates its electrochemical performance. In the counterion drain effect, fewer ions can dope back into the PPy matrix after repeated cycling, due to irreversible insertion/extrusion of counterions [96]. This results in a reduction of electrical conductivity of PPy, which in turn causes cycling instability. The capacitance or cycling stability can also be reduced by dense films of PPy on a current collector since these films decrease the accessibility of dopants to the active sites in the interior region of the polymer matrix [15].

With different factors limiting the electrochemical performance of PPy, researchers have adopted many different approaches. To improve the mechanical stability of PPy based electrodes, flexible current collectors are utilized. To reduce internal resistance and improve charge/ionic transport, direct synthesis of active material is performed without any use of binders. For improving the capacitance and cycling stability of PPy based electrodes, researchers commonly combine PPy with other nanomaterials to obtain composites with enhanced properties [1]. A study reported fabrication of PPy and carbon nanotube-based electrodes for application in high-performance stretchable supercapacitor yarn resulted in a high areal capacitance of 69 mF/cm^2 and reasonable cycling stability [97]. Another study electropolymerized PPy on partially exfoliated graphene to improve its cycling stability [98]. The mechanical flexibility and porosity of graphene sheets provided large elastic buffer space for swelling and shrinking of the PPy matrix during the charging-discharging cycle. This study reported 82% capacitance retention (of the original capacitance of 249 F/g) after 1000 cycles with no cracks or crumbles on the electrodes. Another strategy for improving the cycling stability of PPy supercapacitor electrodes involved deposition of thin carbonaceous shell onto the polymer surface, which resulted in capacitance retention of 85% after 10000 cycles [94]. The carbonaceous shell acts as a buffering layer that alleviates the

structural changes during charging-discharging cycles, and after the pulverization occurs, the flexibility of the shell allows it to serve as a bridge to connect the broken fragments and hence, maintains the mechanical as well as electrochemical stability. The thickness of this shell also plays a crucial role where a thicker shell decreases the capacitance by preventing penetration and reaction of electrolyte ions with PPy chains. Sun et. al. prepared carbonized cotton fabric deposited with PPy for flexible binder-free supercapacitor application that exhibited a high areal capacitance of 500.06 mF/cm^2 at a current density of 2 mA/cm^2, and capacitance retention of 73.6% after 2000 cycles [9]. The porous structure of carbonized cotton provided a large accessible area for PPy loading and enabled conductive pathways for fast electron transfer. Jian et. al. reported a flexible all-solid-state supercapacitor device fabricated by the co-deposition of PPy and carbon quantum dots (CQDs) on an SSWM [23]. This device shows areal capacitance of 315 mF/cm^2 at a current density of 0.2 mA/cm^2, and long cycle life with capacitance retention of 87.5% after 2000 cycles. Thus, combining PPy with other carbon-based nanomaterials is a useful approach in enhancing its cycling stability.

In summary, the performance efficiency of conductive polymers-based supercapacitor highly depends on the interaction between the active electrode material and the current collector. Many different materials have been employed as current collectors for PPy such as carbon cloth, metal-coated textile, SSWM, to name a few. It is necessary to choose a right current collector that can provide mechanical stability to the polymer. As mentioned previously, a common strategy of improving cycling stability of PPy involves forming its composite with carbon-based nanomaterials such as graphene since these composites are capable of providing mechanical support to the polymer that ultimately increases the areal capacitance as well as the cycling

performance of the electrode material [35]. Combining PPy with carbon-based materials also allows to obtain advantages of both EDLC and pseudocapacitance mechanisms. The interaction between these materials changes the surface morphology that, in turn, can vary the charge storage capabilities of resulting composites. Since the charge storage in a supercapacitor depends on the interfacial interactions, it is necessary to maximize the reaction sites at the electrode/electrolyte interface and facilitate efficient ion transport. The design of the electrode configuration should take into account these interfacial interactions to maximize the charge storage capability of the device. Thus, the choice of substrate, the combination of active materials and design of the electrode configuration are crucial for the overall performance of a flexible supercapacitor device.

3.0 Polypyrrole-Graphene-Polypyrrole Sandwich Structure for Supercapacitor Electrode

3.1 Introduction

Over the recent years, portable and wearable electronic devices are being developed at a fast pace for a wide variety of applications like foldable electronic display, military and implantable medical equipment, and new classes of portable power [9]. They are required to be powered using a cheap, flexible and lightweight energy storage device. Conventional energy storage devices are too heavy, bulky, and rigid and impractical for integration into such portable and wearable devices [12]. To meet the customer requirement for flexible energy storage devices, a lot of research is focusing on the development of high performance, flexible quasi-solid-state supercapacitor devices that can exhibit high energy density, high power density and high specific/areal capacitance and cycling stability even under bending conditions. The flexibility of a supercapacitor device depends on the mechanical properties of electrodes, which in turn depends on the properties of the substrate and the active material.

Supercapacitors involve two charge storage mechanisms- electrical double layer mechanism (EDLCs) and pseudocapacitance. Compared to EDLCs, materials exhibiting pseudocapacitance such as metal oxides and conductive polymer possess greater specific/areal capacitance, and hence, higher energy density [15]. Within pseudocapacitors, conductive polymers are cheaper and have higher electrical conductivity, theoretic capacitance and mechanical flexibility [1]. One of the popularly used conductive polymer for flexible supercapacitor electrodes is PPy. Like any conductive polymer, PPy is limited by low cycling stability due to structural pulverization and counterion drain effect during repetitive charging-discharging cycles [96]. One strategy for

improving the cycling stability of PPy supercapacitor electrodes involved deposition of thin carbonaceous shells onto the PPy surface, which resulted in capacitance retention of 85% after 10000 cycles [94]. The carbonaceous shell acted as a buffering layer to alleviate the structural changes during charging-discharging cycles, and the flexibility of the shell allows it to serve as a bridge to connect the broken fragments and maintain the mechanical and electrochemical stability of PPy chains after the pulverization occurs. Shell thickness also played a crucial role since a thicker shell decreased the capacitance by preventing penetration and reaction of electrolyte ions with PPy chains. Another strategy for improving the cycling stability of PPy involves use of flexible substrates. Recent studies have focused on increasing the cycling stability of PPy by addition of high surface area carbon-based materials like graphene in the electrode configuration. Graphene can act as a flexible support material to reduce cycle degradation caused by volume changes during repetitive charging-discharging cycles. Song et. al. electropolymerized PPy on partially exfoliated graphene to improve its cycling stability [98]. The mechanical flexibility and porosity of graphene sheets provided large elastic buffer space for swelling and shrinking of the PPy matrix during the charging-discharging cycle. This study reported 82% capacitance retention (of the original capacitance of 249 F/g) after 1000 cycles with no cracks or crumbles on the electrodes. Li et. al. reported an electrode consisting of PPy/graphene deposited on a polyester fabric that exhibited areal capacitance of 1117 mF/cm^2 at a current density of 1 mA/cm^2 which was 75 times higher than that of the electrode with only graphene-coated on the polyester fabric (15 mF/cm^2) [99]. Another study electrochemically polymerized PPy on carbonized cotton fabric to achieve supercapacitor cells with a large areal capacitance of 500.06 mF/cm^2 at 2 mA/cm^2 current density and 73.7 % capacitance retention after 2000 cycles [9]. All these studies demonstrate that the addition of carbon-based materials such as graphene enhances the

performance of the supercapacitor electrodes and devices. However, there is still some room for improvement, especially for the cycling stability performance of PPy and graphene-based flexible supercapacitors.

The main objective of this section is to assess the role of rGO in enhancement of the electrochemical performance of PPy based electrodes. It discusses the set of experiments conducted for determination of electrode configuration with high electrochemical performance. Different parameters such as drying condition and optimum electrochemical polymerization time are determined using commercially obtained Cu:Ni-PET fabric as the electrode substrate. The electrochemical performance has been assessed in a three-electrode system using CV and EIS methods discussed in Section 2.3.1.

3.2 Experimental Methods and Characterization

3.2.1 Electrode Preparation

GO was synthesized using an improved Hummers' method [100], where a 9:1 mixture of concentrated H_2SO_4/H_3PO_4 (360:40 mL) acids was added to a mixture of graphite flakes (3.0 g) and $KMnO_4$ (18.0 g). The reaction was stirred for 16 h at 50 °C before being cooled by placing it in an ice bath. About 30% H_2O_2 (3 mL) was then added dropwise to the reaction solution. The mixture was then washed with 200 mL of de-ionized water, 200 mL of 30% HCl, and 200 mL of ethanol using centrifugation at 4000 rpm for 1 h. The supernatant was decanted away, and the GO settled at the bottom of the tube were then further washed with de-ionized water till its pH reduced to nearly neutral value and freeze-dried for 3 days to obtained GO flakes. To obtain rGO flakes,

GO flakes were thermally expanded and reduced by placing them in a tube furnace at 1100 °C for 60 seconds under the argon environment [101].

Cu:Ni-PET fabric was used as the substrate material for determining the optimum conditions to obtain high performing electrode configuration. The first layer of PPy was deposited via electrochemical polymerization of pyrrole based on a literature study [9]. Chronoamperometry method was used for this process where a potential of 0.8 V was applied in a three-electrode setup where Cu:Ni-PET fabric of dimensions 2.4x0.6 cm^2 was used as a working electrode, SCE as reference electrode and platinum foil as the counter electrode. The deposition bath consisted of an aqueous solution of 0.3 M p-toluenesulfonic acid (TsOH) as a doping agent and 0.15 M pyrrole monomer. The ratio between TsOH and pyrrole was chosen based on the literature study [9]. The deposition time was varied from 3 min to 20 min to determine the optimum deposition time. The resulting electrode material was rinsed with de-ionized water and dried in a convection oven at 60 °C for 1 hour. The electrode was dip coated with 5 mg/mL of rGO dispersion in 50:50 ratio of water and ethanol for 10 min to deposit rGO flakes onto the first layer of PPy and dried again at 60 °C for 15 min. This process was repeated three times. The second layer of PPy was deposited onto the rGO layer via electrochemical polymerization, similar to the procedure used for the first layer of PPy. The final electrode material with sandwich structure of PPy-rGO-PPy was dried using different methods- convection oven at 60 °C (12 hours), vacuum oven at 110 °C (for 12 hours) and annealing at 150, 180 and 210 °C (for 1 hour, argon environment), to determine an optimum drying method for obtaining high performing supercapacitor electrode material.

3.2.2 Chemical and Structural Characterization

The morphological and structural characteristics of the prepared samples were investigated using a field-emission scanning electron microscope (Quanta FEG-250). A powder X-ray diffractometer (MiniFlex 600, Rigaku) was used with a monochromatized CuK_a radiation source (λ= 0.154178 nm) to record a wide angle (5-85°) X-ray diffraction (XRD).

3.2.3 Electrochemical Characterization

Electrochemical characterization was carried out in a three-electrode configuration using 1M sodium sulfate (Na_2SO_4). PPy-rGO-PPy material deposited on Cu:Ni-PET was used as a working electrode, SCE as a reference electrode and platinum as a counter electrode. The electrochemical properties of electrode material were characterized using cyclic voltammetry (CV) and electrochemical impedance spectroscopy (EIS) on a computer-controlled potentiostat (BioLogic VSP-300). The areal capacitance of electrode material was calculated from CV data (obtained at 10 mV/s scan rate and potential window of -0.8V to 0V) using equation 5 in Section 2.3.1. The EIS was recorded in the frequency range of 10 mHz-100 kHz with a potential amplitude of 5 mV in the three-electrode system.

3.3 Results and Discussion

The supercapacitor electrode designed consisted of a sandwich structure with a layer of rGO deposited between two layers of polypyrrole (PPy-rGO-PPy). Figure 8 shows the schematic illustration for the procedure involved in fabrication of the electrode.

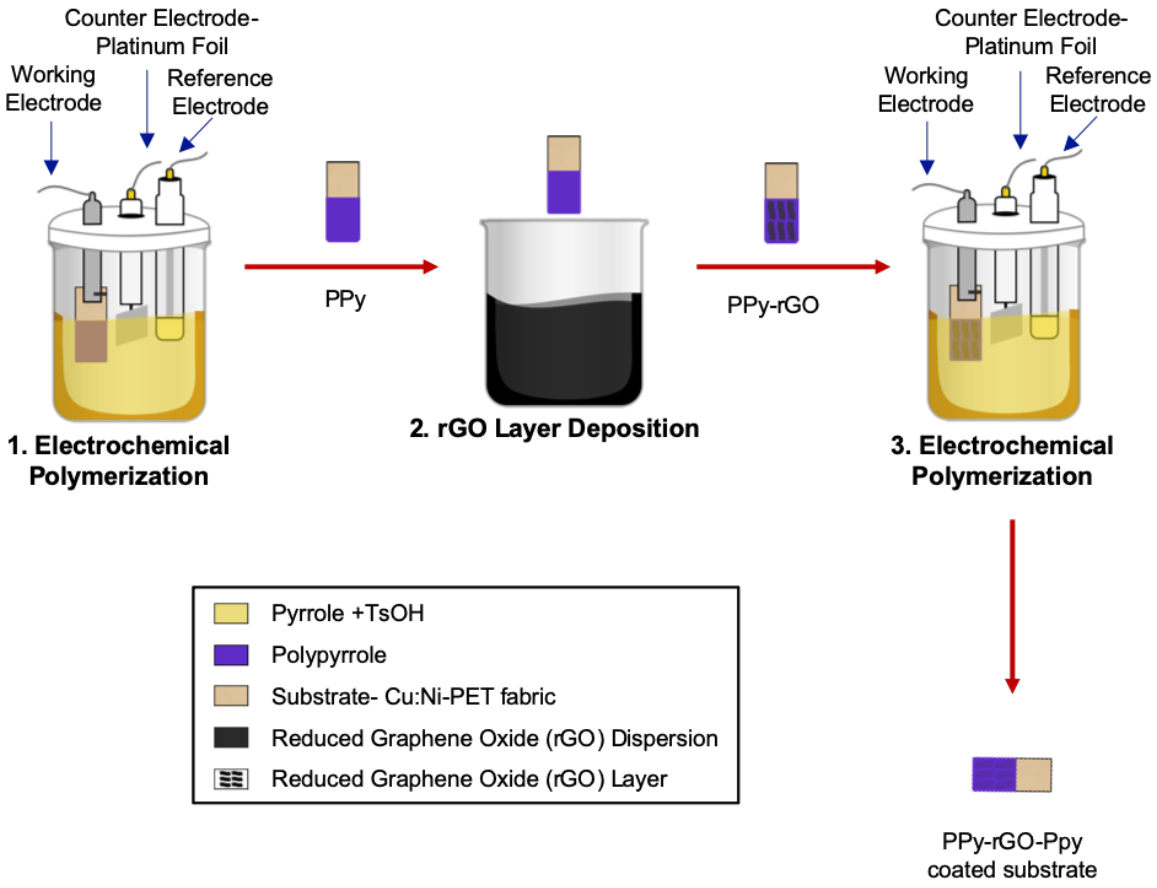

Figure 8: Schematic Illustration for synthesis of PPy-rGO-PPy sandwich structure electrodes.

The commercially obtained Cu:Ni-PET fabric is first coated with PPy using the electrochemical polymerization process. Then, this electrode is dip coated with rGO using the simple dip coating method. The first layer of PPy on Cu:Ni-PET fabric contributes not only as an active material but also as a linker to immobilize rGO via electrostatic interactions and pi-pi interactions on to the conductive fabric [102]. The presence of rGO, in turn, is expected to enhance the stability of the material. GO has more surface functionalities than rGO. However, they suffer from lower electrical conductivity. To obtain rGO, GO is reduced by thermal or chemical reduction methods. The thermally reduced graphene oxides are used in this study instead of chemically reduced graphene oxides because chemical reduction is less efficient. The chemically reduced GO contains

structural defects and a large amount of residual oxygen functionalities that leads to lower conductivity [103]. The second layer of PPy is then deposited onto the electrode using the same electrochemical polymerization process as the first layer and the resulting electrode has polypyrrole-graphene-polypyrrole (PPy-rGO-PPy) sandwich structure.

Figure 9 (a) compares XRD for GO and rGO samples. The representative diffraction peak of GO at 10.2° disappears in the XRD pattern for rGO and a broad peak centered at 26.2° appears indicating exfoliation of graphene. Thermal reduction of GO allows for efficient elimination of oxygenated species from the surface. This result in rGO sheets with a high density of localized electrons that can facilitate strong pi-pi interactions with PPy [104]. Figure 9 (b) compares XRD patterns of black Cu:Ni-PET fabric with the ones coated with PPy and PPy-rGO.

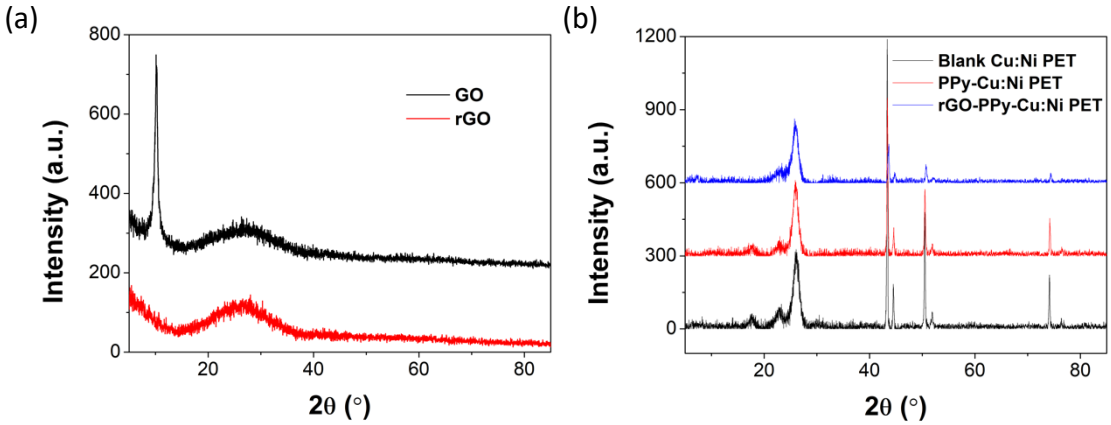

Figure 9: XRD Patterns (a) GO and rGO powder. (b) Blank Cu:Ni-PET substrate, Polypyrrole coated Cu:Ni-PET (PPy-Cu:Ni-PET) and Graphene coated on PPy-Cu:Ni-PET (PPy-rGO-Cu:Ni-PET).

The XRD pattern for blank Cu:Ni-PET fabric shows peaks at 25.9°, 43.6°, 44.6°, 50.5°, 52° and 74.3° where peaks at 43.6°, 50.5° and 74.3° correspond to copper and peaks at 44.6° and 52° correspond to nickel present in the conductive fabric. The reduction in crystallinity can be observed for PPy-Cu:Ni-PET and PPy-rGO-Cu:Ni-PET samples indicating successful deposition of

amorphous PPy polymer films. The peak at 26.6° appears to be broader for PPy-rGO-Cu:Ni-PET compared to PPy-Cu:Ni-PET and blank Cu:Ni-PET, most likely due to deposition of rGO on PPy film.

Surface morphology of the electrode was characterized using a scanning electron microscope (SEM) imaging. The SEM images comparing blank Cu-Ni-PET fabric with the ones coated with PPy, PPy-rGO, and PPy-rGO-PPy are shown in Figure 10 (a). The blank Cu:Ni-PET fabric shows some copper and nickel particles deposited on its smooth surface.

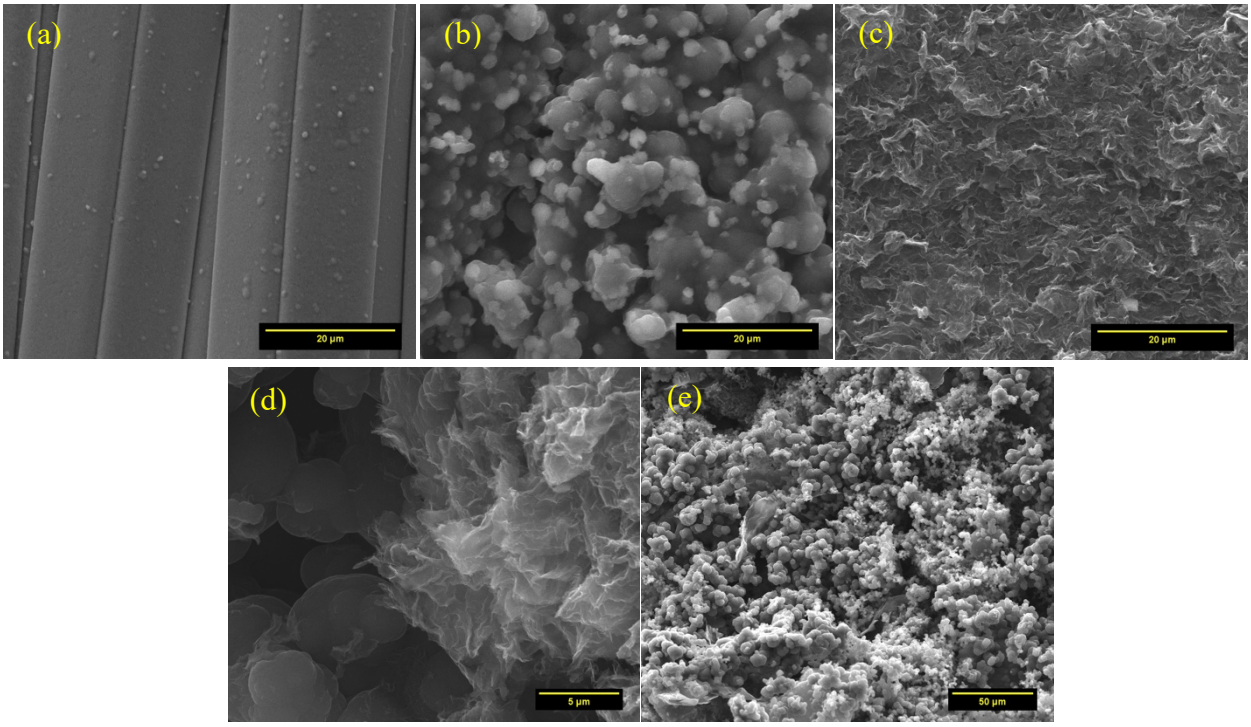

Figure 10: SEM Images of (a) blank Cu:Ni-PET fabric (b) PPy- Cu:Ni-PET (c) rGO-PPy- Cu:Ni-PET at 2000X magnification. (d) SEM image at edge of rGO-PPy- Cu:Ni-PET showing rGO coating on PPy particles at 5000X magnification. (e) SEM image of PPy-rGO-PPy- Cu:Ni-PET.

During electrochemical polymerization, PPy successfully deposits on the fabric and forms a continuous film on the surface of the substrate (Figure 10 (b)). The continuous film of PPy ensures

an increased number of conductive pathways for effective charge transfer. Exfoliated rGO uniformly deposits on the surface of the first layer of PPy, providing high surface area for deposition of the second PPy layer (Figure 10 (c), (d) and (e)). Figure 10 (e) shows the SEM image of PPy-rGO-PPy electrodes. This figure shows that high surface area of rGO layer provides the second layer of PPy with enhanced porous structure.

PPy layers were deposited at different deposition times of 1, 3, 5, 10 and 15 min. All the samples prepared for deposition time determination were dried in the convection oven at 60 °C. In a three-electrode system, CV was performed at 10 mV/s for electrodes fabricated with different deposition times and the optimum time was determined by calculating areal capacitance from the CV data. Electrodes with sandwich design were compared with control samples (PPy-PPy) to investigate the role of graphene layer in the performance enhancement of electrode material. These control samples consist of two separate layers of PPy without rGO layer in the middle. As shown in Figure 11, with an increase in deposition time, the areal capacitance of control samples and electrodes with sandwich structure increases up to 15 min deposition time. Further addition of active material decreases the electrochemical performance since the formation of a thicker and compact PPy film offers resistance to electron transport and diffusion of electrolyte ions in the polymer matrix, preventing participation of all of the active material in the electrochemical activity. Thus, deposition time of 15 min gave highest areal capacitance value and hence, 15 min deposition time was used to form each layer of PPy for all the electrodes.

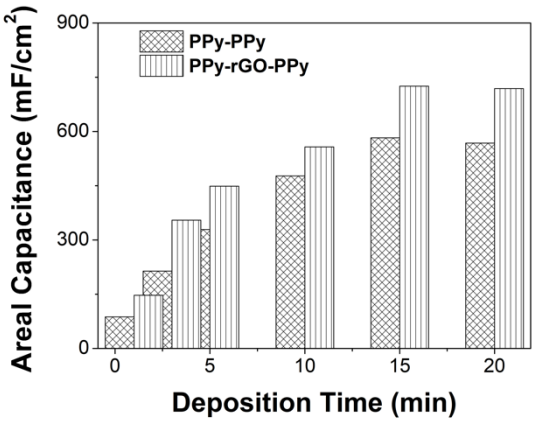

Figure 11: Deposition time for electrochemical polymerization of each layer of PPy in electrode with sandwich configuration (PPy-rGO-PPy) and control samples without rGO layer (PPy-PPy).

For different deposition time, PPy-rGO-PPy structure exhibits larger areal capacitance than control samples, indicating that the layer of rGO enhances the electrochemical performance of the electrode due to its EDLC contribution. At the deposition time of 15 min, PPy-rGO-PPy exhibits larger areal capacitance of 725.3 mF/cm^2 compared to control samples with an areal capacitance of 582.3 mF/cm^2. The larger areal capacitance of PPy-rGO-PPy can be attributed to their sandwich structure that incorporate rGO layer between two PPy films. PPy chains intimately contact the graphene sheets due to the pi-pi interaction between honeycomb lattice and aromatic rings, preventing rGO sheets from re-stacking. The high surface area of graphene provides more surface area for deposition of the second layer of PPy with a porous structure. This porous structure allows for efficient utilization of active materials compared to bulk films that cause resistance to electrolyte ion and electron transport. Thus, addition of rGO layer between two PPy films enhances the areal capacitance of PPy-rGO-PPy electrodes.

Drying method was then determined for PPy-rGO-PPy electrode preparation. Different drying methods used were- 1) simple convection oven drying at 60 °C, 2) vacuum oven drying at 110 °C,

3) annealing at 150 °C, 4) annealing at 180 °C, and 5) annealing at 210 °C. The drying methods are required to ensure proper adherence of active material to Cu:Ni-PET fabric and to remove any water molecules trapped within the polymer matrix that can affect the flow of electrons within the polymer matrix. Figure 12 shows areal capacitance measured from CV scans, at 10 mV/s rate, for each electrode dried using different methods. The cycling stability of these electrodes is also assessed by evaluating capacity retention after 1000 CV cycles at 50 mV/s scan rate.

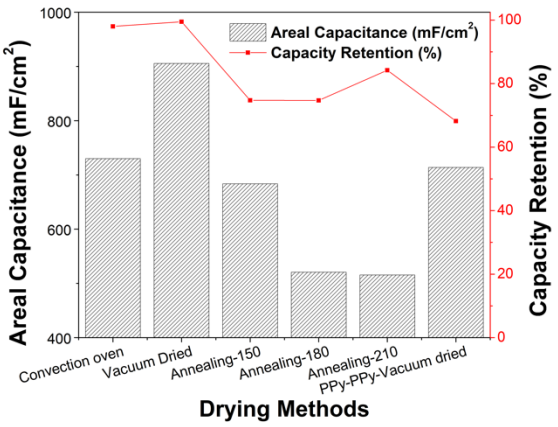

Figure 12: Drying method determination by comparing areal capacitance (mF/cm^2) and capacity retention (%) data.

The areal capacitance and capacity retention for the control sample dried in a vacuum oven at 110 °C is also shown in the figure. The capacity retention determines the cycling stability of the material since it indicates how much capacity is retained by the material after charging and discharging for a certain number of cycles. Out of all these electrodes, PPy-rGO-PPy electrode dried in the vacuum oven at 110 °C shows the best performance with the areal capacitance of 905.4 mF/cm^2. This areal capacitance is larger than 713 mF/cm^2 obtained for PPy-PPy samples dried in the vacuum oven at the same temperature. The high temperature under vacuum allows for complete removal of water molecules without degrading the active materials, which probably results in greater areal capacitance compared to other drying methods. The annealing process was expected

to improve the local ordering of polymer chains. However, degradation in the performance of annealed electrodes is observed. This is probably caused by change in the direct contact between PPy particles due to high temperature during the annealing process [105], [106]. The vacuum dried PPy-rGO-PPy samples also show highest cycling stability of 99.7% after 1000 cycles. High performance of vacuum dried PPy-rGO-PPy samples indicates that drying the samples under vacuum completely removes any water molecules or air bubble trapped within the polymer matrix and allows for proper contact between the three layers of the sandwich structure. The proper contact ensures effective charge transfer during the charging-discharging process, which, in turn, ensures enhancement in the electrochemical performance of the electrode. Thus, vacuum drying was chosen as the drying method to obtain PPy-rGO-PPy electrodes with the highest electrochemical performance.

Figure 13 (a) shows CV scans obtained at different scan rates of 50, 25, 10 and 5 mV/s using PPy-rGO-PPy electrodes dried in a vacuum oven at 110 °C.

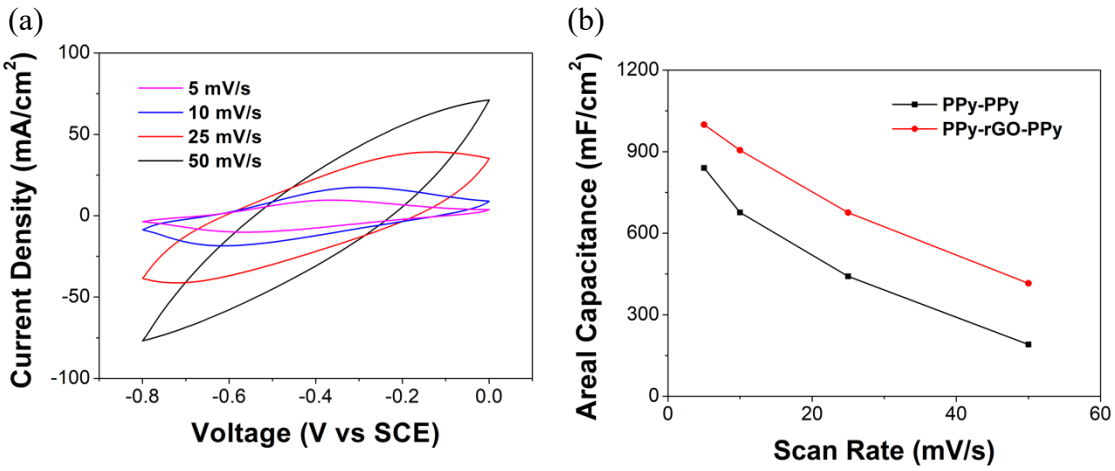

Figure 13: (a) CV curves for electrode with sandwich configuration (PPy-rGO-PPy) at different scan rates. (b) Areal capacitance at different scan rates for electrode with sandwich configuration (PPy-rGO-PPy) and control samples without rGO layer (PPy-PPy).

Figure 13 (b) shows the relationship between the scan rate of CV and its corresponding areal capacitance for PPy-rGO-PPy and PPy-PPy samples. As expected, the areal capacitance decreases with an increase in the scan rate of CV curves since at high scan rate, electrolyte ions do not get enough time to diffuse and utilize all of the active sites for charge storage. This figure also shows that PPy-rGO-PPy electrodes exhibit larger capacitance than PPy-PPy samples at each scan rate. These results demonstrate that graphene layer incorporation between two PPy layers and the porous structure of resulting electrodes enhances the electrochemical performance of the electrode.

EIS test was performed to evaluate the electrical properties of the two electrode materials. The comparison between Nyquist plots of the two electrodes is shown in Figure 14. In the high-frequency region, only one semicircle can be extrapolated for PPy-PPy electrodes. Whereas, PPy-rGO-PPy electrodes have two semicircles, which are most likely due to two interfaces- 1) between the first layer of PPy and rGO, and 2) between rGO and second layer of PPy, in the sandwich configuration of the structure. Thus, the structure of PPy-RGO-PPy electrodes results in two semicircles in the high-frequency region. Internal resistance is obtained using the intersection point between an extrapolated semicircle and the real axis in the high-frequency region. This resistance appears to be quite close for the two electrodes. At low frequency region, the slope of the curve is lower for PPy-PPy electrodes than the one for PPy-rGO-PPy, indicating that PPy-PPy electrodes have higher ion diffusion resistance than the latter electrodes. This demonstrates that the presence of rGO layer and porous morphology of PPy-rGO-PPy electrodes allow for efficient diffusion of ions, utilizing more active material than in the case of bulky films in PPy-PPy electrodes. Thus, incorporation of rGO results in the enhancement of the electrical properties of the electrodes.

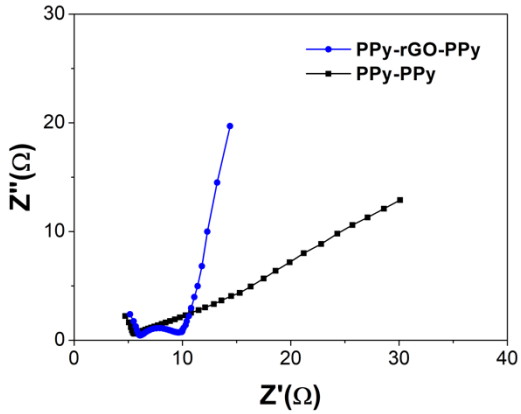

Figure 14: Nyquist plot for PPy-rGO-PPy and PPy-PPy coated on Cu:Ni-PET fabric.

CV scans were performed at 50 mV/s for 1000 cycles to compare the cycle life of PPy-rGO-PPy, PPy-PPy (control sample), and a single layer of PPy electrodes. For all three samples, PPy layer was deposited via electrochemical polymerization using 15 min as deposition time. The capacity retention was calculated using CV data, as shown in Figure 15.

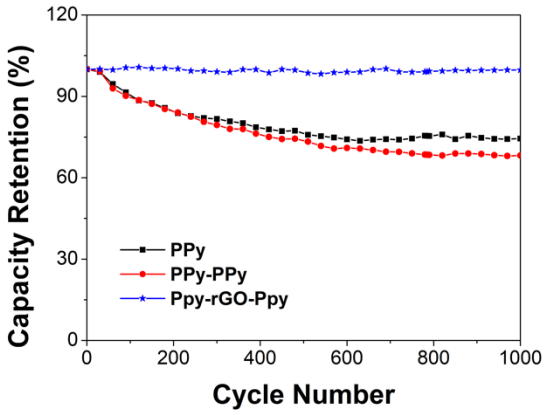

Figure 15: Cycling stability comparison between electrode with sandwich configuration (PPy-rGO-PPy), control samples without rGO layer (PPy-PPy) and single layer of PPy deposited on Cu:Ni-PET fabric for 1000 cycles.

PPy-rGO-PPy electrode gives high capacity retention of 99.7% after 1000 cycles compared to 68.2% and 74.4% for PPy-PPy and PPy electrodes, respectively. The higher capacity retention of

PPy-rGO-PPy electrodes can be attributed to the role of graphene in enhancing the cycling stability of PPy chains. As discussed previously in Section 2.5.2, like any conductive polymer, PPy tends to shrink and swell upon repetitive doping-dedoping of polymer chains during charging-discharging cycles. This leads to poor cyclic stability of PPy as depicted by PPy and PPy-PPy samples in the figure. However, addition of high surface area carbon material can provide mechanical support to polymer chains, increasing cycling stability of the material. In the sandwich structure, the high surface area of rGO provides a greater amount of PPy loading on the substrate. Thus, greater loading of PPy is achieved without formation of a bulk film of polymer. The rGO layer in the middle of two PPy layers can facilitate penetration of electrolyte ions, allowing for utilization of more active sites. The rGO layer can also serve as a physical buffer to suppress structural changes of the first layer of PPy during a charging-discharging process similar to the carbonaceous shells in a study that enhanced the stability of PPy layers [94]. The rGO layer might also hold together the electrode fragments in the first layer by serving as a conductive network. Thus, incorporation of rGO layer in PPy-rGO-PPy electrodes provides them with higher cycling stability compared to PPy-PPy and PPy electrodes.

Further, CV scans for PPy-rGO-PPy electrode were performed for 3000 cycles at 50 mV/s, which resulted in capacity retention of 96.6%, as shown in Figure 16 (a). The figure shows that CV curves retain their shape even after testing over 26 hours (Figure 16 (b)), suggesting that PPy-rGO-PPy electrodes can achieve long term cycling stability without any significant degradation in their electrochemical performance.

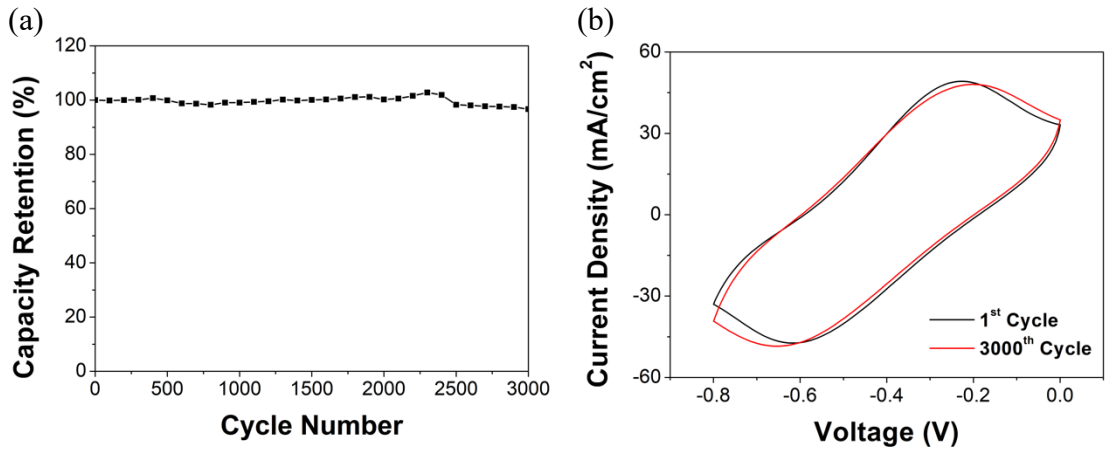

Figure 16: (a) Cycling stability of electrode with sandwich configuration (PPy-rGO-PPy) for 3000 cycles. (b) CV scans at 50 mV/s for first and 3000th cycle for PPy-rGO-PPy electrodes.

In conclusion, PPy and rGO-based electrode with sandwich configuration exhibit good electrochemical performance in terms of their areal capacitance and cycling stability, due to their synergistic effect. The first layer of PPy film allows for the deposition of rGO flakes via pi-pi interactions, and rGO layer, in turn, acts as a buffering layer for the PPy films during repetitive charging and discharging cycles. The high surface area of rGO layer provides the second layer of PPy film with porous morphology and enhances the electrolyte ion accessible active sites. rGO layer also provides mechanical support for the second layer of PPy as they undergo swelling and shrinking by repeated insertion and extraction of dopant atoms during charging and discharging processes. PPy-rGO-PPy electrodes show larger areal capacitance and capacitance retention compared to the control samples PPy-PPy, indicating that presence of rGO layer enhances the electrochemical performance of the electrode. EIS results show that the rGO layer can decrease the ion diffusion impedance, allowing for the effective utilization of active sites. PPy-rGO-PPy electrodes prepared using 15 min deposition time for electrochemical polymerization and dried under vacuum at 110 ºC show largest areal capacitance of 905.4 mF/cm^2 at 10 mV/s and cycling

stability of 96.6% after 3000 cycles at 50 mV/s compared to other samples. Thus, the sandwich configuration of PPy-rGO-PPy results in an electrode with larger areal capacitance and cycling stability.

4.0 Impact of Substrates on Supercapacitor Performance

4.1 Introduction

An electrode forms the main component of a flexible supercapacitor device and consists of active materials and a flexible substrate. Although active materials make the main contribution to the electrochemical performance of the supercapacitor, it is important to understand the role of flexible substrates. Few studied have reported self-supporting films using active materials alone, without any additional substrate. However, these materials generally have low mechanical strength limiting their application in flexible energy storage devices. As a result, different research studies have reported variety of substrate materials such as metals foils or meshes, carbon cloth, carbonized fabrics or metal-coated fabrics for application in flexible supercapacitors. These flexible substrates are required to act as a current collector while keeping the active material adhered under applications involving bending conditions. The substrate can either have inherent conductivity or must be made conductive via various surface treatments.

Metal foils or meshes based on aluminum, copper or stainless-steel [23], [78] have been widely used as current collectors in supercapacitors. These substrates can be coated with different active materials through electrochemical deposition or polymerization methods. A study has shown that SSWM is a better choice than stainless steel foils for deposition of conductive polymer (PPy) since thick and bulky films of PPy forms on the foils that lower the cycling stability of their supercapacitor device [79]. The foil also suffers from poor adherence to PPy compared to SSWM. Jian et. al. reported a flexible all-solid-state supercapacitor device fabricated by the co-deposition of PPy and carbon quantum dots (CQDs) on SSWM [23]. CQDs were combined with PPy to

enhance their cycling stability. This device shows areal capacitance of 315 mF/cm^2 at a current density of 0.2 mA/cm^2 and long cycle life capacitance retention of 87.5% after 2000 cycles.

Textile based substrates have gained a lot of interest ever since the focus has shifted towards wearable supercapacitor devices. Carbon cloth is a popular, inexpensive, conducting textile, made from woven bundles of carbon fibers, that is used as an excellent support material [14], [80]. It is highly flexible with excellent strength [81]. A study sequentially electrodeposited MnO_2 and PPy on carbon cloth to obtain flexible electrodes that possessed high specific capacitance of 325 F/g at a current density of 0.2 A/g and 70% capacitance retention at a high current density of 5 A/g after 1000 cycles [22].

Other textile materials such as cotton, polyester, nylon have also gained interest for application in flexible supercapacitors due to their excellent mechanical flexibility, feeling of comfort and breathability, enabling their easy integration within wearable electronics [107], [108]. Carbonization of cotton fabric is a common procedure for making the material conductive [9]. Even though carbonization process enhances the electrochemical performance due to formation of high surface area of carbon network, mechanical strength of the material seems to be reduced by the carbonization process [109]. The textile materials are also made conductive by depositing carbon-based nanomaterials such as graphene sheets or CNTs [63], [110] or metallic coating of nickel, copper or silver [43], [83], [84]. Carbon-based nanomaterials are often coated on the textile via simple dip coating or impregnation methods. This method involves repetitive immersion of fabric in a concentrated solution of CNTs or graphene ink followed by drying to deposit the material on the textile. However, it is difficult to achieve a uniform coating with such a method.

The coating thickness also needs to be carefully controlled since high thickness can lead to flaking of the material. To increase adherence to the fabric, a binder is often added to the ink. However, this can lower the electrochemical performance of the active ingredient by blocking some of the active sites. For making a textile fabric conductive, metals are a better choice than carbon-based nanomaterials due to their higher conductivity. Today many conductive textile fabrics are commercially available in the market, especially for application in electrochemical shielding in flexible electronics.

Although different substrates have been proposed separately in a variety of research papers, there are very few studies comparing these substrates using the same active material deposited under the same condition [111]. This section uses the electrode configuration PPy-rGO-PPy, discussed in Section 3, as active materials to compare three different substrate materials- carbon cloth, SSWM and commercially obtained Cu:Ni-PET fabric for flexible supercapacitors. These three materials are good substrates for flexible supercapacitor applications due to their good flexibility and bendability, high conductivity compared to textile-based substrates, and low cost. However, they can be compared based on their wettability, electrical conductivity value, structures in terms of knitting and surface morphology (porosity). The conductivity is an important property since high conductivity allows the substrate to act as a good current collector. High conductivity also leads to higher rate of electrochemical polymerization, providing porous morphology to PPy film as discussed in Section 2.5.1 [85]. The electrical conductivity of a film can be measured using a four-point probe method. Another important property is the good wettability of material towards water that can aid in the deposition of active material where aqueous solvents are involved in the process. The wettability of material towards water can be qualitatively analyzed by simply comparing the

shape of the water droplet on its surface and assessing the contact angle formed at the interface between water and the material. Structure and surface morphology of the substrate are also important factors since they, in turn, affect the surface morphology of the active material deposited on them. These features are assessed using SEM images of the blank and coated substrates.

The first objective of this section is to compare three different substrates to study substrate effects on the electrochemical performance of flexible supercapacitor electrodes. The second objective is to prepare three full cells from each substrate using an aqueous gel electrolyte and analyze the impact of a substrate on the electrochemical performance of flexible supercapacitors. To achieve these objectives, the optimized electrode configuration, PPy-rGO-PPy, is deposited on each substrate under the same synthesis conditions to minimize the influence of synthesis processes on electrochemical properties of the electrode material, and to demonstrate the impact of the substrates on such properties. The three-electrode tests were conducted using 1M Na_2SO_4 electrolytes, to compare the three substrates for their electrochemical performance in supercapacitor application. Further, an aqueous electrolyte was chosen for the preparation of PVA based gel electrolyte to assemble flexible supercapacitor cells. The electrochemical characterizations were performed using CV, GCD, and EIS in both three- and two-electrode system to compare the three substrates. The results indicate that various factors must be considered when choosing a substrate material for flexible supercapacitors, such as its conductivity, wettability, surface morphology, and structure of the material.

4.2 Experimental Methods and Characterization

4.2.1 Electrode Preparation using different Substrates

To compare performance of electrode prepared using different substrate materials, active material was deposited on different conductive substrates using the method optimized in Section 3. Carbon cloth (obtained from Fuel Cell Earth LLC) and stainless-steel wire mesh (325 woven mesh, obtained from Alfa Aesar) and commercially obtained conductive fabric (obtained from Adafruit Industries) were used as substrates for supercapacitor preparation.

For carbon cloth-based electrode, carbon cloth was first treated with nitric acid to make its surface hydrophilic before electrochemically polymerizing pyrrole onto its surface. This treatment involved soaking the carbon cloth with 1 M nitric acid overnight followed by thorough rinsing with de-ionised water [112]. The carbon cloth was then rinsed with acetone to further remove any oil particles or other impurities, followed by drying overnight in the fume hood. A piece of carbon cloth was then used as working electrode and PPy was deposited onto its surface using electrochemical polymerization discussed in Section 3.2.1.

In case of stainless-steel wire mesh (SSWM) based electrode, SSWM was first flattened using roll press machine. They were then polished with a sand paper followed by treatment with 1 M sulfuric acid for 4 hours to enhance the surface roughness of the material [113]. The modified SSWM were then rinsed with de-ionized water and acetone and dried under N_2 gas flow. The dried SSWM were used as working electrode to deposit PPy via electrochemical polymerization method.

PPy-rGO-PPy material were deposited on the three substrates using procedure described in Section 3.2.1. These electrodes were then rinsed with de-ionized water followed by drying under vacuum at 110 ºC for 12 hours.

4.2.2 Device Assembly

The full cells were prepared using the two electrodes with filter paper as a separator and PVA/Na_2SO_4 as a gel electrolyte. The gel electrolyte was prepared by first preparing a 5 wt% PVA solution. Then 1M Na_2SO_4 was added such that the ratio between PVA and Na_2SO_4 was at 7:3 ratio [114], [115]. The electrodes and filter paper were immersed in the gel electrolyte for 12 hours before being assembled into a supercapacitor device for electrochemical test.

4.2.3 Materials and Electrochemical Characterization

Material characterization was performed using procedure described in Section 3.2.2. A four-point probe method was used for determining the in-plane electrical conductivity of the blank substrates (Equation 11). Keysight digit multimeter 34465A and Agilent 34401A were used as ammeter and voltmeter, respectively, and QuadTech programmable DC power supply 42006-100-25 was used as the power source. Electrochemical characterization was carried out in a three-electrode configuration using 1M sodium sulfate (Na_2SO_4). For three electrode tests, three different substrates with PPy-rGO-PPy material deposited on them were used as working electrodes, SCE as a reference electrode and platinum as the counter electrode. For two electrode tests, assembled full cells were used directly. Electrochemical properties of electrode material and assembled full cells were characterized using cyclic voltammetry (CV), galvanostatic charging discharging (GCD) and electrochemical impedance spectroscopy (EIS) methods on a computer-controlled

potentiostat (BioLogic VSP-300). EIS was recorded in the frequency range of 10 mHz-100 kHz with a potential amplitude of 5 mV in three-electrode system and two-electrode system.

4.3 Results and Discussion

4.3.1 Three-electrode Tests

For studying substrate effects on the electrochemical performance of electrode material, commercially obtained Cu and Ni coated polyester fabric (Cu:Ni-PET), carbon cloth and stainless steel wire mesh (SSWM) were used as substrates to deposit PPy-rGO-PPy active material. Out of the three substrates, carbon cloth is popularly used substrate material for flexible supercapacitors due to its low cost, good conductivity, and flexibility with its textile fabrics like knitted structure. Moreover, the network of the carbon fibers in carbon cloth based electrodes provide them with EDLC contribution for charge storage [14]. SSWM is another substrate commonly used for application in flexible supercapacitors due to its good conductivity, flexibility and mechanical strength [23]. The third substrate, Cu:Ni-PET fabric, is being used for the first time for the supercapacitor application. It has been chosen as a potential substrate for the material due to its high conductivity provided by copper and nickel coating on polyester (PET) fabric, good flexibility with a finely knitted structure of PET fabric and low cost.

Figure 17 (a) shows images of blank samples and PPy-rGO-PPy coated substrates. Out of the three substrates, SSWM has lower normalized cost value of \$1.75/ 500 cm^2 than Cu:Ni-PET substrate with cost value of \$6.2/ 500 cm^2, followed by carbon cloth of \$14.1/ 500 cm^2. The electrical conductivity of blank substrates was measured using a four-point probe system (Figure 17 (b)). Cu:Ni-PET substrate show highest in-plane electrical conductivity of 304.7 S/cm, followed by

carbon cloth with 124.2 S/cm and SSWM with 71.1 S/cm. The high electrical conductivity of Cu:Ni-PET is associated with the polyester fabric being coated with highly conductive metals copper and nickel. The wettability of the substrate is another important parameter to consider since the electrochemical polymerization process involves an aqueous medium in this work. The degree of wetting of a substrate depends on intermolecular forces within (solid-solid or liquid-liquid) and between the materials (solid-liquid) involved. The wettability of three substrates was qualitatively assessed using the contact angle formed by a drop of liquid on the surface of the three substrates (Figure 17 (c)). Out of the three substrates, Cu:Ni-PET substrate has higher conductivity and higher degree of wetting towards water than the other two substrates, which are beneficial for polymer deposit and electrochemical performance.

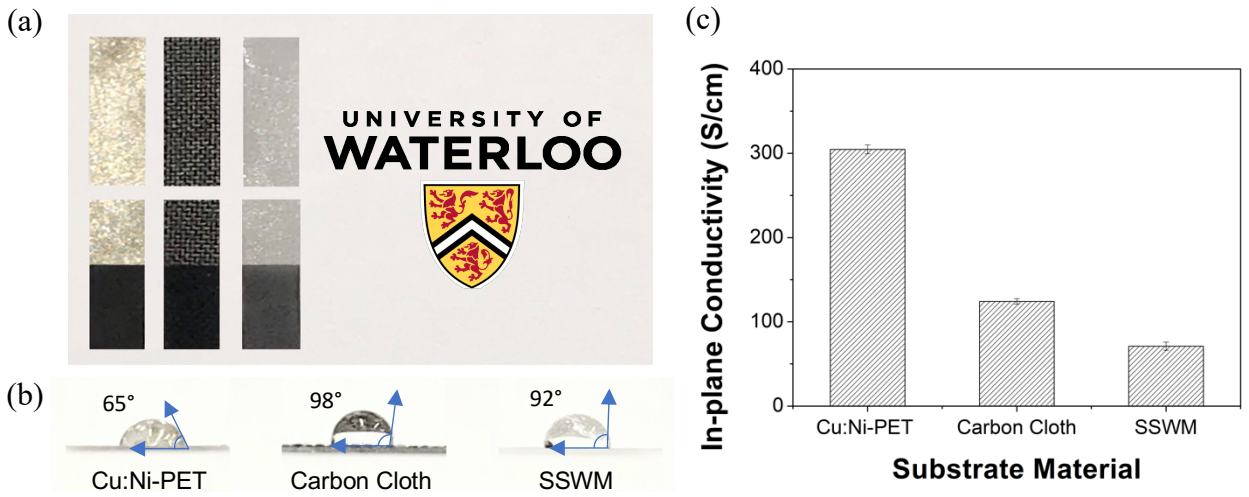

Figure 17: (a) Images of blank (top) and PPy-rGO-PPy coated (bottom) Cu:Ni-PET (left), Carbon cloth (centre), SSWM (right) substrates. (b) Qualitative analysis of contact angle using images of water droplet on blank substrates. (c) In-plane electrical conductivity of blank substrates.

The surface morphology of the blank substrates and the ones coated with PPy-rGO-PPy were characterized using SEM, as shown in Figure 18. SEM images of blank Cu:Ni-PET fabric shows its fine knitted structure (Figure 18 (a)). The fibers of this commercially obtained material are

uniformly coated with copper and nickel metal as can be observed from the SEM image. Figure 18 (b) shows SEM image of blank carbon cloth material where bundles of carbon fibers are knitted together. SEM image of SSWM (Figure 18 (c)) shows its structure with uniform mesh size.

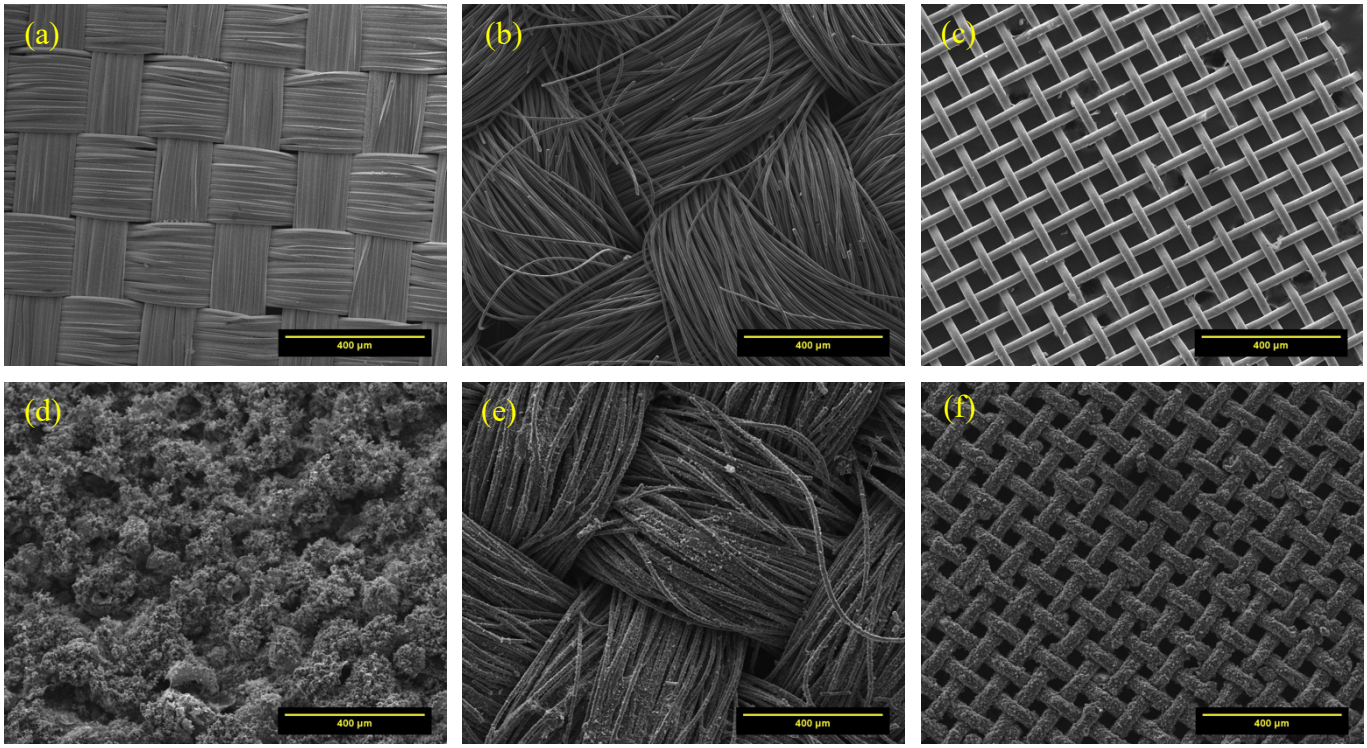

Figure 18: SEM images at 100X magnification of blank substrates- (a) Cu:Ni-PET fabric, (b) Carbon cloth, (c) SSWM and substrates coated with PPy-rGO-PPy electrode material- (d) Cu:Ni-PET fabric, (e) Carbon cloth, (f) SSWM.

Upon coating Cu:Ni-PET, carbon cloth, SSWM substrates with the electrode material, different morphologies are obtained as shown in Figure 18 (d), (e) and (f), respectively. For Cu:Ni-PET fabric, the smooth surface of fabric changes to a rough surface due to successful deposition and growth of PPy particles on its surface. The knitted structure of the substrate completely gets covered by PPy film with porous morphology. Some curled rGO flakes can also be observed on the surface of the material. This curling of flakes probably results from vacuum drying of the material. For carbon cloth-based electrodes, less rough surface is obtained. SSWM based electrodes retained their mesh structure, but the mesh size decreased due to the successful

deposition of the electrode material. Out of the three substrates, Cu:Ni-PET based electrode appears to have the most porous morphology. The porous morphology can be attributed to the fact that this substrate has higher conductivity and a higher degree of wetting towards water which results in increased efficiency of electrochemical polymerization of PPy that provides them with porous morphology. The finely knitted structure of the material also contributes to the dense morphology of PPy particles, which further allows for greater rGO deposition via π - π interactions. The porous structure of Cu:Ni-PET based electrode compared to carbon cloth and SSWM based electrodes facilitate access of electrolyte and reduce the ion diffusion distance. The higher amount of electrolyte ion accessible active sites provides Cu:Ni-PET based electrodes with an ability to store a greater amount of charge compared to the other two electrodes. Therefore, greater electrochemical performance can be expected from the electrodes prepared using this substrate.

The electrochemical performance of the three electrodes was first analyzed using CV, GCD and EIS tests in a three-electrode system. CV curves for Cu:Ni-PET, carbon cloth and SSWM based electrodes were obtained at different scan rates from 5 mV/s to 50 mV/s using -0.8 V to 0 V voltage window as shown in Figure 19 (a), (b), (c) respectively. Both Cu:Ni-PET and carbon cloth based electrodes maintain rectangular shape even at 50 mV/s scan rate, whereas SSWM deviates from rectangular shape. The electrode with Cu:Ni-PET substrate has the largest enclosed area, indicating that these electrodes have better capacitance behavior. Figure 19 (d) shows areal capacitance calculated from CV curve at each scan rate.

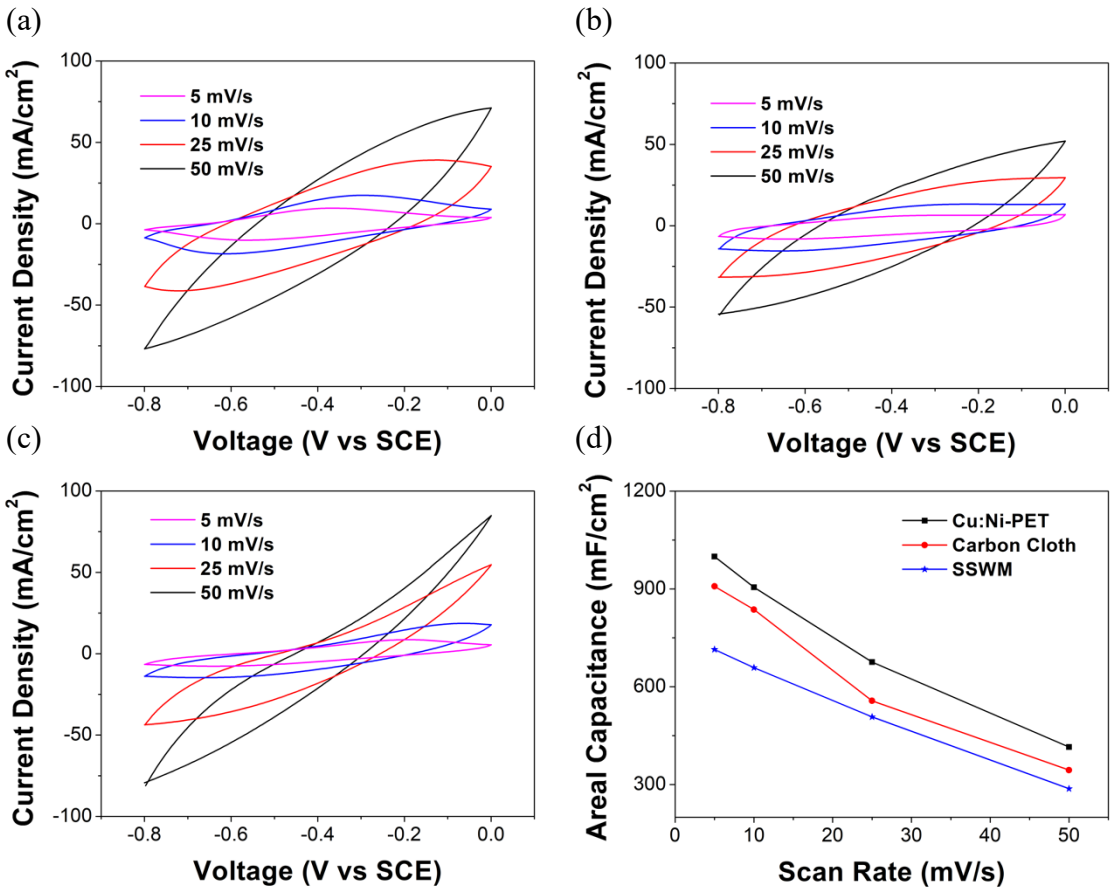

Figure 19: CV data of PPy-rGO-PPy on different substrates. CV curves at different scan rates for (a) Cu:Ni-PET (b) Carbon cloth (c) SSWM. (d) Areal capacitance values at different scan rates comparing the three substrates.

For all the scan rates, Cu:Ni-PET based electrode shows larger areal capacitance than electrodes with carbon cloth and SSWM as substrates. At scan rate of 5 mV/s, Cu:Ni-PET based electrode provides an areal capacitance of 999.4 mF/cm^2 compared to carbon cloth based electrode with 908.15 mF/cm^2 and SSWM based electrode with 714.6 mF/cm^2. The larger areal capacitance of Cu:Ni-PET based electrodes compared to carbon cloth and SSWM based electrodes can be attributed to high conductivity and wettability of Cu:Ni-PET that allows for increased efficiency of electrochemical polymerization and provide electrodes with porous morphology. The high conductivity of Cu:Ni-PET also allows them to act as a good current collector, reducing the equivalent series resistance of their electrodes. The Cu:Ni-PET substrate provides a porous

structure to the active materials, as observed in SEM images. This porous structure of Cu:Ni-PET based electrodes contribute to the larger areal capacitance since they allow access of electrolyte ions to more active sites than in the case of other two electrodes.

Figure 20 (a), (b) and (c) shows GCD profiles of Cu:Ni-PET, carbon cloth and SSWM based electrodes, among which Cu:Ni-PET based electrodes show the longest charge/discharge time.

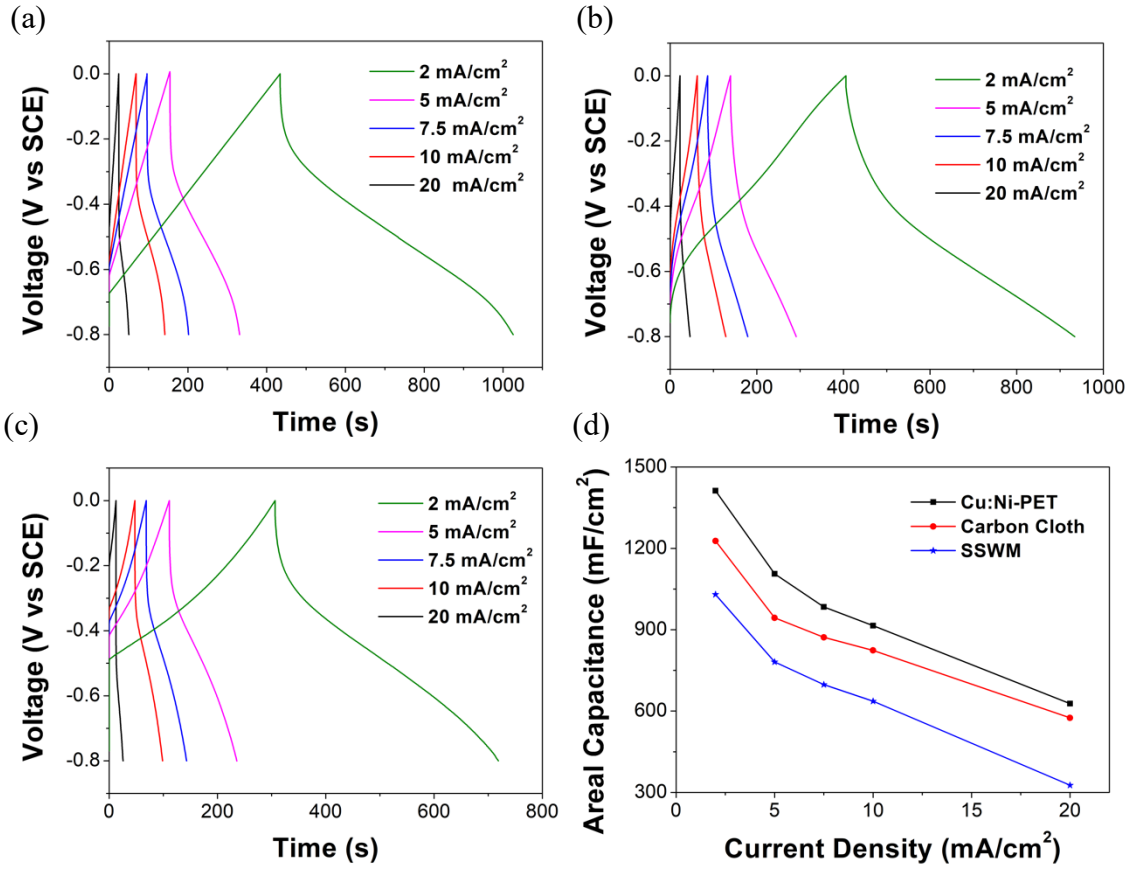

Figure 20: GCD data of PPy-rGO-PPy on different substrates. GCD curves at different current densities for (a) Cu:Ni-PET (b) Carbon cloth (c) SSWM. (d) Areal capacitance values at different current densities comparing the three substrates.

GCD curves keep nearly symmetric triangular shape demonstrating fast, successive reversible Faradaic reactions of the electrodes. Cu:Ni-PET substrate based electrodes also exhibit better rate capability compared with the other two electrodes (Figure 20 (d)). At current density of 2 mA/cm^2,

areal capacitance of 1412 mF/cm^2, 1227 mF/cm^2, 1030 mF/cm^2 were obtained for Cu:Ni-PET, carbon cloth and SSWM based electrodes respectively. These results indicate that higher conductivity, better wettability and finely knitted structure of Cu:Ni-PET substrates provide porous structure to their corresponding electrodes. This, in turn, provides them with large areal capacitance and better rate capability compared to other two electrodes.

The cycling stability of the three substrates was assessed using CV scans at 50 mV/s scan rate as shown in Figure 21.

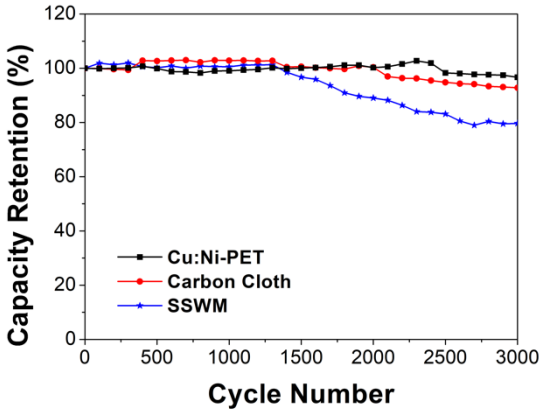

Figure 21: Stability test of PPy-rGO-PPy on different substrates at scan rate of 50 mV/s.

This figure shows that Cu:Ni-PET based electrode has good cycling stability, retaining 96.6 % capacitance retention after 3000 cycles, which is better than that of carbon cloth based electrode (92.8 % after 3000 cycles) and SSWM based electrodes (79.7 % after 3000 cycles). The higher cycling stability of Cu:Ni-PET based electrodes can be attributed to their structure and surface morphology. The finely knitted structure of Cu:Ni-PET substrate results in the deposition of porous and continuous PPy film on its surface. The surface morphology of Cu:Ni-PET based electrodes allows them to accommodate the volume expansion of PPy chains when they undergo

repeated charging and discharging, providing their full cells with higher cycling stability compared to other carbon cloth and SSWM based cells.

EIS measurements were performed for three different electrodes to obtain Nyquist plots shown in Figure 22 (a), (b) and (c).

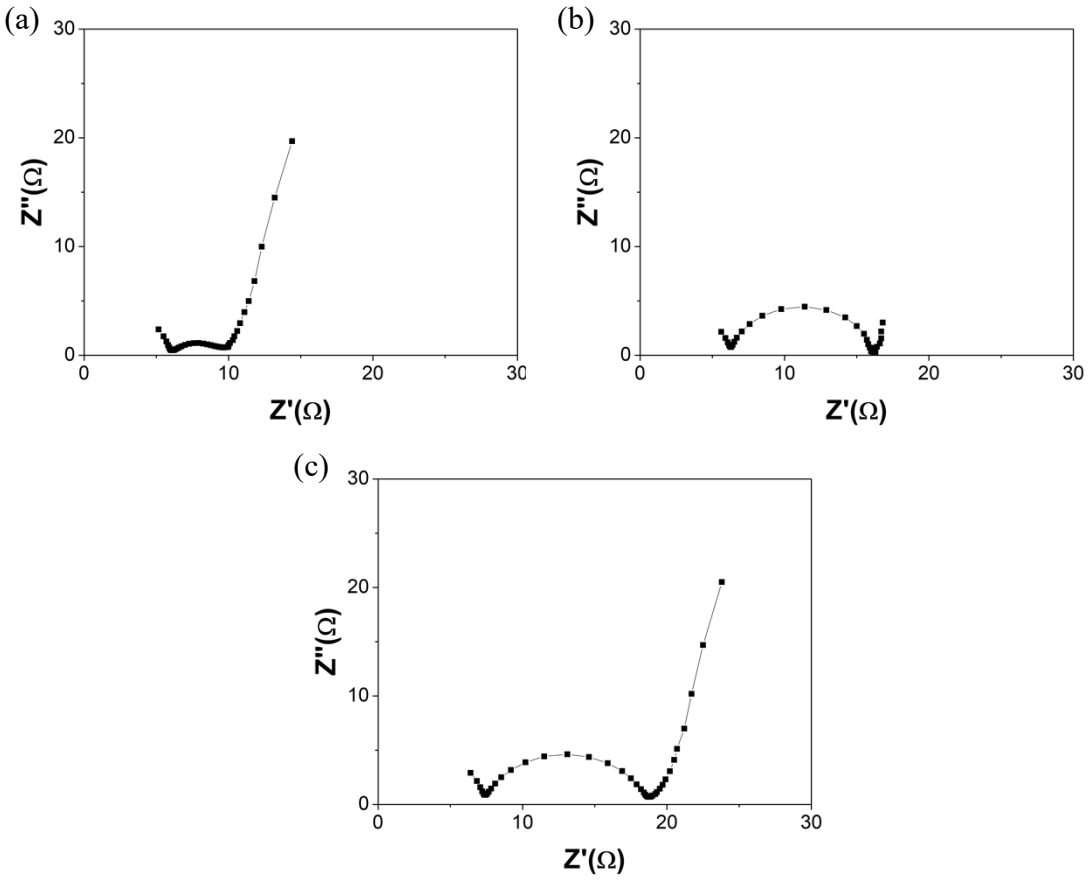

Figure 22: Nyquist curves of PPy-rGO-PPy on different substrates- (a) Cu:Ni-PET (b) Carbon cloth (c) SSWM.

All three electrodes show two semicircles in high and-mid frequency region which is most likely due to the two interfaces appearing in the sandwich configuration of PPy-rGO-PPy electrodes. The internal resistance of the electrodes was determined by extrapolating the semicircle in high-frequency regions, where Cu:Ni-PET based electrodes show lowest internal resistance followed

by carbon cloth and SSWM based electrodes. This is due to the higher conductivity of blank Cu:Ni-PET substrates compared to carbon cloth and SSWM. The high conductivity of the substrate inherently increases the conductivity of their respective electrodes. The charge transfer resistance is determined from the diameter of the second semicircle in mid-frequency region and represents impedance caused by mass transport phenomenon as the electrolyte ions navigate through sandwich structure of electrodes [116], [117]. This resistance was found to be minimum for Cu:Ni-PET based electrodes compared to carbon cloth and SSWM based ones. The fast charge transfer reaction in Cu:Ni-PET based electrodes is probably due to their structure being more porous than the other two electrodes. Thus, the EIS data indicates that the electrical conductivity of a substrate and the morphology of the active material can influence the internal resistance and charge transfer impedance, and hence the electrochemical performance of its corresponding electrode.

The mechanical flexibility of electrodes was compared by performing bending tests where electrodes were bent 0, 250, 500, 750 and 1000 number of times at 90° angle, and the areal capacitance was measured after each set of cycles. Figure 23 (a), (b) and (c) show CV curves for Cu:Ni-PET, carbon cloth and SSWM electrodes after 0, 250, 500, 750 and 1000 bending cycles at 10 mV/s scan rate. These figures show that CV curves nearly maintain their rectangular shapes even after 1000 bending cycles for all three substrates. Obviously, there is a small amount of loss in the area under the CV curve with an increase in the number of bending cycles, especially for Cu:Ni-PET based-electrode, indicating its electrode has good mechanical flexibility which allows it to retain its performance even after repetitive bending Figure 23 (d)). This can be attributed to the structure of the substrate and their corresponding electrodes. The SEM image of Cu:Ni-PET substrates show finely knitted structure of the material, and the image of their electrodes show a

continuous porous morphology (Figure 18 (a) and (b)). The structure of Cu:Ni-PET enables their electrodes to undergo minimum fraying from the edges of the electrodes during bending cycles compared to carbon cloth and SSWM. Fraying of electrodes can result in loss of active material which, in turn, can lower the charge storage capability of the material. Thus, upon bending, Cu:Ni-PET undergoes minimum fraying and hence, exhibit better bending performance than the other two substrates.

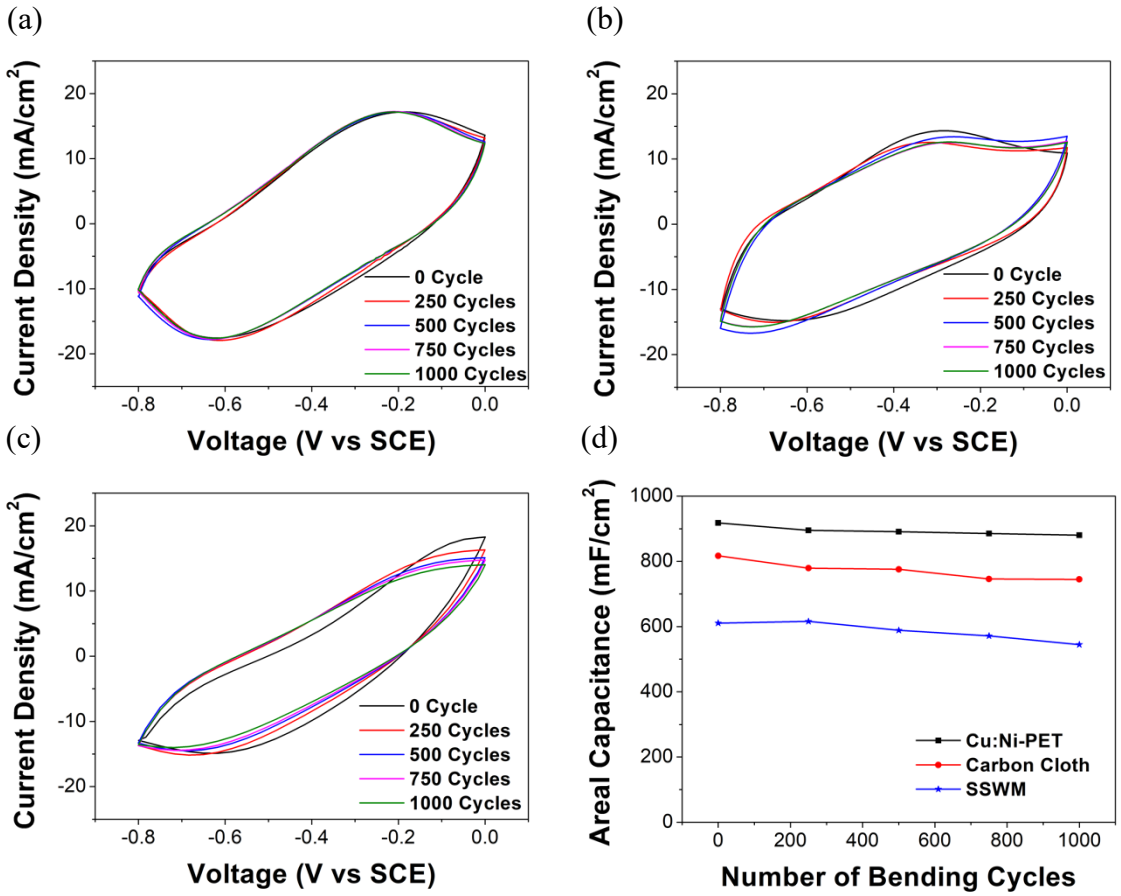

Figure 23: Bending test of PPy-rGO-PPy on different substrates (a) Cu:Ni-PET (b) Carbon cloth (c) SSWM. (d) Areal capacitance as a function of number of bending cycles for three different substrates.

In summary, three flexible and conductive substrates- Cu:Ni-PET, carbon cloth and SSWM have been compared for application in flexible supercapacitor electrodes. These substrates were

deposited with PPy-rGO-PPy as active materials using an optimized procedure discussed in Section 3. The blank Cu:Ni-PET substrate shows higher wettability towards water and higher in-plane electrical conductivity than the blank carbon cloth and SSWM substrates, which increases electrochemical polymerization efficiency and provides Cu:Ni-PET electrodes with porous morphology. SEM images of electrodes and blank substrates show how conductivity, wettability, surface morphology and structure of substrates affected the overall surface morphology of the active material deposited on them. The electrochemical performance results for the electrodes show that Cu:Ni-PET based electrodes exhibit larger areal capacitance of 1412 mF/cm^2 compared to carbon cloth based (1227 mF/cm^2) and SSWM based (1030 mF/cm^2) electrodes, at a current density of 2 mA/cm^2. Cu:Ni-PET based electrodes also show higher capacitance retention of 96.6% after 3000 charging-discharging cycles compared to carbon cloth and SSWM based electrodes. This indicates that Cu:Ni-PET substrate provides electrodes with porous morphology that can accommodate the volume expansion of PPy chains during charging-discharging cycles. The EIS results show that Cu:Ni-PET based electrodes had lower internal resistance and charge transfer resistance than carbon cloth and SSWM based electrodes. This can be attributed to the high conductivity of Cu:Ni-PET substrate and porous morphology of their electrodes. The flexibility of the electrodes was also compared, where Cu:Ni-PET based electrodes show highest performance, followed by carbon cloth and SSWM based electrodes. This indicates that the finely knitted structure and surface morphology of Cu:Ni-PET substrate provide their electrodes with mechanical stability under bending conditions. Thus, the results from electrochemical characterization indicate that various properties of a substrate such as conductivity, wettability, surface morphology, and knitted structure can influence the surface morphology of their electrodes and hence, impact its overall electrochemical performance.

4.3.2 Two-electrode Tests

The full cells were assembled for each substrate material by immersing the electrode and a filter paper (separator) in gel electrolytes and placing them in a sandwich structure, as shown in the schematic in Figure 24.

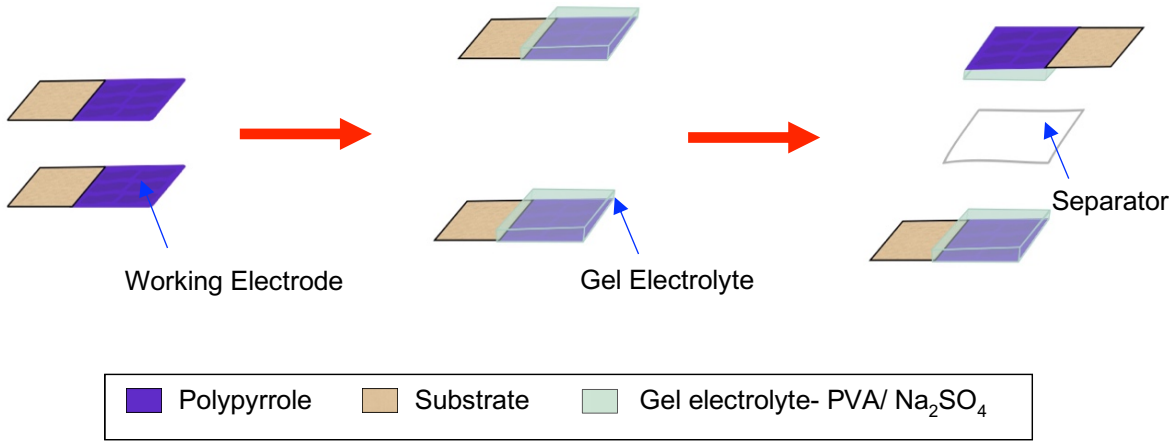

Figure 24: Schematic illustration for assembling full cell using PVA/Na_2SO_4 gel electrolyte.

Aqueous electrolytes such as H_3PO_4 and H_2SO_4 are commonly used in gel electrolyte preparation for PPy-based electrodes. However, substrates such as SSWM and Cu:Ni-PET are not compatible because they corrode in acidic conditions. Even a basic electrolyte, KOH, was found to be incompatible with all the electrodes because, within few hours of immersing the electrodes in the PVA/KOH gel electrolyte, the color of gel around the electrode turned into yellow color indicating some dissolution of the active material (Figure 25).

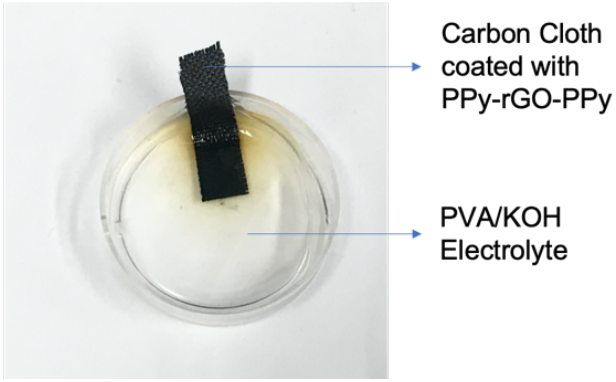

Figure 25: Carbon cloth coated with PPy-rGO-PPy in PVA/KOH electrolyte.

Upon further investigation, it was discovered that this dissolution is probably due to the de-doping of p-toluenesulfonate anions from polymer films in the presence of a strong oxidizing agent (KOH). Prolonged treatment with an oxidizing agent can reduce electrochemical performance. Extended treatment with an oxidizing agent increases the extent of oxidation of carbon atoms of polymer and make it lose its conjugation [105], [118]. This was experimentally observed where, the full cells prepared using PVA/KOH retained only about 50% of their initial capacity after only 1000 cycles. Thus, a neutral electrolyte Na_2SO_4 was chosen for gel electrolyte preparation and was used with the three different electrodes to assemble full cells. In this gel electrolyte, no dissolution or coloration of gel electrolyte was observed for any of the three electrodes.

Full cells assembled were compressed and dried before being analyzed using the CV test. First, voltage window was determined for full cells prepared using Cu:Ni-PET substrates. Figure 26 shows the CV scans obtained from 0 to 0.6-1.2 V voltage window. A voltage window of 0 to 1 V was used for all the two-electrode system-based characterization because, within this voltage range, the CV curve maintained a rectangular shape without any tailing.

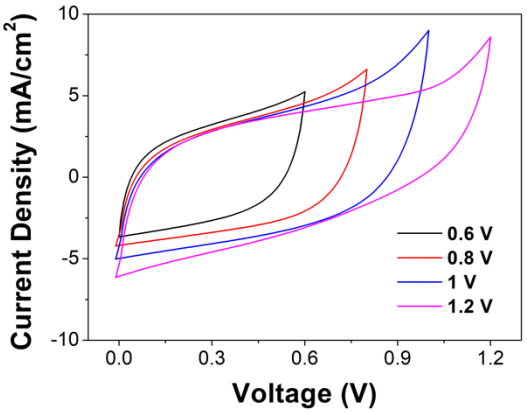

Figure 26: Voltage window determination using SC full cells prepared with Cu:Ni-PET fabric coated with PPy-rGO-PPy as electrodes.

Figure *27*Figure 27 (a), (b) and (c) show CV scans for full cells assembled using the three different substrates- Cu:Ni-PET, carbon cloth and SSWM respectively. These figures show that the full cells seem to maintain their rectangular shapes for different scan rates from 5 mV/s to 80 mV/s. The CV scans of full cell with Cu:Ni-PET substrate have larger enclosed area compared to full cells with carbon cloth and SSWM as the substrate, indicating that it exhibits largest areal capacitance. At a scan rate of 5 mV/s, Cu:Ni-PET based full cells exhibit large areal capacitance of 570 mF/cm^2, compared to capacitance of 527 mF/cm^2 for carbon cloth based, and 353 mF/cm^2 for SSWM based full cells. These results agree with the three-electrode results, where higher conductivity and better wettability of Cu:Ni-PET substrate resulted in electrodes with porous structure. The porous surface morphology of resulting electrodes, in turn, increases the charge storage capability of the resulting full cells. The relationship between areal capacitance and scan rates is shown in Figure 27 (d), where the areal capacitance was found to decrease with an increase in scan rate due to the slow diffusion of electrolyte ions into all the active sites.

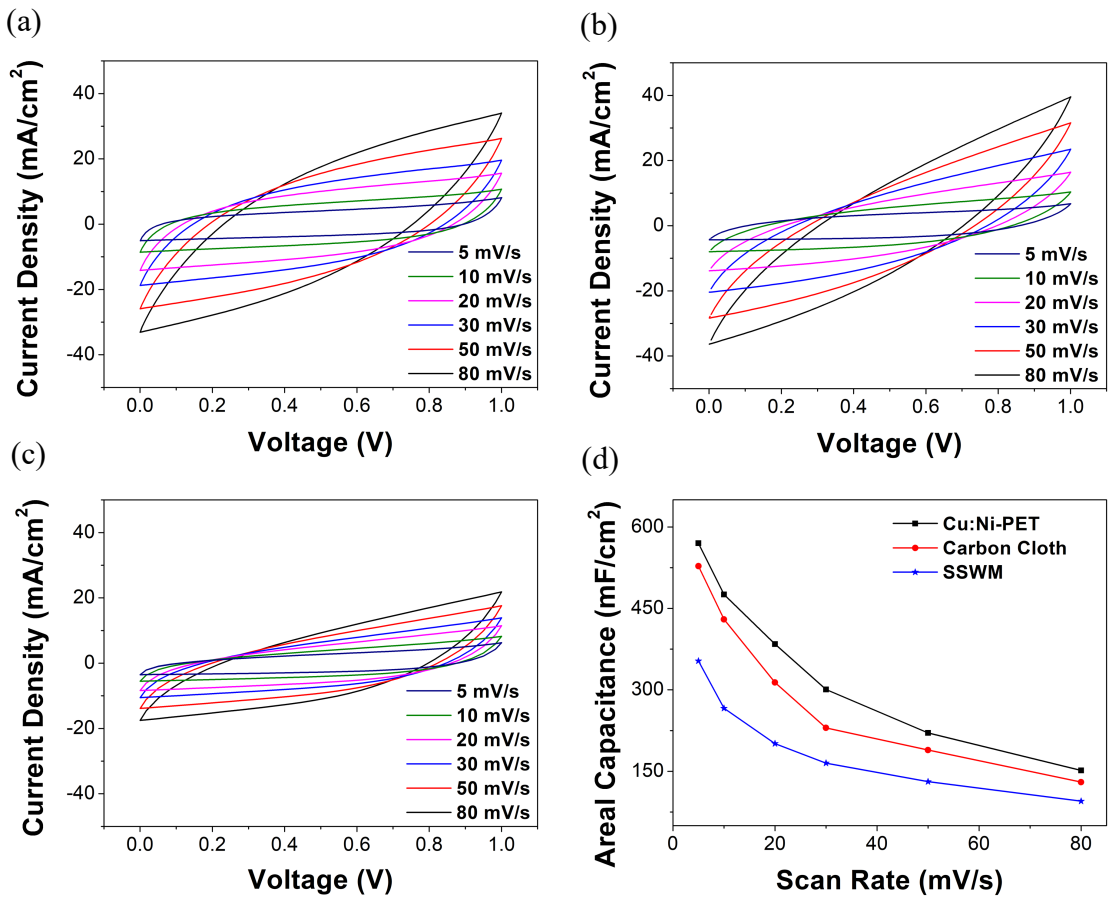

Figure 27: CV data of PPy-rGO-PPy based full cells with different substrates. CV curves at different scan rates for (a) Cu:Ni-PET (b) Carbon cloth (c) SSWM. (d) Areal capacitance values at different scan rates comparing the three substrates.

The GCD profiles obtained for full cells with Cu:Ni-PET, carbon cloth and SSWM substrates are shown in Figure 28 (a), (b) and (c). All the GCD profiles maintain a nearly triangular shape and have symmetry, indicating good capacitive behavior. They all show larger IR drop at higher current densities since more irreversible reactions would occur at high charge/discharge rates. Similar to results shown for the three-electrode system, cells with Cu:Ni-PET substrate exhibit the longest charge-discharge time compared to other substrates. They also show a smaller IR drop, which is attributed to the lower contact resistance at the interface between the active material and current collector/substrate. The smaller IR drop of Cu:Ni-PET based full cells indicates intimate

contact between the substrate and PPy films. The better wettability and higher conductivity of Cu:Ni-PET substrates most probably result in intimate contact formation between substrate and PPy films produced during the electrochemical polymerization process.

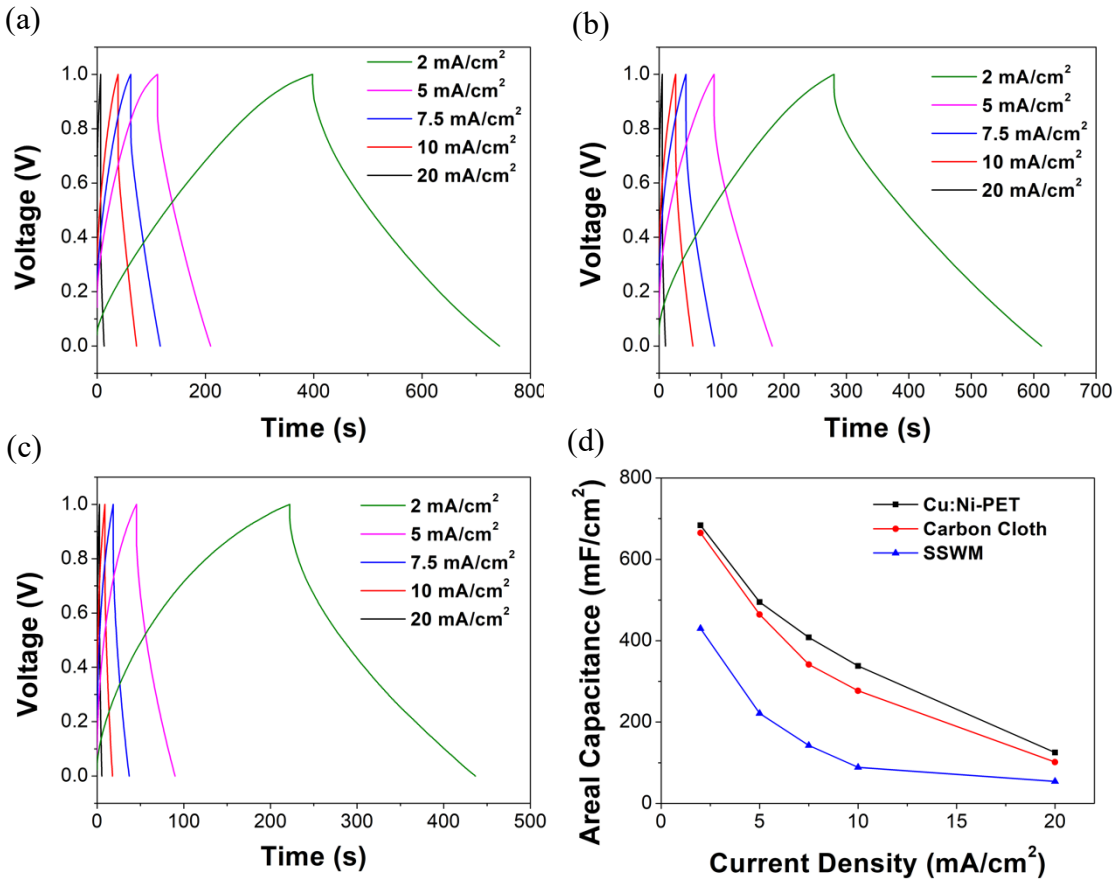

Figure 28: GCD data of PPy-rGO-PPy based full cells with different substrates. CV curves at different scan rates for (a) Cu:Ni-PET (b) Carbon cloth (c) SSWM. (d) Areal capacitance values at different scan rates comparing the three substrates.

The areal capacitance versus current densities are plotted for the full devices with different substrates in Figure 28 (d), where areal capacitance in case of Cu:Ni-PET and carbon cloth substrates are much larger than that in the case of SSWM. At 2 mA/cm^2, Cu:Ni-PET based full cells exhibit larger areal capacitance of 684 mF/cm^2, compared to capacitance of 664 mF/cm^2 for carbon based, and 430 mF/cm^2 for SSWM based full cells. This is probably due to the difference

in conductivity, wettability, and morphology of the material. The higher conductivity and better wettability of Cu:Ni-PET allows for increased efficiency of electrochemical polymerization, providing the resulting electrodes with a porous structure, which ultimately increases the charge storage capability of their full cells. This substrate also has higher conductivity than the other two substrates, which allows it to act as a better current collector. The structure of Cu:Ni-PET also contributes to the formation of continuous porous PPy layer, which allows access to more active sites for electrolyte ion diffusion, increasing the areal capacitance of resulting full cell. Thus, Cu:Ni-PET based full cells exhibit larger areal capacitance compared to other two cells.

Ragone plot for the full cell devices using different substrates are shown in Figure 29.

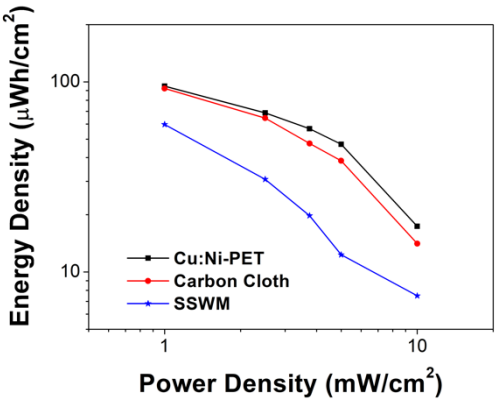

Figure 29: Ragone plot comparing PPy-rGO-PPy based full cells with different substrates.

The areal energy density and areal power density were calculated using Equations 8 and 9 in Section 2.3.2 based on different current densities. The full cells prepared using Cu:Ni-PET substrate has a high areal energy density of 95 μWh/cm^2 at an areal power density of 1 mW/cm^2, which is higher than those prepared from SSWM and carbon cloth substrates. Factors such as high conductivity, good wettability and structure of Cu:Ni-PET substrates enhance the surface morphology of their corresponding electrodes such that their full cells exhibit larger areal

capacitance. This, in turn, results in full cells with higher areal energy density and areal power density.

The cycling stability of full cells were evaluated by performing CV scans at 80 mV/s scan rate. Figure 30 compares the cycling stability of full cells prepared from three different substrates. The full cells with Cu:Ni-PET substrate show high capacitance retention of 94.2 % after 4000 cycles, demonstrating its good cycling stability. The carbon cloth substrates show capacitance retention of 92% after 4000 cycles and SSWM substrates show only 68.3% capacitance retention. This is probably due to the intrinsic properties of Cu:Ni-PET fabric substrate which results in a unique surface morphology of active materials (Figure 18 (d)) and accommodates a large volumetric expansion of polypyrrole chains, alleviating the structural pulverization and enhancing the stability of polypyrrole [18].

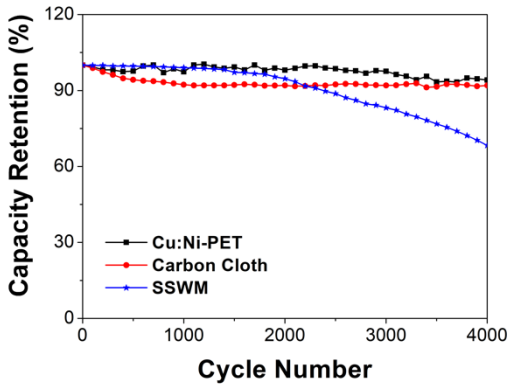

Figure 30: Stability test of PPy-rGO-PPy based full cells with different substrates at scan rate of 80 mV/s.

Nyquist plots were obtained from EIS characterization of the full cell devices. Figure 31 shows these plots for the three full cell devices prepared using three different substrates.

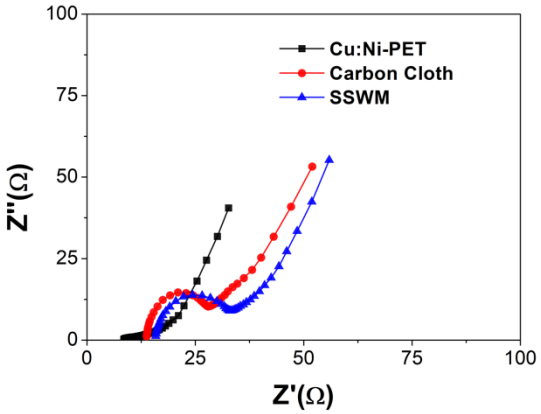

Figure 31: Nyquist curves of PPy-rGO-PPy based full cells with different substrates.

The figure shows that Cu:Ni-PET based full cells have lower internal resistance and charge transfer resistance indicating that they exhibit better electrical conductivity than carbon cloth and SSWM based devices. These results comply with EIS results from the three-electrode test, where higher conductivity of the substrate and high porosity of respective electrode provided Cu:Ni-PET based electrodes with lower internal resistance and charge transfer resistance, respectively.

To analyze importance of substrate on the flexibility of a supercapacitor cell, bending tests were performed where the cells were bent 0, 250, 500, 750 and 1000 number of times similar to the bending test performed in the three-electrode system. All the three devices maintained their electrochemical performance as indicated by the nearly similar CV scans of the material as shown in Figure 32 (a), (b) and (c). However, carbon cloth and SSWM based cells lose some of the area under the curve indicating a decrease in the areal capacitance of the cell with an increase in number of bending cycles.

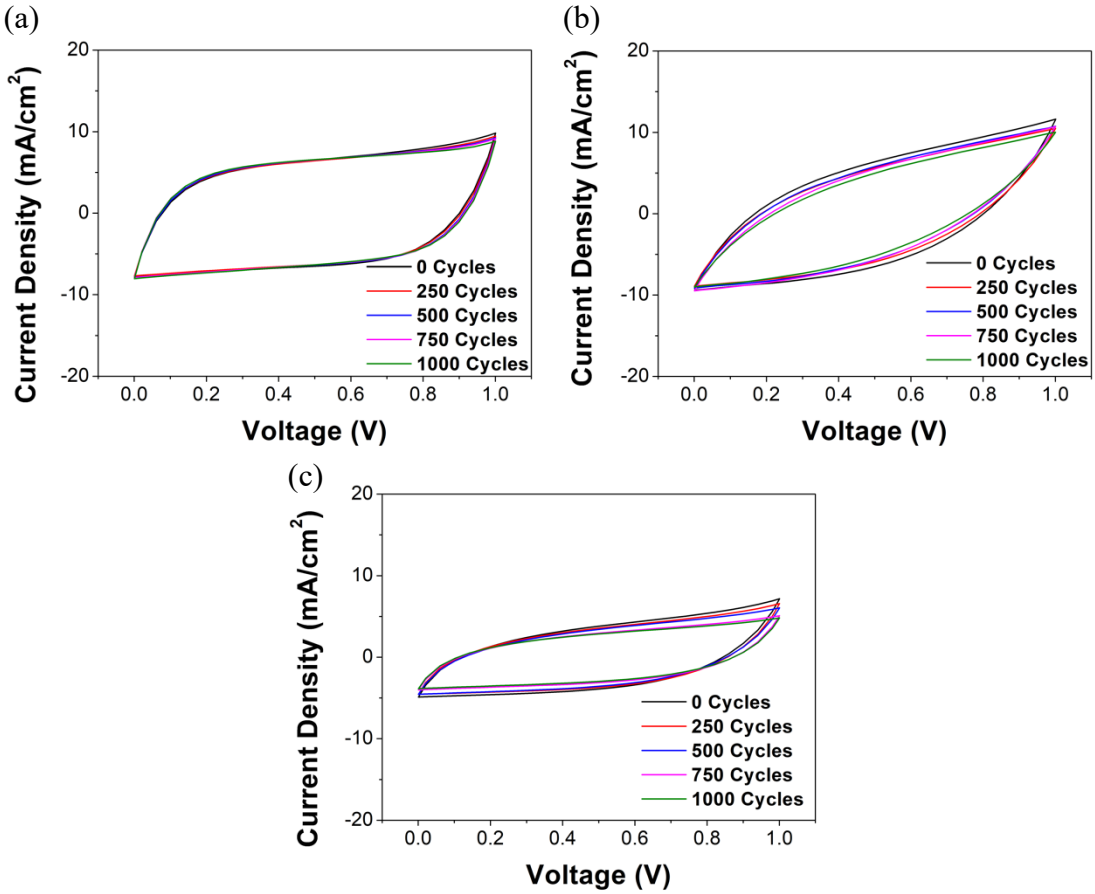

Figure 32: Bending test: CV scans of PPy-rGO-PPy based full cells with different substrates after different number of bending cycles at 10 mV/s (a) Cu:Ni-PET (b) Carbon cloth (c) SSWM.

Figure 32 (a) shows that in case of Cu:Ni-PET based full cell, the areal capacitance decreased after initial 250 cycles but with further bending the decrease in areal capacitance is less significant than other two devices. This indicates that Cu:Ni-PET does not undergo significant structural failure, which is an important requirement for flexible supercapacitor device. To further access the flexibility of supercapacitor device, CV scans of the three devices were obtained under flat and bent condition (Figure 33 (a), (b) and (c)), with a radius of curvature of 0.8 cm.

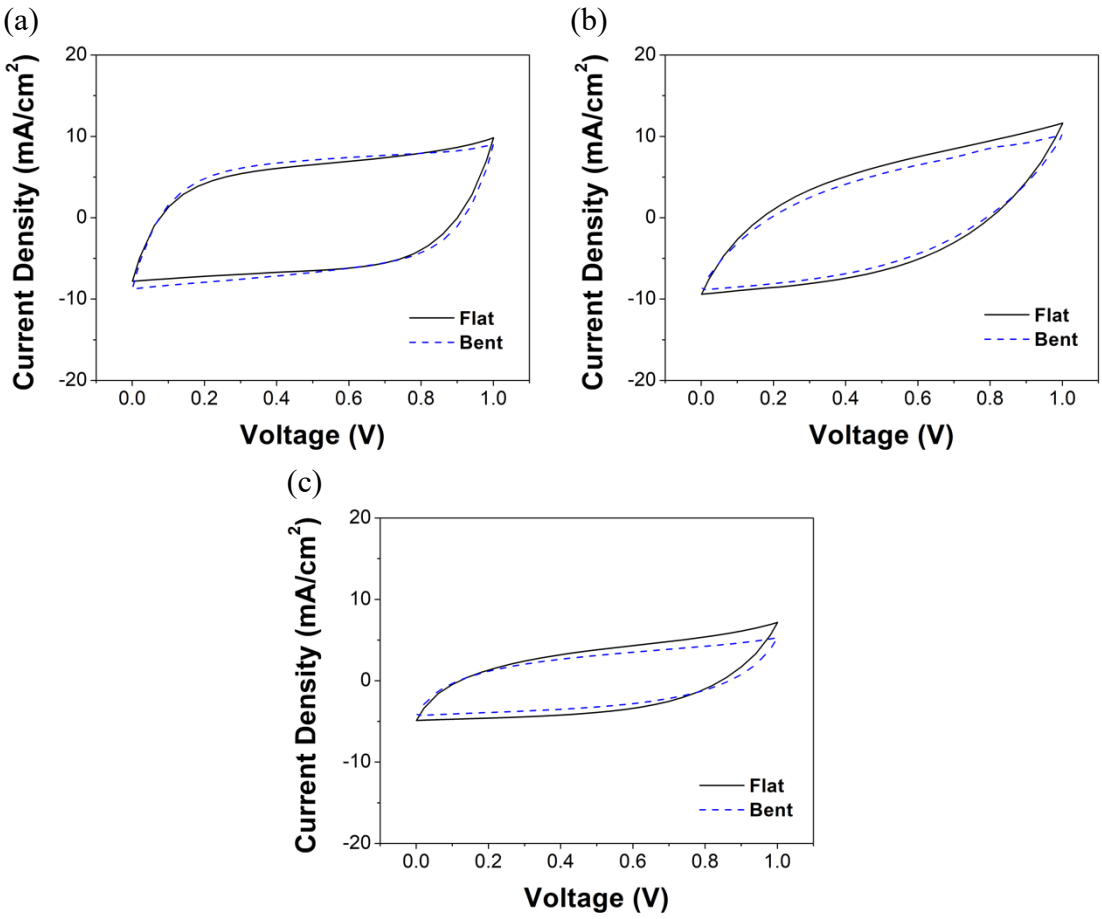

Figure 33: Bending test: CV scans of PPy-rGO-PPy based full cells with different substrates under flat and bent conditions at 10 mV/s (a) Cu:Ni-PET (b) Carbon cloth (c) SSWM.

These figures show that the shape of CV curve is nearly maintained by Cu:Ni-PET based devices but carbon cloth and SSWM based devices seem to lose more area under the curve when tested under bent condition. The better bending performance of Cu:Ni-PET based full cells can be attributed to the finely knitted structure of Cu:Ni-PET substrate that enhances the morphology of the corresponding electrodes. The finely knitted structure of Cu:Ni-PET substrate minimizes fraying of their electrodes upon bending. The structure of Cu:Ni-PET substrate result in electrodes with a continuous porous structure of PPy film that provides their respective full cells with excellent electrochemical stability even under bending conditions. Thus, the morphology and

structure of a substrate are important factors for ensuring that the supercapacitor cell prepared using it retains its electrochemical performance even under bending conditions.

Overall, three electrodes based on different substrates were compared in the two-electrode system to study their influence on the electrochemical performance of their corresponding full cell. Each electrode was immersed in PVA/Na_2SO_4 gel electrolyte to prepare supercapacitor cells with a sandwich structure. Cu:Ni-PET based full cells exhibit large areal capacitance of 684 mF/cm^2 at 2 mA/cm^2 and demonstrate highest cycling stability 94.2% after 4000 cycles compared to carbon cloth and SSWM based full cells. Cu:Ni-PET based cells also exhibit higher electrochemical performance than most PPy composite based flexible symmetric supercapacitors reported in literature (Table 1). Cu:Ni-PET based full cells also show a high areal energy density of 95 μWh/cm^2 at a power density of 1 mW/cm^2. Higher conductivity and wettability of Cu:Ni-PET substrates provided porous morphology to their corresponding electrodes and hence, high electrochemical performance was achieved for Cu:Ni-PET based full cells. Bending performance of cells was assessed by obtaining CV curves after repeatedly bending the cell from 0 to 1000 times and under flat and bent conditions. The finely knitted structure of Cu:Ni-PET substrates provided their full cells with better bending performance than carbon cloth based and SSWM based full cells. Thus, properties of a substrate such as conductivity, wettability, structure, and surface morphology influence the surface morphology of their electrodes. Modification in surface morphology, in turn, impacts the electrochemical performance of electrodes and their respective full cells. Hence, these properties of substrate must be carefully considered when selecting it for high performance flexible supercapacitor fabrication.

Table 1: Comparison of electrochemical performance of PPy composite based flexible symmetric supercapacitors.

Electrode Materials	**Areal Capacitance (mF/cm^2)**	**Cycling Stability (Cycles)**	**Electrolyte**	**Year/ Ref.**
Graphite flakes/ PPy lapping film	23 ($0.1\ mA/cm^2$)	95.2% (5000)	PVA/H_3PO_4	2015 [87]
rGO/PPy hybrid paper (Free standing)	440 ($1.35\ mA/cm^2$)	75% (1000)	$1M\ H_2SO_4$	2016 [119]
PPy/graphene/bacterial cellulose paper	790 ($1\ mA/cm^2$)	75.8% (3000)	$1M\ NaNO_3$	2016 [120]
CQD/PPy/SSWM	315 ($0.2\ mA/cm^2$)	85.7% (2000)	PVA/LiCl	2017 [23]
PPy/rGO/Modified PET	474 ($1\ mA/cm^2$)	100% (10,000)	PVA/H_2SO_4	2018 [99]
PPy/carbonized cotton fabric	500.06 ($2\ mA/cm^2$)	73.6% (2000)	PVA/LiCl	2019 [9]
PPy/rGO/PET	230 (1 mV/s)	76% (6000)	PVA/H_2SO_4	2019 [110]
PPy-rGO-PPy/Cu:Ni-PET fabric	**684 ($2\ mA/cm^2$)**	**94.4% (4000)**	**PVA/Na_2SO_4**	**This work**

5.0 Conclusions

With the growth in wearable technologies, there is an increasing need for development of flexible energy storage devices such as supercapacitors that can easily be integrated with portable wearable electronics. The rigid structure of conventional supercapacitor make them impractical for integration with wearable technologies and hence, current research studies focus on the development of flexible supercapacitors. PPy is one of the popular conductive polymer used for flexible supercapacitor applications due to its low cost, large specific/areal capacitance, high energy density and high flexibility. However, they suffer from poor cycling stability. This limitation is often overcome by combining PPy with carbon-based materials such as graphene. This study proposes an optimized sandwich configuration for PPy and rGO-based supercapacitor electrodes (PPy-rGO-PPy) that exhibit good electrochemical performance in terms of areal capacitance and cycling stability.

The first layer of PPy films on a conductive and flexible substrate allows for deposition of rGO flakes via pi-pi interactions. In turn, rGO layer acts as a buffering layer for the first PPy film when the electrode undergoes repeated charging and discharging cycles. The high surface area of rGO layer allows for the deposition of the second layer of PPy film with porous morphology. PPy-rGO-PPy electrodes prepared using 15 min electrochemical polymerization time and dried under vacuum at 110 ºC provided largest areal capacitance and capacitance retention after 1000 cycles. rGO layer between PPy films enhanced the areal capacitance of the material from 713 mF/cm^2 (control samples PPy-PPy) to 905.4 mF/cm^2 (PPy-rGO-PPy samples) at 10 mV/s scan rate. The porous morphology of PPy-rGO-PPy samples increases the electrolyte ion accessible active sites

that participate in charge storage mechanism and hence, lead to larger areal capacitance for PPy-rGO-PPy electrodes. PPy-rGO-PPy electrodes also increased capacitance retention from 68.2 % for PPy-PPy to 99.7 % for PPy-rGO-PPy samples after 1000 cycles. The increase in capacitance retention is associated with the presence of rGO layer that provides mechanical support to the second layer of PPy as they undergo swelling and shrinking during charging and discharging processes. They probably also serve as a physical buffer to suppress structural changes of the first layer of PPy during a charging-discharging process, enhancing cycling stability of the electrode. Since sandwich structure prevents formation of bulk films of PPy, effective utilization of active sites occurs and the ion diffusion impedance for PPy-rGO-PPy electrodes decreases as shown in EIS data. Thus, the sandwich configuration of PPy-rGO-PPy results in an electrode with large areal capacitance and cycling stability.

Over recent years, researchers have separately reported many different flexible substrates for flexible supercapacitor applications. However, there is a lack of study comparing these flexible substrates deposited with same active material to study the impact of substrate properties on the electrochemical performance of flexible supercapacitors. To overcome this limitation, the optimized PPy-rGO-PPy electrode configuration was deposited on three different types of flexible substrates- a commercially obtained conductive substrate PET fabric (Cu:Ni-PET), carbon cloth and stainless steel wire mesh (SSWM), to study substrate effects on the electrochemical performance of flexible supercapacitors. The blank Cu:Ni-PET substrates have highest in-plane electrical conductivity of 304.7 S/cm compared to carbon cloth with 124.2 S/cm and SSWM with 71.1 S/cm. They also exhibit highest wettability towards water. The substrate properties such as conductivity, wettability, structure and surface morphology were found to influence the overall

surface morphology of the deposited active material. Highly conductive and finely knitted Cu:Ni-PET fabric provided deposition of a continuous layer of PPy with porous structures creating conductive pathways for fast charge transfer. The electrochemical performance of these electrodes, as well as their respective full cells, was compared in three- and two-electrode systems, respectively. At a current density of 2 mA/cm^2, Cu:Ni-PET based electrodes show larger areal capacitance of 1412 mF/cm^2 compared to carbon cloth based electrodes (1227 mF/cm^2) and SSWM based electrodes (1030 mF/cm^2). This can be attributed to the substrate's high conductivity and wettability which increases the efficiency of polymerization process and provide them with a porous morphology. The higher conductivity of Cu:Ni-PET also allows it to act as a better current collector. EIS results show that Cu:Ni-PET based electrodes exhibit lower internal resistance and charge transfer resistance compared to other two electrodes, indicating that an electrode's electrical properties depend on the conductivity of their substrates. Cu:Ni-PET based electrodes also show higher capacitance retention of 96.6% after 3000 cycles at 50 mV/s compared to 92.8 % retention by carbon cloth based electrodes and 79.7 % retention by SSWM based electrodes. The morphology and structure of the substrate were found to influence the bending performance and cycling stability of the electrode material. Thus, properties of a substrate influence the morphology and electrochemical properties of their respective flexible supercapacitor electrodes.

Full cells were prepared from three substrate-based electrodes using PVA/Na_2SO_4 gel electrolyte that was found to be compatible with both active materials and three substrates. Cu:Ni-PET based full cells exhibit a larger areal capacitance of 684 mF/cm^2 and higher capacity retention of 94.2% after 4000 cycles compared to carbon cloth based and SSWM based full cells. The electrochemical performance of Cu:Ni-PET based full cells is also higher than most PPy composite based flexible

supercapacitors reported in literature. EIS results show that Cu:Ni-PET based electrodes and full cells have lower internal resistance and charge transfer resistance compared to carbon cloth and SSWM based full cells. Bending performance of full cells also complied with three-electrode results, where Cu:Ni-PET based electrode's structure and morphology provided better bending performance to their full cells. Thus, Cu:Ni-PET substrate based full cells show the best electrochemical performance compared to carbon cloth based and SSWM based full cells due to higher conductivity, higher wettability and finely knitted structure of Cu:Ni-PET substrate, and porous morphology of Cu:Ni-PET based electrodes. Hence, this work demonstrates that properties of a substrate such as conductivity, wettability, surface morphology, and structure must be taken into consideration when selecting it for application in a flexible supercapacitor device.

6.0 Recommendations

Following are some recommendations to further enhance the electrochemical performance of PPy-rGO-PPy sandwich structure and evaluate substrate effects on the electrochemical properties of the supercapacitor electrodes and cells:

- A simple drying method was used for rGO deposition and was kept consistent for all the samples. Further studies can be conducted to optimize rGO loading by taking into consideration immersion speed and duration. The impact of the amount of rGO loading on the overall electrochemical property of the supercapacitor electrodes can also be evaluated.

- For polypyrrole films, although the doping agent (TsOH), provides high conductivity as reported in previous studies [9], it limits the type of electrolyte that can be used since TsOH ions dissolve in basic electrolytes (Figure 25). Thus, alternative doping agents such as sodium dodecylbenzene sulfonate, that are compatible with a wide range of electrolytes [121], [122], can be investigated to achieve electrodes with high electrochemical performance.

- During the analysis of drying methods for PPy-rGO-PPy electrodes, annealing of samples resulted in degradation in their performance even at a low temperature of 150 ºC. Whereas, when vacuum dried at 110 ºC, the electrodes exhibit good electrochemical performance (Figure 12). To further understand the phenomenon behind the degradation of samples and whether the temperature is a lead cause of sample degradation during annealing, electrodes can be annealed at a same temperature used for vacuum drying (110 ºC), and their electrochemical performance can be characterized.

- Enhancement in areal capacitance and cycling stability is achieved with the sandwich structure consisting of a layer of rGO between two polymer layers. This structure can be further evaluated by using alternative graphene-like 2D materials such as MXenes, graphene nanoribbons, graphite-carbon nitride nanosheets, in place of rGO flakes to investigate if the sandwich structure indeed aids in enhancing the cycling stability of polypyrrole based electrodes.

- Performance of the quasi-solid-state flexible supercapacitor is still lower than the expected value since the PVA based gel electrolytes experience limited ion conductivity and penetrability. Recently researchers are exploring new gel electrolytes such as cross-linked polymer hydrogels that have higher ionic conductivity, to obtain high-performance solid-state supercapacitors [123]. Thus, further research can be conducted on applying these new gel electrolytes to obtain high performance flexible solid-state supercapacitor devices using PPy-rGO-PPy active material and Cu:Ni-PET substrate.

References

[1] Y. Huang *et al.*, "Nanostructured Polypyrrole as a flexible electrode material of supercapacitor," *Nano Energy*, vol. 22, pp. 422–438, Apr. 2016.

[2] X. Chen, R. Paul, and L. Dai, "Carbon-based supercapacitors for efficient energy storage," *Natl. Sci. Rev.*, vol. 4, no. 3, pp. 453–489, 2017.

[3] Q. Li, M. Horn, Y. Wang, J. MacLeod, N. Motta, and J. Liu, "A Review of Supercapacitors Based on Graphene and Redox-Active Organic Materials," *Materials (Basel).*, vol. 12, no. 5, p. 703, 2019.

[4] D. P. Dubal, N. R. Chodankar, D. H. Kim, and P. Gomez-Romero, "Towards flexible solid-state supercapacitors for smart and wearable electronics," *Chem. Soc. Rev.*, vol. 47, no. 6, pp. 2065–2129, 2018.

[5] C. Meng, C. Liu, L. Chen, C. Hu, and S. Fan, "Highly flexible and all-solid-state paperlike polymer supercapacitors," *Nano Lett.*, vol. 10, no. 10, pp. 4025–4031, 2010.

[6] M. F. El-Kady and R. B. Kaner, "Scalable fabrication of high-power graphene micro-supercapacitors for flexible and on-chip energy storage," *Nat. Commun.*, vol. 4, 2013.

[7] X. Peng, L. Peng, C. Wu, and Y. Xie, "Two dimensional nanomaterials for flexible supercapacitors," *Chem. Soc. Rev.*, vol. 43, no. 10, pp. 3303–3323, 2014.

[8] F. Su, X. Lyu, C. Liu, and M. Miao, "Flexible two-ply yarn supercapacitors based on carbon nanotube/stainless steel core spun yarns decorated with Co 3 O 4 nanoparticles and MnO x composites," *Electrochim. Acta*, vol. 215, pp. 535–542, Oct. 2016.

[9] C. Sun, X. Li, Z. Cai, and F. Ge, "Carbonized cotton fabric in-situ electrodeposition polypyrrole as high-performance flexible electrode for wearable supercapacitor," *Electrochim. Acta*, vol. 296, pp. 617–626, Feb. 2019.

[10] L. Hu *et al.*, “Stretchable, Porous, and Conductive Energy Textiles,” *Nano Lett.*, vol. 10, no. 2, pp. 708–714, Feb. 2010.

[11] C. Wan, Y. Jiao, and J. Li, “Flexible, highly conductive, and free-standing reduced graphene oxide/polypyrrole/cellulose hybrid papers for supercapacitor electrodes,” *J. Mater. Chem. A*, vol. 5, no. 8, pp. 3819–3831, 2017.

[12] Y. Lin *et al.*, “In-situ growth of high-performance all-solid-state electrode for flexible supercapacitors based on carbon woven fabric/ polyaniline/ graphene composite,” *J. Power Sources*, vol. 384, no. March, pp. 278–286, 2018.

[13] B. K. Kim, S. Sy, A. Yu, and J. Zhang, “Electrochemical Supercapacitors for Energy Storage and Conversion,” in *Handbook of Clean Energy Systems*, Chichester, UK: John Wiley & Sons, Ltd, 2015, pp. 1–25.

[14] R. Tjandra, W. Liu, M. Zhang, and A. Yu, “All-carbon flexible supercapacitors based on electrophoretic deposition of graphene quantum dots on carbon cloth,” *J. Power Sources*, vol. 438, p. 227009, Oct. 2019.

[15] I. Shown, A. Ganguly, L. C. Chen, and K. H. Chen, “Conducting polymer-based flexible supercapacitor,” *Energy Sci. Eng.*, vol. 3, no. 1, pp. 1–25, 2015.

[16] A. Yu, V. Chabot, and J. Zhang, *Electrochemical Supercapacitors for Energy Storage and Delivery: Fundamentals and Applications*. Taylor & Francis Group, 2013.

[17] B. Yue, C. Wang, X. Ding, and G. G. Wallace, “Polypyrrole coated nylon lycra fabric as stretchable electrode for supercapacitor applications,” *Electrochim. Acta*, 2012.

[18] Y. Song, T.-Y. Liu, X.-X. Xu, D.-Y. Feng, Y. Li, and X.-X. Liu, “Pushing the Cycling Stability Limit of Polypyrrole for Supercapacitors,” *Adv. Funct. Mater.*, vol. 25, no. 29, pp. 4626–4632, Aug. 2015.

[19] R. Ansari, “Polypyrrole Conducting Electroactive Polymers: Synthesis and Stability Studies,” *E-Journal Chem.*, vol. 3, no. 4, pp. 186–201, 2006.

[20] M. Guo, Y. Zhou, H. Sun, G. Zhang, and Y. Wang, “Interconnected polypyrrole nanostructure for high-performance all-solid-state flexible supercapacitor,” *Electrochim. Acta*, vol. 298, pp. 918–923, 2019.

[21] Y. Shi, L. Peng, Y. Ding, Y. Zhao, and G. Yu, “Nanostructured conductive polymers for advanced energy storage,” *Chem. Soc. Rev.*, vol. 44, no. 19, pp. 6684–6696, 2015.

[22] X. Fan, X. Wang, G. Li, A. Yu, and Z. Chen, “High-performance flexible electrode based on electrodeposition of polypyrrole/MnO2 on carbon cloth for supercapacitors,” *J. Power Sources*, vol. 326, pp. 357–364, Sep. 2016.

[23] X. Jian, H. Yang, J. Li, E. Zhang, L. Cao, and Z. Liang, “Flexible all-solid-state high-performance supercapacitor based on electrochemically synthesized carbon quantum dots/polypyrrole composite electrode,” *Electrochim. Acta*, vol. 228, pp. 483–493, Feb. 2017.

[24] C. Zhang *et al.*, “A high-performance all-solid-state yarn supercapacitor based on polypyrrole-coated stainless steel/cotton blended yarns,” *Cellulose*, vol. 26, no. 2, pp. 1169–1181, 2019.

[25] H. I. . Becker, “Low voltage electrolytic capacitor,” US 2800616, Jul-1957.

[26] C. Largeot, C. Portet, J. Chmiola, P. L. Taberna, Y. Gogotsi, and P. Simon, “Relation between the ion size and pore size for an electric double-layer capacitor,” *J. Am. Chem. Soc.*, vol. 130, no. 9, pp. 2730–2731, 2008.

[27] G. Wang, L. Zhang, and J. Zhang, “A review of electrode materials for electrochemical supercapacitors,” *Chem. Soc. Rev.*, vol. 41, no. 2, pp. 797–828, 2012.

[28] C. Zhong, Y. Deng, W. Hu, J. Qiao, L. Zhang, and J. Zhang, “A review of electrolyte materials and compositions for electrochemical supercapacitors,” *Chem. Soc. Rev.*, vol. 44, no. 21, pp. 7484–7539, 2015.

[29] A. González, E. Goikolea, J. A. Barrena, and R. Mysyk, “Review on supercapacitors: Technologies and materials,” *Renew. Sustain. Energy Rev.*, vol. 58, pp. 1189–1206, 2016.

[30] S. Zhang and N. Pan, “Supercapacitors Performance Evaluation,” *Adv. Energy Mater.*, vol. 5, no. 6, p. 1401401, Mar. 2015.

[31] F. Béguin, V. Presser, A. Balducci, and E. Frackowiak, “Carbons and electrolytes for advanced supercapacitors,” *Adv. Mater.*, vol. 26, no. 14, pp. 2219–2251, 2014.

[32] M. Endo, T. Takeda, Y. J. Kim, K. Koshiba, and K. Ishii, “High Power Electric Double Layer Capacitor (EDLC ’ s); from Operating Principle to Pore Size Control in Advanced Activated Carbons,” *Carbon Sci.*, vol. 1, no. 3, pp. 117–128, 2001.

[33] C. Brett, *Fundamentals of electrochemistry*. 2008.

[34] B. E. Conway, V. Birss, and J. Wojtowicz, “The role and utilization of pseudocapacitance for energy storage by supercapacitors,” *J. Power Sources*, vol. 66, no. 1–2, pp. 1–14, May 1997.

[35] W. Raza *et al.*, “Recent advancements in supercapacitor technology,” *Nano Energy*, vol. 52, no. August, pp. 441–473, 2018.

[36] Z. Z. Zhu, G. C. Wang, M. Q. Sun, X. W. Li, and C. Z. Li, “Fabrication and electrochemical characterization of polyaniline nanorods modified with sulfonated carbon nanotubes for supercapacitor applications,” *Electrochim. Acta*, vol. 56, no. 3, pp. 1366–1372, 2011.

[37] S. S. Jayaseelan *et al.*, “Mesoporous 3D NiCo 2 O 4 /MWCNT nanocomposite aerogels

prepared by a supercritical CO 2 drying method for high performance hybrid supercapacitor electrodes," *Colloids Surfaces A Physicochem. Eng. Asp.*, vol. 538, no. September 2017, pp. 451–459, 2018.

[38] M. Cakici, K. R. Reddy, and F. Alonso-Marroquin, "Advanced electrochemical energy storage supercapacitors based on the flexible carbon fiber fabric-coated with uniform coral-like MnO2structured electrodes," *Chem. Eng. J.*, vol. 309, pp. 151–158, 2017.

[39] Y. Zhang *et al.*, "Progress of electrochemical capacitor electrode materials: A review," *Int. J. Hydrogen Energy*, vol. 34, no. 11, pp. 4889–4899, 2009.

[40] P. Simon, Y. Gogotsi, P. Simon, Y. Gogotsi, and N. Materials, "Materials for electrochemical capacitors," vol. 7, no. 11, pp. 845–854, 2019.

[41] M. Seredych, M. Koscinski, M. Sliwinska-Bartkowiak, and T. J. Bandosz, "Active pore space utilization in nanoporous carbon-based supercapacitors: Effects of conductivity and pore accessibility," *J. Power Sources*, vol. 220, pp. 243–252, 2012.

[42] J. Huang, B. G. Sumpter, and V. Meunier, "A universal model for nanoporous carbon supercapacitors applicable to diverse pore regimes, carbon materials, and electrolytes," *Chem. - A Eur. J.*, vol. 14, no. 22, pp. 6614–6626, 2008.

[43] Y. Yang *et al.*, "Waterproof, Ultrahigh Areal-Capacitance, Wearable Supercapacitor Fabrics," *Adv. Mater.*, vol. 29, no. 19, p. 1606679, May 2017.

[44] K. Koziol *et al.*, "High-performance carbon nanotube fiber," *Science (80-.).*, vol. 318, no. 5858, pp. 1892–1895, 2007.

[45] H. Chen, M. B. Müller, K. J. Gilmore, G. G. Wallace, and D. Li, "Mechanically strong, electrically conductive, and biocompatible graphene paper," *Adv. Mater.*, vol. 20, no. 18, pp. 3557–3561, 2008.

[46] M. Pumera, “Graphene-based nanomaterials and their electrochemistry,” *Chem. Soc. Rev.*, vol. 39, no. 11, pp. 4146–4157, 2010.

[47] X. Zhang, H. Zhang, C. Li, K. Wang, X. Sun, and Y. Ma, “Recent advances in porous graphene materials for supercapacitor applications,” *RSC Adv.*, vol. 4, no. 86, pp. 45862–45884, 2014.

[48] Y. Gao, “Graphene and Polymer Composites for Supercapacitor Applications: a Review,” *Nanoscale Res. Lett.*, vol. 12, no. 1, 2017.

[49] P. Simon and A. Burke, “Nanostructured carbons: Double-layer capacitance and more,” *Electrochem. Soc. Interface*, vol. 17, no. 1, pp. 38–43, 2008.

[50] J. P. Zheng and T. R. Jow, “A New Charge Storage Mechanism for Electrochemical Capacitors,” *J. Electrochem. Soc.*, vol. 142, no. 1, pp. 6–8, 1995.

[51] S. C. Pang and M. A. Anderson, “Novel electrode materials for electrochemical capacitors: Part II. Material characterization of sol-gel-derived and electrodeposited manganese dioxide thin films,” *J. Mater. Res.*, vol. 15, no. 10, pp. 2096–2106, 2000.

[52] C. Lin, J. A. Ritter, and B. N. Popov, “Characterization of sol-gel-derived cobalt oxide xerogels as electrochemical capacitors,” *J. Electrochem. Soc.*, vol. 145, no. 12, pp. 4097–4103, 1998.

[53] K. C. Liu and M. A. Anderson, “Porous nickel oxide/nickel films for electrochemical capacitors,” *J. Electrochem. Soc.*, vol. 143, no. 1, pp. 124–130, 1996.

[54] M. Zhi, C. Xiang, J. Li, M. Li, and N. Wu, “Nanostructured carbon-metal oxide composite electrodes for supercapacitors: A review,” *Nanoscale*, vol. 5, no. 1, pp. 72–88, 2013.

[55] Y. Wang, J. Guo, T. Wang, J. Shao, D. Wang, and Y. W. Yang, “Mesoporous transition metal oxides for supercapacitors,” *Nanomaterials*, vol. 5, no. 4, pp. 1667–1689, 2015.

[56] P. Simon and Y. Gogotsi, “Materials for electrochemical capacitors,” *Nat. Mater.*, vol. 7, no. 11, pp. 845–854, 2008.

[57] T. H. Le, Y. Kim, and H. Yoon, “Electrical and electrochemical properties of conducting polymers,” *Polymers (Basel).*, vol. 9, no. 4, 2017.

[58] G. Sabouraud, S. Sadki, and N. Brodie, “The mechanisms of pyrrole electropolymerization,” *Chem. Soc. Rev.*, vol. 29, no. 5, pp. 283–293, 2000.

[59] T. Patois, B. Lakard, S. Monney, X. Roizard, and P. Fievet, “Characterization of the surface properties of polypyrrole films: Influence of electrodeposition parameters,” *Synth. Met.*, vol. 161, no. 21–22, pp. 2498–2505, 2011.

[60] Y. Wang, Y. Song, and Y. Xia, “Electrochemical capacitors: Mechanism, materials, systems, characterization and applications,” *Chem. Soc. Rev.*, vol. 45, no. 21, pp. 5925–5950, 2016.

[61] G. Panta and D. Subedi, “Electrical characterization of aluminum (Al) thin films measured by using four- point probe method,” *Kathmandu Univ. J. Sci. Eng. Technol.*, vol. 8, no. 2, pp. 31–36, 2013.

[62] F. Algahtani, K. B. Thulasiram, N. M. Nasir, and A. S. Holland, “Four point probe geometry modified correction factor for determining resistivity,” *Micro/Nano Mater. Devices, Syst.*, vol. 8923, p. 89235D, 2013.

[63] W. Liu, X. Yan, J. Lang, C. Peng, and Q. Xue, “Flexible and conductive nanocomposite electrode based on graphene sheets and cotton cloth for supercapacitor,” *J. Mater. Chem.*, vol. 22, no. 33, p. 17245, 2012.

[64] Y. Deng, Y. Xie, K. Zou, and X. Ji, “Review on recent advances in nitrogen-doped carbons: Preparations and applications in supercapacitors,” *J. Mater. Chem. A*, vol. 4, no.

4, pp. 1144–1173, 2015.

[65] K. Li and J. Zhang, “Recent advances in flexible supercapacitors based on carbon nanotubes and graphene,” *Sci. China Mater.*, vol. 61, no. 2, pp. 210–232, Feb. 2018.

[66] Y. Shao *et al.*, “Graphene-based materials for flexible supercapacitors,” *Chem. Soc. Rev.*, vol. 44, no. 11, pp. 3639–3665, 2015.

[67] W. Liu *et al.*, “Hair-based flexible knittable supercapacitor with wide operating voltage and ultra-high rate capability,” *Nano Energy*, vol. 34, no. February, pp. 491–499, 2017.

[68] R. Reit, J. Nguyen, and W. J. Ready, “Growth time performance dependence of vertically aligned carbon nanotube supercapacitors grown on aluminum substrates,” *Electrochim. Acta*, vol. 91, pp. 96–100, 2013.

[69] D. C. Singu, B. Joseph, V. Velmurugan, S. Ravuri, and A. N. Grace, “Combustion Synthesis of Graphene from Waste Paper for High Performance Supercapacitor Electrodes,” *Int. J. Nanosci.*, vol. 17, no. 1–2, pp. 1–5, 2018.

[70] J. X. Feng, Q. Li, X. F. Lu, Y. X. Tong, and G. R. Li, “Flexible symmetrical planar supercapacitors based on multi-layered MnO 2/Ni/graphite/paper electrodes with high-efficient electrochemical energy storage,” *J. Mater. Chem. A*, vol. 2, no. 9, pp. 2985–2992, 2014.

[71] L. Chen *et al.*, “Flexible all-solid-state supercapacitors based on freestanding, binder-free carbon nanofibers@polypyrrole@graphene film,” *Chem. Eng. J.*, vol. 334, no. August 2017, pp. 184–190, 2018.

[72] C. Wei *et al.*, “An all-solid-state yarn supercapacitor using cotton yarn electrodes coated with polypyrrole nanotubes,” *Carbohydr. Polym.*, vol. 169, pp. 50–57, 2017.

[73] S. Shi, C. Xu, C. Yang, Y. Chen, J. Liu, and F. Kang, “Flexible asymmetric

supercapacitors based on ultrathin two-dimensional nanosheets with outstanding electrochemical performance and aesthetic property," *Sci. Rep.*, vol. 3, pp. 1–7, 2013.

[74] N. Suganya, V. Jaisankar, and E. K. T. Sivakumar, "Conducting Polymeric Hydrogel Electrolyte Based on Carboxymethylcellulose and Polyacrylamide/Polyaniline for Supercapacitor Applications," *Int. J. Nanosci.*, vol. 17, no. 1–2, pp. 1–6, 2018.

[75] X. Li, J. Zhao, Z. Cai, and F. Ge, "A dyeing-induced heteroatom-co-doped route toward flexible carbon electrode derived from silk fabric," *J. Mater. Sci.*, vol. 53, no. 10, pp. 7735–7743, 2018.

[76] Z. Zhou, X. F. Wu, and H. Fong, "Electrospun carbon nanofibers surface-grafted with vapor-grown carbon nanotubes as hierarchical electrodes for supercapacitors," *Appl. Phys. Lett.*, vol. 100, no. 2, 2012.

[77] X. Wang, H. Liu, X. Chen, D. G. Evans, and W. Yang, "Fabrication of manganese dioxide nanosheet-based thin-film electrode and its electrochemical capacitance performance," *Electrochim. Acta*, vol. 78, pp. 115–121, 2012.

[78] Y. Huang *et al.*, "Super-high rate stretchable polypyrrole-based supercapacitors with excellent cycling stability," *Nano Energy*, vol. 11, pp. 518–525, 2015.

[79] K. P. Díaz-Orellana and M. E. Roberts, "Scalable, template-free synthesis of conducting polymer microtubes," *RSC Adv.*, vol. 5, no. 32, pp. 25504–25512, 2015.

[80] I. Aldama, V. Barranco, T. A. Centeno, J. Ibañez, and J. M. Rojo, "Composite Electrodes Made from Carbon Cloth as Supercapacitor Material and Manganese and Cobalt Oxide as Battery One," *J. Electrochem. Soc.*, vol. 163, no. 5, pp. A758–A765, Feb. 2016.

[81] Y. Wang, S. Tang, S. Vongehr, J. Ali Syed, X. Wang, and X. Meng, "High-Performance Flexible Solid-State Carbon Cloth Supercapacitors Based on Highly Processible N-

Graphene Doped Polyacrylic Acid/Polyaniline Composites," *Sci. Rep.*, vol. 6, no. February, pp. 1–10, 2016.

[82] N. Kumar, R. T. Ginting, and J. W. Kang, "Flexible, large-area, all-solid-state supercapacitors using spray deposited PEDOT:PSS/reduced-graphene oxide," *Electrochim. Acta*, vol. 270, pp. 37–47, 2018.

[83] L. Liu, Y. Yu, C. Yan, K. Li, and Z. Zheng, "Wearable energy-dense and power-dense supercapacitor yarns enabled by scalable graphene–metallic textile composite electrodes," *Nat. Commun.*, vol. 6, no. 1, p. 7260, Nov. 2015.

[84] C. Cheng, J. Xu, W. Gao, S. Jiang, and R. Guo, "Preparation of flexible supercapacitor with RGO/Ni-MOF film on Ni-coated polyester fabric," *Electrochim. Acta*, vol. 318, pp. 23–31, 2019.

[85] S. Patil, J. . Mahajan, M. . More, and P. . Patil, "Influence of substrate conductivity on electrochemical polymerization of O-methoxyaniline," *Mater. Sci. Eng. B*, vol. 87, no. 2, pp. 134–140, Nov. 2001.

[86] Y. Shi, L. Peng, Y. Ding, Y. Zhao, and G. Yu, "Nanostructured conductive polymers for advanced energy storage," *Chem. Soc. Rev.*, vol. 44, no. 19, pp. 6684–6696, 2015.

[87] C. J. Raj *et al.*, "Highly Flexible and Planar Supercapacitors Using Graphite Flakes/Polypyrrole in Polymer Lapping Film," *ACS Appl. Mater. Interfaces*, vol. 7, no. 24, pp. 13405–13414, 2015.

[88] S. Machida, S. Miyata, and A. Techagumpuch, "Chemical synthesis of highly electrically conductive polypyrrole," *Synth. Met.*, vol. 31, no. 3, pp. 311–318, Sep. 1989.

[89] G. A. Snook, P. Kao, and A. S. Best, "Conducting-polymer-based supercapacitor devices and electrodes," *J. Power Sources*, vol. 196, no. 1, pp. 1–12, 2011.

[90] Y. Tan and K. Ghandi, “Kinetics and mechanism of pyrrole chemical polymerization,” *Synth. Met.*, vol. 175, pp. 183–191, 2013.

[91] R. Bouldin *et al.*, “Synthesis of polypyrrole with fewer structural defects using enzyme catalysis,” *Synth. Met.*, vol. 161, no. 15–16, pp. 1611–1617, 2011.

[92] A. Kausaite-Minkstimiene, V. Mazeiko, A. Ramanaviciene, and A. Ramanavicius, “Evaluation of chemical synthesis of polypyrrole particles,” *Colloids Surfaces A Physicochem. Eng. Asp.*, vol. 483, pp. 224–231, 2015.

[93] A. F. Diaz *et al.*, “Polypyrrole: An electrochemically synthesized conducting organic polymer,” *Synth. Met.*, vol. 1, no. 3, pp. 329–336, 2003.

[94] T. Liu *et al.*, “Polyaniline and Polypyrrole Pseudocapacitor Electrodes with Excellent Cycling Stability,” *Nano Lett.*, vol. 14, no. 5, pp. 2522–2527, May 2014.

[95] L. Yuan, B. Yao, B. Hu, K. Huo, W. Chen, and J. Zhou, “Polypyrrole-coated paper for flexible solid-state energy storage,” *Energy Environ. Sci.*, vol. 6, no. 2, pp. 470–476, 2013.

[96] J. Wang, Y. Xu, J. Wang, J. Zhu, Y. Bai, and L. Xiong, “Study on Capacitance Evolving Mechanism of Polypyrrole during Prolonged Cycling,” *J. Phys. Chem. B*, vol. 118, no. 5, pp. 1353–1362, Feb. 2014.

[97] J. Sun *et al.*, “High-performance stretchable yarn supercapacitor based on PPy@CNTs@urethane elastic fiber core spun yarn,” *Nano Energy*, vol. 27, pp. 230–237, Sep. 2016.

[98] Y. Song, J.-L. Xu, and X.-X. Liu, “Electrochemical anchoring of dual doping polypyrrole on graphene sheets partially exfoliated from graphite foil for high-performance supercapacitor electrode,” *J. Power Sources*, vol. 249, pp. 48–58, Mar. 2014.

[99] X. Li *et al.*, “High-Performance Polypyrrole/Graphene/SnCl 2 Modified Polyester Textile

Electrodes and Yarn Electrodes for Wearable Energy Storage," *Adv. Funct. Mater.*, vol. 28, no. 22, p. 1800064, May 2018.

[100] D. C. Marcano *et al.*, "Improved Synthesis of Graphene Oxide," *ACS Nano*, vol. 4, no. 8, pp. 4806–4814, Aug. 2010.

[101] F. Ahmed *et al.*, "Graphene oxide humidity sensor built entirely by additive manufacturing approaches," *J. Mater. Sci. Mater. Electron.*, vol. 30, no. 9, pp. 8980–8988, 2019.

[102] B. Wu, N. Zhao, S. Hou, and C. Zhang, "Electrochemical Synthesis of Polypyrrole, Reduced Graphene Oxide, and Gold Nanoparticles Composite and Its Application to Hydrogen Peroxide Biosensor," *Nanomaterials*, vol. 6, no. 11, p. 220, Nov. 2016.

[103] X. Gao, J. Jang, and S. Nagase, "Hydrazine and thermal reduction of graphene oxide: Reaction mechanisms, product structures, and reaction design," *J. Phys. Chem. C*, vol. 114, no. 2, pp. 832–842, 2010.

[104] S. J. Li *et al.*, "Application of thermally reduced graphene oxide modified electrode in simultaneous determination of dihydroxybenzene isomers," *Sensors Actuators, B Chem.*, vol. 174, pp. 441–448, 2012.

[105] K. G. Neoh, T. T. Young, E. T. Kang, and K. L. Tan, "Structural and mechanical degradation of polypyrrole films due to aqueous media and heat treatment and the subsequent redoping characteristics," *J. Appl. Polym. Sci.*, vol. 64, no. 3, pp. 519–526, 1997.

[106] X. B. Chen, J. P. Issi, J. Devaux, and D. Billaud, "The stability of polypyrrole and its composites," *J. Mater. Sci.*, vol. 32, no. 6, pp. 1515–1518, 1997.

[107] L. Dong *et al.*, "Flexible electrodes and supercapacitors for wearable energy storage: A

review by category," *J. Mater. Chem. A*, vol. 4, no. 13, pp. 4659–4685, 2016.

[108] K. Jost, G. Dion, and Y. Gogotsi, "Textile energy storage in perspective," *J. Mater. Chem. A*, vol. 2, no. 28, pp. 10776–10787, 2014.

[109] X. Chen *et al.*, "Environmentally Friendly Flexible Strain Sensor from Waste Cotton Fabrics and Natural Rubber Latex," *Polymers (Basel).*, vol. 11, no. 3, p. 404, Mar. 2019.

[110] M. Barakzehi, M. Montazer, F. Sharif, T. Norby, and A. Chatzitakis, "A textile-based wearable supercapacitor using reduced graphene oxide/polypyrrole composite," *Electrochim. Acta*, vol. 305, pp. 187–196, 2019.

[111] W.-L. Hong and L.-Y. Lin, "Studying the substrate effects on energy storage abilities of flexible battery supercapacitor hybrids based on nickel cobalt oxide and nickel cobalt oxide@nickel molybdenum oxide," *Electrochim. Acta*, vol. 308, pp. 83–90, Jun. 2019.

[112] J. Shen *et al.*, "Flexible carbon cloth based solid-state supercapacitor from hierarchical holothurian-morphological NiCo2O4@NiMoO4/PANI," *Electrochim. Acta*, vol. 320, pp. 1–10, 2019.

[113] X. Peng, S. Chen, L. Liu, S. Zheng, and M. Li, "Modified stainless steel for high performance and stable anode in microbial fuel cells," *Electrochim. Acta*, vol. 194, pp. 246–252, 2016.

[114] S. Totaro Yamagata and K. Shuji Banno, "Process for separating polyvinyl alcohol from its solution," US4078129A, 1975.

[115] N. Batisse and E. Raymundo-Piñero, "A self-standing hydrogel neutral electrolyte for high voltage and safe flexible supercapacitors," *J. Power Sources*, vol. 348, pp. 168–174, 2017.

[116] R. Zhang, Y. Xu, D. Harrison, J. Fyson, and D. Southee, "A study of the electrochemical performance of strip supercapacitors under bending conditions," *Int. J. Electrochem. Sci.*,

vol. 11, no. 9, pp. 7922–7933, 2016.

[117] B. A. Mei, J. Lau, T. Lin, S. H. Tolbert, B. S. Dunn, and L. Pilon, "Physical Interpretations of Electrochemical Impedance Spectroscopy of Redox Active Electrodes for Electrical Energy Storage," *J. Phys. Chem. C*, vol. 122, no. 43, pp. 24499–24511, 2018.

[118] A. Bello *et al.*, "Electrochemical performance of polypyrrole derived porous activated carbon-based symmetric supercapacitors in various electrolytes," *RSC Adv.*, vol. 6, no. 72, pp. 68141–68149, 2016.

[119] C. Yang, L. Zhang, N. Hu, Z. Yang, H. Wei, and Y. Zhang, "Reduced graphene oxide/polypyrrole nanotube papers for flexible all-solid-state supercapacitors with excellent rate capability and high energy density," *J. Power Sources*, vol. 302, pp. 39–45, 2016.

[120] K. Shu, C. Wang, C. Zhao, Y. Ge, and G. G. Wallace, "A Free-standing Graphene-Polypyrrole Hybrid Paper via Electropolymerization with an Enhanced Areal Capacitance," *Electrochim. Acta*, vol. 212, pp. 561–571, 2016.

[121] R. Zhang, J. Xu, and E. H. Yang, "Fabrication and chacterization of an all-solid-state stretchable supercapacitor using polypyrrole-CNT hybrid partially embedded in PDMS," *TechConnect Briefs 2018 - Adv. Mater.*, vol. 2, pp. 71–74, 2018.

[122] R. Zhang, K. Yan, A. Palumbo, J. Xu, S. Fu, and E. H. Yang, "A stretchable and bendable all-solid-state pseudocapacitor with dodecylbenzenesulfonate-doped polypyrrole-coated vertically aligned carbon nanotubes partially embedded in PDMS," *Nanotechnology*, vol. 30, no. 9, 2019.

[123] T. Lv, M. Liu, D. Zhu, L. Gan, and T. Chen, "Nanocarbon-Based Materials for Flexible

All-Solid-State Supercapacitors," *Adv. Mater.*, vol. 30, no. 17, pp. 1–17, 2018.